c-Myb Regulates the Survival of CD4+CD8+ Double Positive Thymocytes

Joan Yuan
Lund, Sweden

M.Sc, Lund University, Sweden, 2003

A Dissertation presented to the Graduate Faculty
of the University of Virginia in Candidacy for the Degree of
Doctor of Philosophy

Department of Microbiology

University of Virginia
December, 2009

Abstract

The peripheral T cell repertoire is selected during the $CD4^+CD8^+$ double positive (DP) stage of T cell development for optimized pathogen recognition while maintaining self-tolerance. *Bcl2l1* encodes the survival factor Bcl-xL, which is specifically upregulated in DP thymocytes to prolong the window of time available for *Tcrα* rearrangements and the generation of a diverse T cell repertoire. However, despite the importance of *Bcl2l1* during T cell development, the regulation of its expression remains poorly understood. The *Myb* proto-oncogene encodes an essential transcription factor that plays critical roles during several stages of T cell development including DN to DP thymocyte development, DP thymocyte survival and the development of CD4SP thymocytes. Work in this thesis demonstrates that *Myb* mRNA expression is specifically upregulated in the small, pre-selection DP stage during T cell development. Using a conditional deletion model in which deletion at the *Myb* locus takes place in DP thymocytes, we demonstrate that *Myb* deficient DP thymocytes undergo premature apoptosis, resulting in a limited *Tcrα* repertoire biased towards 5' *Jα* segment usage. Premature apoptosis occurs in an αβ-TCR independent manner and is a consequence of decreased Bcl-xL expression. Re-introduction of c-Myb restores both Bcl-xL expression and the small pre-selection DP compartment and forced Bcl-xL expression is able to rescue survival. However, prolonged survival alone cannot restore the CD4SP compartment in *Myb* deficient mice, suggesting that c-Myb is able to enhance CD4SP lineage representation independent of

its ability to prolong DP thymocyte survival. Work in this thesis makes clear that c-Myb promotes *Bcl2l1* transcription *in vivo* via a novel genetic pathway independent of the expression of TCF-1 or RORγt, two transcription factors previously reported to induce Bcl-xL expression during T cell development. In conclusion, this thesis work establishes Bcl-xL as a novel mediator of c-Myb activity and sheds new light on the regulation of cell survival during a critical stage of normal T cell development.

Acknowledgements

It is an honor to thank my thesis advisor Dr Timothy Bender. I truly appreciate all of his encouragement and constructive criticism, which helped push me to become the best and most meticulous thinker, speaker and writer of science that I can be. Most importantly, his trust in me gave me a great sense of responsibility early on in the development of my thesis project and the confidence to pursue my own ideas, making my time in his laboratory a time of tremendous scientific and personal growth and fulfillment. This thesis would not have been possible without my outstanding thesis advisory committee, Drs Kodi Ravichandran, Victor Engelhard, Ulrike Lorenz, and John Buschweller whose intelligence and guidance has been invaluable and will continue to inspire me.

I would like to thank the Department of Microbiology for providing a nurturing environment for young scientists and in particular for harboring prominent female investigators who have served as role models to me personally. I am indebted to the staff of the Department of Microbiology, especially Sandra Weirich for her incredible problem solving skills. I am grateful to the Robert Wagner fellowship for providing financial support for my thesis work as well as sponsoring my first participation in a national scientific meeting. Finally, I am deeply grateful to all past and present members of the Bender laboratory including Matthew Thomas, Amanda Duley, Erin Yarde, Shawn Fahl, Christopher Kremer and Rowena Crittenden for their support and precious friendship.

They have made me feel at home in a foreign land and made everyday fun and memorable.

I owe all of my ambition and success to my mother and father whose love, hard work and personal sacrifice to provide a better future for our family has paved the way for me and remind everyday to have endurance, diligence and a sense of humor in all of my endeavors. I dedicate this thesis to my husband, Jeremy Daniel, with whom I share my passion for biomedical science. His unconditional love and support has been my greatest source of motivation and inner balance and made me into a better scientist and person than I could be on my own.

Table of contents

List of Figuures

List of Tables

Chapter I. INTRODUCTION

1.1 αβ T cell development

Vertebrates are uniquely equipped with an adaptive immune system that enables them to recognize, eradicate and remember a seemingly infinite number of specific foreign antigens (Boehm and Bleul, 2007). T cells are characterized by the surface expression of an antigen specific clonal T cell receptor (TCR) and play a central role in the adaptive immune response. Unlike all other hematopoietic lineages that develop in the bone marrow, T cell precursors mature in the thymus. αβ T cell development revolves around the two-step assembly of an αβ-TCR heterodimer with the goal to generate a diverse TCR repertoire that allows broad recognition of foreign antigens while maintaining self-tolerance. Diversity is accomplished by somatic recombination of the variable (V), diversity (D) and joining (J) segments encoded at the *Tcrβ* locus and the V and J segments encoded at the *Tcrα* locus through an error-prone process known as V(D)J recombination (Jung and Alt, 2004). V(D)J recombination at the *Tcrβ* and *Tcrα* loci takes place during temporally distinct stages of T cell development and relies on two waves of the recombination activating genes, *Rag1* and *Rag2* expression (Wilson et al., 1994), as well as changes in chromatin accessibility induced by active chromatin remodeling of the TCR-coding loci at the appropriate stages (Cobb et al., 2006). Successful V(D)J recombination at the *Tcrβ* and *Tcrα* loci are enforced by two

developmental checkpoints known as β-selection and repertoire selection respectively (von Boehmer, 2004).

CD4 and CD8 are co-receptors that assist TCR signaling by direct association with MHC class II and class I molecules respectively and recruitment of intracellular signaling components. The generation of mature αβ T cells can be separated into three major stages based on changes in the cell surface expression of CD4 and CD8 (Fig. 1.1). Recombination of *Tcrβ* takes place in early T cell progenitors that lack the surface expression of both CD4 and CD8 ($CD4^-CD8^-$ double negative (DN) thymocytes). Productive *Tcrβ* rearrangement leads to the surface expression of a pre-TCR complex, signaling through which drives continued development into the $CD4^+CD8^+$ DP stage (von Boehmer et al., 1999). This process represents the first major developmental checkpoint during T cell development and is termed β-selection. During the DP stage, productive recombination at the *Tcrα* locus results in the production of a TCRα chain and the surface expression of a mature αβ-TCR complex that will be tested for reactivity towards self-peptide/MHC complex in a second developmental checkpoint termed repertoire selection (Starr et al., 2003). Thymocytes that fail to make a productive rearrangement or produce potentially autoreactive TCRs are eliminated by way of apoptosis. Only around 5% of all DP thymocytes produce an αβ-TCR with an intermediate level of affinity towards self-peptide/MHC complexes and qualify for positive selection and continued development. Positively selected DP thymocytes differentiate into either CD4 or the CD8 single positive (SP) thymocytes in a MHC dependent fashion and go on to constitute the peripheral T helper and T cytotoxic compartments respectively (Singer et al., 2008).

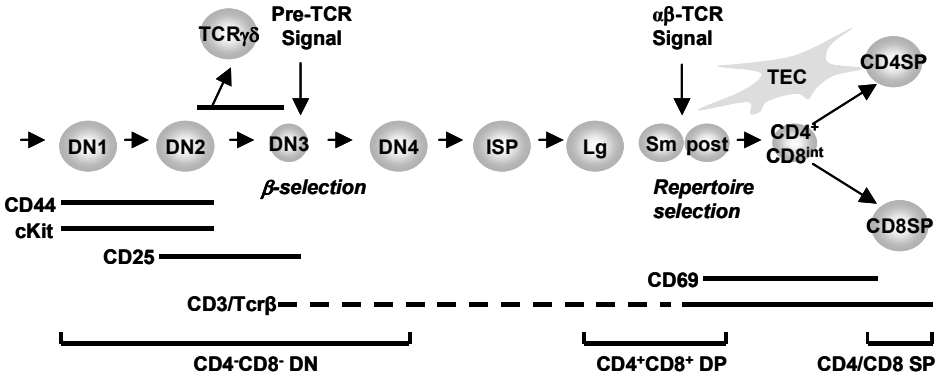
TCRγδ
Pre-TCR Signal
αβ-TCR Signal
TEC
CD4SP
DN1
DN2
DN3
DN4
ISP
Lg
Sm
post
CD4+ CD8int
β-selection
Repertoire selection
CD8SP
CD44
cKit
CD25
CD69
CD3/Tcrβ
CD4-CD8- DN
CD4+CD8+ DP
CD4/CD8 SP

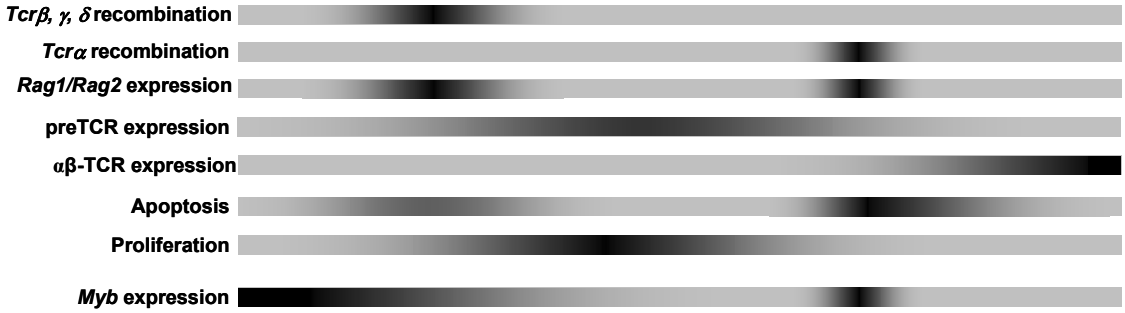
Tcrβ, γ, δ recombination
Tcrα recombination
Rag1/Rag2 expression
preTCR expression
αβ-TCR expression
Apoptosis
Proliferation
Myb expression

Figure 1.1 Summary normal mouse T cell development. The major stages and events of T cell development are outlined in the diagram. Solid lines indicate high surface expression and dotted lines indicate low surface expression. Bars mark stages with high incidence (black) of V(D)J recombination, expression of the TCR-coding loci, Rag1/2 expression, cell death and proliferation. c-Myb mRNA expression pattern as determined by work in this thesis is illustrated on the bottom. DN thymocytes can subdivided into four stages based on changes in the surface expression of cKit, CD44 and CD25 as depicted. DP thymocytes can be divided into large pre-selection (Lg), small pre-selection (Sm) and post-selection (post) thymocytes. The two major developmental checkpoints, β-selection and repertoire selection are indicated. Thymic epithelial cells (TEC) provide self-peptide MHC complexes, which engage the newly assembled αβ-TCR during repertoire selection. Other branch points such as those to the NKT and T_{reg} lineages also exist but are not depicted.

Early thymocyte development and β-selection

$CD4^-CD8^-$ double negative (DN) thymocytes represent the most immature thymocyte compartment and can be further divided into four developmental stages based on differential expression of c-Kit (CD117), CD44 and CD25 (Fig. 1.1) (Godfrey et al., 1993). Multipotent bone-marrow derived lymphoid progenitors are recruited from the blood into the postnatal thymus at the corticomedullary junction (CMJ) (Misslitz et al., 2006). Early T-lineage progenitors (ETP) ($c\text{-}Kit^{hi}$, $CD44^+$, $CD25^-$) represent the most recent settlers of the thymus and undergo proliferation while retaining the potential to differentiate into the natural killer, macrophage and dendritic cell lineages (Balciunaite et al., 2005; Schmitt et al., 2004; Shen et al., 2003). Differentiation to the DN2 ($c\text{-}Kit^+$, $CD44^+$, $CD25^+$) and subsequently the DN3 ($c\text{-}Kit^{low}$, $CD44^{low}$, $CD25^+$) stages is accompanied by cell migration from the CMJ towards the outer cortex of the thymus. During this time, continuous cytokine and Notch signaling from the thymic microenvironment drives the expression of T lineage associated genes or T lineage specification (Radtke et al., 1999; Sambandam et al., 2005; Wilson et al., 2001). V(D)J recombination at the *Tcrβ* locus is initiated upon commitment to the T lineage whereby the potential to differentiate into other hematopoietic lineages is irreversibly lost (Masuda et al., 2007). The recombination process occurs in a temporal order involving first the joining of *Dβ* and *Jβ* segments and subsequently the joining of *Vβ* segments to the *DβJβ* joint in DN2 and DN3 thymocytes (Jung and Alt, 2004). If rearrangement is productive, the resulting TCRβ chain will attempt to associate with an invariant pre-TCRα (pTα) protein as well as proteins of the CD3 complex to form a pre-TCR complex (Groettrup et

al., 1993). αβ T cell development is blocked at the DN3 stage in mice that lack *pTα*, *Tcrβ*, *CD3ε* or *CD3γ* (von Boehmer et al., 1999). V(D)J recombination at the *Tcrγ* and *Tcrδ* loci also take place during the DN2 and DN3 stages (Fig. 1.1). While the vast majority of thymocytes differentiate down the αβ T-lineage, a minor fraction (<5%) successfully produce a γδ TCR and differentiate down the γδ T-lineage. It is believed that signals emanating from the Notch receptor and the γδ-TCR or pre-TCR play instructive roles during the αβ/γδ Tlineage decision (Garbe and von Boehmer, 2007). However, the mechanisms underlying γδ T cell development are poorly understood and will not be discussed in this thesis.

Thymocytes that receive signaling through a functional pre-TCR complex are eligible to pass the first major developmental checkpoint known as β-selection. In addition to its role in granting survival exclusively to those progenitors that express a productive pre-TCR complex, β-selection signaling also down-regulates *Rag1/2* mRNA expression and prevents further rearrangement at the Tcrβ loci through a process known as allelic exclusion, as well as drives entry into the cell cycle, down-regulates CD25 surface expression prior to up-regulating first the CD8 and then the CD4 co-receptors (von Boehmer et al., 1999). Thus, β-selection drives the differentiation of the DN3 thymocyte into the DN4 (c-Kit$^-$, CD44$^-$, CD25$^-$), immature single positive (ISP) (TCRβ^{lo}, CD8$^+$, CD4$^-$) and subsequently the DP (CD4$^+$CD8$^+$) stage.

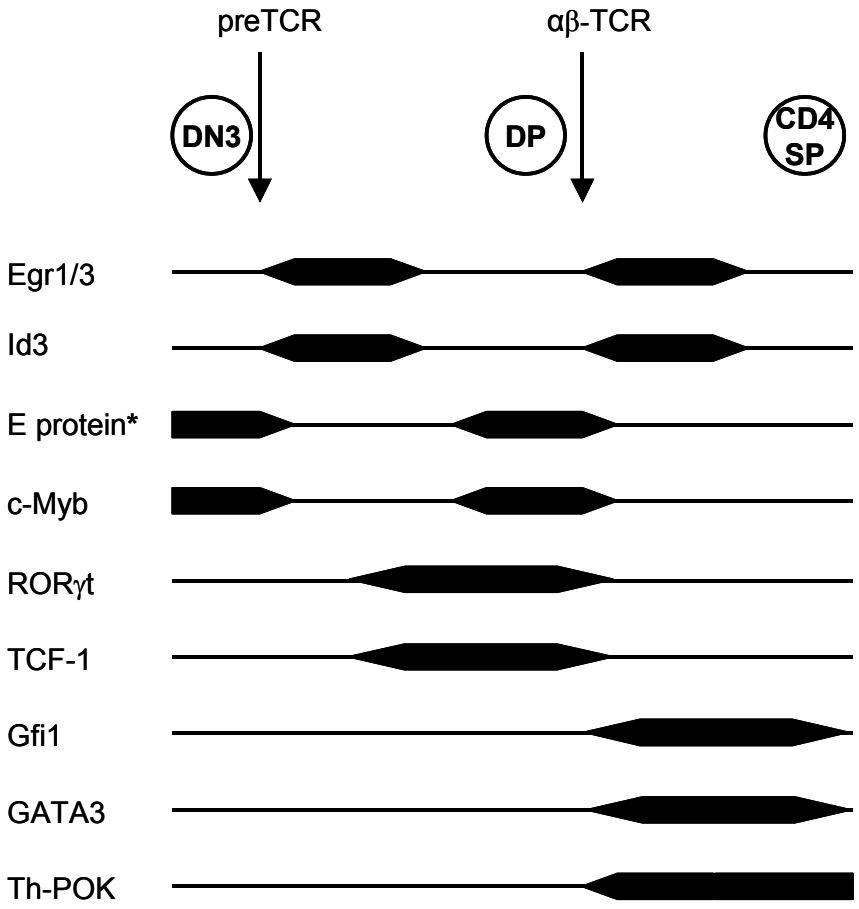

Figure 1.2 Summary of the expression patterns of several transcription factors during normal mouse T cell development. Diagram summarizes known changes in the expression of important transcription factors discussed in this thesis. Lines represent little to no expression and bars represent high expression. * Represents net changes in E protein activity based on changes in protein expression and activation state. The timing of pre-TCR signaling and αβ-TCR signaling are indicated. The CD8SP subset was not depicted since CD8SP lineage specific transcription factors were not extensively discussed in this thesis.

Becoming a DP thymocyte

Thymocytes undergo the greatest proliferative burst following β-selection during the DN4 and ISP stages and enter the DP stage as large blasts. Shortly upon becoming a DP thymocyte, cells enter a quiescent phase, where they have an intrinsic lifespan of 3-4 days, and begin V(D)J recombination at the *Tcrα* locus (Egerton et al., 1990; Petrie et al., 1993). Thymocytes that qualify for the criteria of β-selection are relatively rare and must endure a second stringent developmental checkpoint that is referred to as repertoire selection and takes place in the DP stage. The extensive expansion of clones that express a functional TCRβ chain following β-selection is therefore crucial to ensure sufficient input into the DP compartment thymocytes that express productive TCRβ chains. This allows the same TCRβ chain to audition many TCRα chains and increases the opportunities for its positive selection and inclusion into the mature αβ-TCR repertoire.

Following the post β-selection proliferative phase, it is imperative that DP thymocytes enter a resting state as V(D)J recombination at the *Tcrα* locus generates DNA double-stand breaks and is therefore incompatible with DNA replication. Recent evidence suggests that pre-TCR signaling triggers sequential changes in the expression and activity of several transcription factors, which orchestrates the temporal distinction between rapid proliferation and *Tcrα* gene rearrangements. A key player in the establishment of quiescence in DP thymocytes is the orphan nuclear hormone receptor RORγt (Sun et al., 2000; Xi et al., 2006). RORγt is an isoform of the *RORγ* gene that is expressed predominantly in DP thymocytes. *RORγ*$^{-/-}$ mice display decreased ISP to DP differentiation, an inability of DP thymocytes to withdraw from cell cycle, and

insufficient *Tcrα* recombination due to a failure of DP thymocytes to up-regulate both Rag2 and Bcl-xL expression (Guo et al., 2002; He, 2000; Sun et al., 2000; Yu et al., 2004). These findings are consistent with an anti-proliferative role of RORγt during the DP stage of T cell development to enable efficient *Tcrα* recombination. RORγt expression is up-regulated in normal DP thymocytes in a manner that is dependent on the activities of the E-protein family of transcription factors (E12, E47, E2-2, and HEB) (Xi et al., 2006). Up-regulation of RORγt expression requires pre-TCR signals but is delayed following β-selection to allow sufficient proliferation of DN4 and ISP thymocytes (Xi and Kersh, 2004b) (Fig. 1.2). This controlled delay in RORγt up-regulation is thought to be established by the repressive activity of a transient burst of early growth response gene 3 (Egr3) expression following β-selection (Fig. 1.2 and 1.3). Mice that express a constitutive Egr3 transgene fail to up-regulate RORγt expression following pre-TCR signaling and closely resemble RORγ$^{-/-}$ mice in phenotype (Xi and Kersh, 2004b), while mice lacking Egr3 expression exhibit impaired proliferation following β-selection (Xi and Kersh, 2004a), suggesting that Egr3 prevents RORγt induction while facilitating proliferation following β-selection. More recently, it has been reported that Egr3 interferes with the E-protein dependent induction of RORγt by up-regultating the expression of the inhibitor of differentiation 3 (Id3), a negative regulator of E protein function (Xi et al., 2006) (Fig. 1.3). In the same study, Egr3 was also reported to interact with RORγt at the protein level to prevent induction of RORγt target genes. These findings are in accordance with a model where RORγt is required for the establishment of the resting DP phenotype required for efficient V(D)J recombination, while transient Egr3 expression induced by pre-TCR signaling creates a window immediately following

β-selection for sufficient clonal expansion, at least in part by delaying both the up-regulation and function of RORγt (Fig. 1.3).

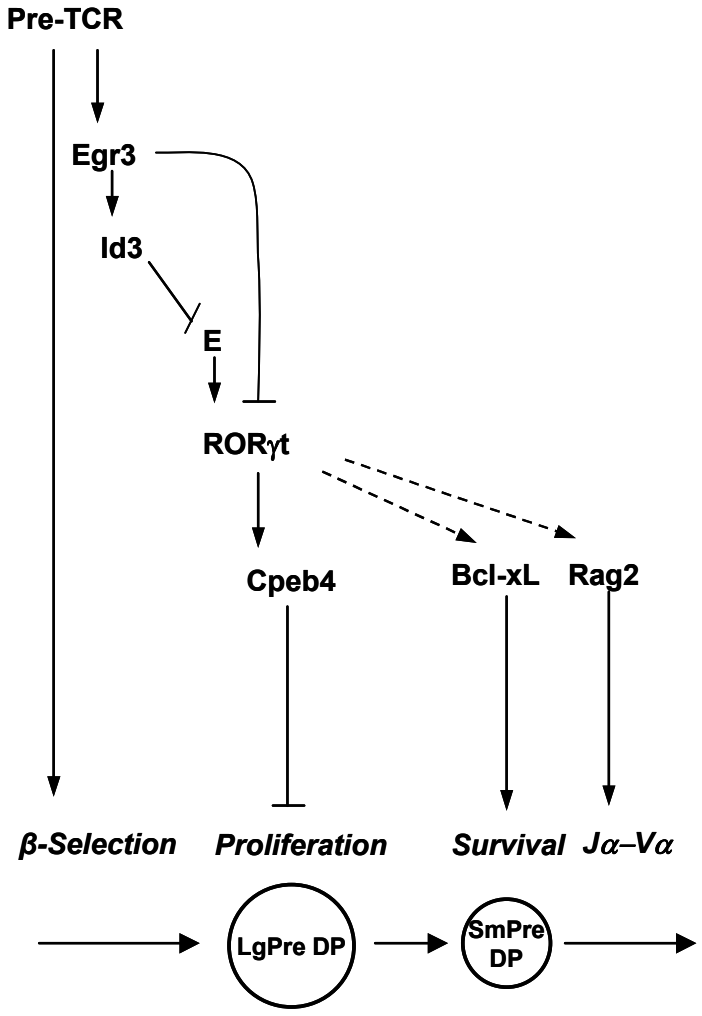

Figure 1.3 Model of the transcriptional network controlling proliferation, quiescence and *Tcrα* V(D)J recombination in response to pre-TCR signaling. The initiation and cessation of the post-β-selection proliferative burst is strictly regulated by an interplay of Egr3, the E-proteins and RORγt. Egr3 is transiently induced upon β-selection to promote thymocyte proliferation, at least in part by delaying the expression and activity of RORγt. RORγt is activated in an E-protein dependent manner upon down-regulation of Egr3 and facilitates recombination at the *Tcrα* locus by promoting cell cycle withdrawal and DP thymocyte survival.

Repertoire selection

The vast majority of cortical thymocytes are small, quiescent cells undergoing V(D)J recombination at the *Tcrα* locus. Several unique features distinguish *Tcrα* rearrangements from *Tcrβ* rearrangements. First, the *Tcrα* locus lacks diversity gene segments. Second, initial rearrangements occur between proximally located 3' *Vα* and 5' *Jα* segments (Petrie et al., 1995; Thompson et al., 1990; Xi and Kersh, 2004b). Third, non-productive recombination events can be rescued by repeated rearrangements between further distally located *Vα* and *Jα* segments that replace prior *VαJα* joins (Petrie et al., 1993). This process is known as receptor editing and occurs simultaneously at both alleles in a coordinated fashion such that nearby *Jα* segments are used in both alleles at any given time (Davodeau et al., 2001). Receptor editing continues until *Rag1/2* expression is diminished by a positive selection signal as a result of productive αβ-TCR engagement (Borgulya et al., 1992; Huang and Kanagawa, 2001b; Petrie et al., 1993; Wang et al., 1998). Finally, there is an apparent lack of allelic exclusion at the *Tcrα* locus (Malissen et al., 1992). These features of *Tcrα* recombination allow flexible sampling of TCRα chains by the pre-existing TCRβ chain within each DP thymocyte and maximizes the chances for positive selection within a limited intrinsic lifespan of 3-4 days (Egerton et al., 1990). Secondary rearrangements at the *Tcrα* locus occur in the majority of DP thymocytes (Yannoutsos et al., 2001) and contribute significantly to the frequency of positive selection and the diversity of the peripheral T cell repertoire. The survival window of pre-selection DP thymocytes limits the extent of secondary

rearrangements and premature cell death results in an unusually 5' biased TCR repertoire (Guo et al., 2002).

If a functional TCRα chain that is able to pair with the existing TCRβ chain is produced, a mature αβ-TCR complex is inserted into the plasma membrane. At this stage, the DP thymocyte is subjected to repertoire selection based on the reactivity of its αβ-TCR towards the self-peptide/MHC complex (Starr et al., 2003). Despite secondary rearrangements, ~90% of all DP thymocytes fail to produce an αβ-TCR complex that can productively engage self-peptide/MHC complexes presented by thymic epithelial cells (TEC) within the limited survival window (Fig. 1.1). Thymocytes that fail to undergo positive selection are not useful to the immune system and undergo death by neglect. DP thymocytes that receive positive selection signals undergo phenotypical changes including increased surface expression of CD69, CD5, CD53, BTLA, TCRβ and CCR7 (Han et al., 2004; Kwan and Killeen, 2004; Sudo et al., 1993; Tomlinson et al., 1995; Ueno et al., 2004; Witt and Robey, 2004). Importantly, CCR7 facilitates migration of DP thymocytes from the thymic cortex, across the CMJ, into the thymic medulla. The transcription factor AIRE (autoimmuneregulator) promotes the expression of peripheral tissue-restricted antigens in thymic medullary epithelial cells (Anderson et al., 2002; Liston et al., 2003). Upon migration into the medulla, those thymocytes that bind self-peptide/MHC complexes with high affinity are deleted by way of negative selection. Less than 5% of all DP thymocytes will express an αβ-TCR with an intermediate affinity towards self peptide-MHC complexes and receive the vital signal for positive selection based on their ability to engage MHC while preserving self-tolerance.

Like β-selection, positive selection initiates signals for survival and continued differentiation, but unlike β-selection, positive selection does not stimulate rapid cell division. From an evolutionary standpoint, further clonal expansion in the thymus does not provide additional benefits once the αβ-TCR specificity is finalized. The establishment of a working adaptive immune system and its reactivity towards antigens presented by self-peptide/MHC relies on an intact repertoire selection checkpoint. Thus, despite being an extremely wasteful process in terms of energy cost to the individual, repertoire selection has provided vital advantages through vertebrate evolution.

CD4/CD8 lineage decision

Completion of positive selection requires continuous TCR interactions and results in the development of DP thymocytes into either the CD4 single positive (SP) ($TCRb^{hi}$, $CD4^{+}$, $CD8^{-}$) or the CD8SP ($TCRb^{hi}$, $CD4^{-}$, $CD8^{+}$) stage (Wilkinson et al., 1995). This transition follows a complex pattern of coordinated changes in co-receptor expression involving a common transitional stage ($CD4^{+}$, $CD8^{int}$, $CD69^{+}$) during which CD4/CD8 lineage commitment is thought to initiate (Singer et al., 2008). It has long been known that the CD4/CD8 lineage decision takes place in a MHC specific manner such that thymocytes that receive a positive selection signal through engagement of class II MHC differentiate into CD4SP cells and those that receive a positive selection signal through class I MHC differentiate into CD8SP cells (Teh et al., 1988). The mechanism underlying this binary cell fate decision has been the subject of extensive experimental analysis and intense debate and is still not fully understood (Singer et al., 2008).

However, recent advances make clear that CD4/CD8 lineage fate depends both on the nature of αβ-TCR signaling and a sophisticated interplay between transcription factors, leading first to lineage specification and then lineage commitment (Egawa, 2009; Rothenberg, 2009).

Lineage commitment is by definition the process during which lineage plasticity is lost through the loss of gene expression that is required for the alternative cell fate. In the case of the CD4/CD8 lineage decision, lineage commitment leads to the permanent down-regulation of one of the co-receptors. The stage-specific expression of *Cd8a/CD8b* genes is dependent on the activation of stage-specific enhancers while the stage specific expression of *Cd4* is regulated by the activity of a silencer element (Singer et al., 2008). The e8III enhancer is sufficient to activate *Cd8* expression in pre-selection DP thymoytes (Feik et al., 2005). Such expression is down-regulated upon positive selection regardless of the MHC specificity of the αβ-TCR engagement resulting in a $CD4^{+}CD8^{int}CD69^{+}$ phenotype (Bosselut et al., 2003; Singer, 2002). If positively selecting TCR signals are MHC class II dependent, signaling requires only the CD4 co-receptor and persists in $CD4^{+}CD8^{int}CD69^{+}$ thymocytes. Thus, class II MHC mediated TCR engagement is uninterrupted and believed to up-regulate the expression of the CD4 lineage specific transcription factor GATA3. GATA3 up-regulation is a critical CD4 lineage specification event that in turn induces Th-Pok (*Zbtb7b*) expression (Fig. 1.4). Th-Pok is a zinc-finger transcription factor believed to induce CD4 lineage commitment at least in part by blocking Runx3 expression and antagonizing Runx dependent repression at the *Cd4* silencer (Egawa, 2009) (Fig. 1.4). Alternatively, if the positively selecting αβ-TCR

signal is MHC class I dependent, signaling is interrupted upon down-regulation of surface CD8 in $CD4^{+}CD8^{int}CD69^{+}$ thymocytes. Signal cessation has been linked to increased Il7Rα expression, induction of Runx3 and re-expression of *Cd8* mediated by a different enhancer element (e8I) (Singer et al., 2008). Runx3 in turn silences both *Zbtb7b* expression and *Cd4* transcription and achieves commitment to the CD8 lineage. Early SP thymocytes continue to be susceptible to negative selection. Further functional maturation of SP thymocytes drives the upregulation of S1P1, a cell surface molecule that facilitates movement into the blood stream via blood vessels in the thymic medulla (Weinreich and Hogquist, 2008).

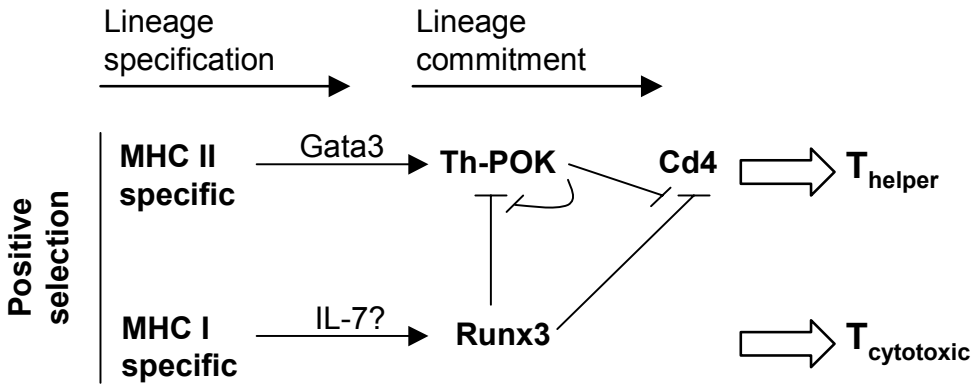

Figure 1.4 Model of the antagonistic interplay between Th-POK (*Zbtb7b*) and Runx3 that brings about CD4/CD8 lineage commitment during T cell development. GATA3 expression is highly induced by MHC II specific positive selection signals, whereas Runx3 expression is induced by MHC I specific positive selection signals. In the absence of Th-POK, Runx3 expression silences *Zbtb7b* and *Cd4* transcription and directs development towards the $T_{cytotoxic}$ lineage. GATA3 activity promotes transcription at the *Zbtb7b* locus. Th-POK is able to block Runx3 mediated repression at the *Zbtb7b* and *Cd4* loci and thereby mediate commitment to the T_{helper} lineage.

1.2 Life and death in T cell development.

Apoptosis is the evolutionarily conserved process of programmed cell death and can be induced through two distinct, but ultimately converging pathways, referred to as the intrinsic and extrinsic apoptotic pathways (Fig. 1.5) (Hengartner, 2000). Apoptosis serves to eliminate unwanted and potentially dangerous cells during normal development and homeostasis in metazoans and is morphologically characterized by cell shrinking, membrane blebbing, DNA fragmentation and degradation of cellular structure without the loss of membrane integrity. Apoptotic bodies express surface signaling molecules that mediate their clearance by phagocytes in a non-inflammatory manner (Ravichandran, 2003). Apoptosis through the intrinsic pathway is marked by the involvement of the mitochondria and is triggered by signals that originate from within the cell such as DNA damage, nutrient starvation, hypoxia, a defective cell cycle, loss of survival factors and other forms of severe cell stress. In contrast, the extrinsic apoptotic pathway is triggered in response to ligation of cell surface death receptors. During thymopoiesis, apoptosis through the intrinsic as well as the extrinsic pathway strictly enforce the two TCR controlled checkpoints during thymocyte development and ensure only thymocytes that bear potentially useful TCRs are granted continued survival (Opferman, 2008) (Fig. 1.6).

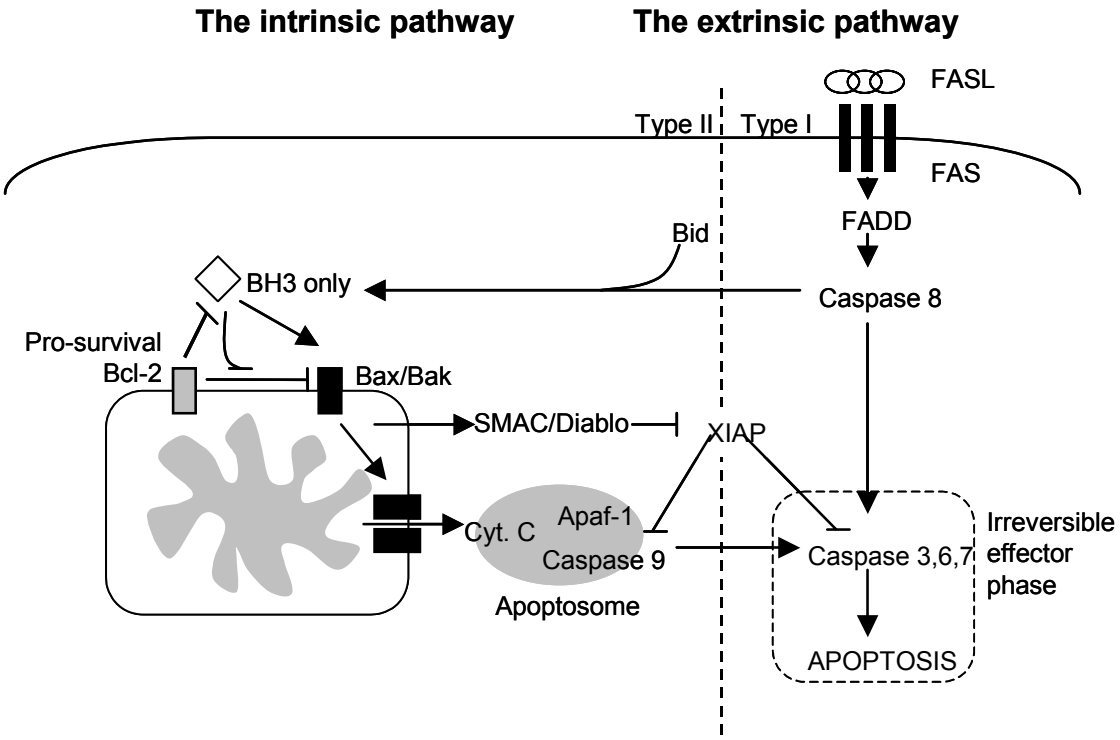
The intrinsic pathway
The extrinsic pathway
FASL
Type II
Type I
FAS
FADD
Bid
BH3 only
Caspase 8
Pro-survival
Bcl-2
Bax/Bak
SMAC/Diablo
XIAP
Cyt. C
Apaf-1
Caspase 9
Apoptosome
Caspase 3,6,7
Irreversible
effector
phase
APOPTOSIS

Figure 1.5 Model of the intrinsic and extrinsic apoptotic signaling pathways.

Two major pathways lead to activaton of the effector caspases, caspase-3, -6 and -7, which trigger an irreversible cascade of cellular breakdown. The intrinsic apoptotic pathway is controlled by the balanced actions of pro- and anti-apoptotic members of the Bcl-2 family, which reside in the mitochondrial outer membrane. Cell intrinsic death signals causes a shift in the balance of the activities of Bcl-2 family members, which can lead to permeabilization of the mitochondrial outer membrane, mitochondrial dysfunction and the release of various apoptotic factors such as Cytochrome C and SMAC/Diablo into the cytoplasm. Cytochrom C forms a complex, apoptosome, with Apaf-1 and pro-caspase-9, which catalyzes caspase-9 activation. Active caspase-9 catalyzes cleavage of effector caspases. SMAC/Diablo inactivates the caspase inhibitor XIAP and thereby licenses caspase activation. Death receptor signaling activates the extrinsic apoptotic signaling pathway through recruitment of FADD and pro-caspase-8. Caspase-8 becomes activated and catalyzes cleavage of effector caspases. In type I cells, death receptor induced apoptosis does not require the enrollment of the intrinsic apoptotic pathway due to low XIAP expression. In type II cells, caspase-8 mediated cell death requires involvement of the intrinsic apoptotic pathway to relieve the caspase inhibition exerted by high XIAP expression.

The intrinsic apoptotic pathway

During apoptosis, deconstruction of a cell is mediated by aspartate-specific cysteine proteases called caspases. Caspases themselves contain internal cleavage sites and are normally present in the cell in an inactive zymogen form. They are activated by proteolytic cleavage and in turn cleave and activate other caspases and enzymes including the caspase-activated deoxyribonuclease (Enari et al., 1998) that initiate and amplify a catalytic cascade leading to irreversible cell death. The extrinsic and intrinsic apoptotic pathways activate the initiator caspases, caspase-8 and -9 respectively, in response to normal or pathological signals. The two initiator caspases mediate the activation of the common effector caspases-3, -6 and -7 that are responsible for cellular degradation (Hengartner, 2000).

The intrinsic apoptotic pathway is mainly controlled by the balance of the activities of pro- and anti-apoptotic Bcl-2 family members in the mitochondrial outer membrane. The Bcl-2 family can be divided into three subgroups based on structure and function. All Bcl-2 family members contain homology to the α-helical Bcl-2 homology (BH) domain. The anti-apoptotic members include Bcl-2, Bcl-xL, Mcl-1, A1 and Bcl-w all of which contain four BH domains (BH1-4) and all but Bcl-w are known to actively regulate T cell development. Targeted gene deletions in mice have demonstrated that different anti-apoptotic Bcl-2 proteins are critical for the survival of different cell types (Opferman, 2008). This is largely due to tissue and stage specific expression (Fig. 1.6), as over expression of one member can often compensate for the loss of another.

However, Bcl-2 cannot compensate for the loss of A1 during T cell development and forced expression of Bcl-2 but not Bcl-xL is able to inhibit negative selection (Grillot et al., 1995; Mandal et al., 2005; Strasser et al., 1991). Thus, anti-apoptotic Bcl-2 family members appear to possess distinct functions through mechanisms not yet fully understood. Members of the multi-domain pro-apoptotic subgroup contain three BH domains (BH1-3) and includes Bax, Bad and Bok. Despite high structural similarity to the anti-apoptotic subgroup, these proteins are essential for intrinsic apoptotic cell death. Activation of Bax and Bak is associated with conformational changes that lead to homo-oligomerization. Gene-targeting experiments have demonstrated that Bax and Bak have largely redundant functions that are essential for apoptosis induction through the intrinsic pathway (Rathmell et al., 2002). The third and last group of the Bcl-2 family is the BH3-only pro-apoptotic subgroup and includes Bad, Bik, Hrk, Bid, Bim, Bmf, Bbc3 and Noxa. BH3-only proteins contain only the minimal BH3 domain and require Bax/Bak function to induce apoptosis (Zong et al., 2001). In healthy cells, different pro-apoptotic BH3 only proteins have been found to be sequestered by different anti-apoptotic Bcl-2 family members (Cheng et al., 2001; Willis et al., 2007) to prevent activation of Bax and/or Bak. Selective binding of BH3 only proteins to anti-apoptotic Bcl-2 family members is thought to contribute to the non-redundant functions of the latter (Chen et al., 2005). Various types of cellular stress can cause specific BH3 proteins to become activated after which they are believed to inactivate the protective function of the anti-apoptotic Bcl-2 family and facilitate Bax/Bax effector functions. This results in the loss of mitochondrial membrane potential, likely through the formation of supramolecular pores by Bax/Bak on the outer mitochondrial membrane (Fig. 1.5). As a consequence, Cytochrome-c is

released from the mitochondrial intermembrane space into the cytoplasm where it associates with Apaf-1 and pro-caspase-9 to assemble the 'apoptosome' protein complex, which triggers the activation of caspase-9 and thereby activates downstream effector caspases (Opferman, 2008). In addition to Cytochrome-c, other apoptosis augmenting mitochondrial proteins are released during this process including Smac/Diablo (Fig. 1.5), which upon entry into the cytoplasm binds to and inhibits the X chromosome-linked inhibitor of apoptosis protein (XIAP) (Du et al., 2000; Verhagen et al., 2000). XIAP is a potent inhibitor of effector caspases and acts to prevent unnecessary caspase activation in healthy cells (Chai et al., 2001; Deveraux et al., 1997; Riedl et al., 2001). Many questions remain regarding the mechanisms of Bcl-2 family member functions. For example, it is known that pro-apoptotic Bcl-2 family members can induce caspase activation in an apoptosome independent fashion during T cell development, suggesting that Bcl-2 family members have a broader function than is currently understood to control caspase activation (Marsden et al., 2002; Villunger et al., 2004).

The extrinsic apoptotic pathway

The extrinsic apoptotic pathway is induced by the ligation of death receptors of the tumor necrosis factor receptor super family such as CD95 and TNFR-1 (Opferman, 2008). Ligand engagement induces the recruitment of the death adaptor protein Fas-associated death domain (FADD) and procaspase-8 forming the death inducing signaling complex (DISC) (Chinnaiyan et al., 1995). Clustering of procaspase-8 facilitates its autocatalytic activation and release into the cytoplasm where it activates the common effector

caspases-3, -6 and -7 and thereby enroll the same machinery as the intrinsic pathway (Bao and Shi, 2007) (Fig. 1.5).

Caspase-8 is able to catalyze the activation of the BH3 only pro-apoptotic Bcl-2 family member Bid and thereby cooperate with the intrinsic apoptotic pathway (Yin et al., 1999). Reports have demonstrated that Bid mediated amplification of CD95 induced apoptosis signaling is necessary for death induction in certain cell types, leading to the classification cells into two types based on the requirement of Bid in CD95 mediated apoptosis (Scaffidi et al., 1998) (Fig. 1.5). In type I cells such as thymocytes, engagement of CD95 is accompanied by rapid caspase-3 activation that is not affected by the over-expression of Bcl-2 or loss of Bid. In type II cells such as hepatocytes, CD95 cross-linking is unable to induce caspase-3 activation without the help from the intrinsic apoptotic pathway mediated by Bid function. For many years little was known about how death receptor ligation could activate substantially different apoptotic pathways in different cell types. New evidence suggests that changes in XIAP expression in response to CD95 stimulation may be the discriminating factor between type I and type II cells (Jost et al., 2009). XIAP is present at comparable levels in healthy thymocytes and hepatocytes. Upon CD95 stimulation, XIAP expression declines in thymocytes while becoming dramatically upregulated in hepatocytes. Importantly, loss of XIAP function in hepatocytes results in a type I like behavior, such that CD95 stimulation is now able to activate caspase-3 in the absence of Bid (Jost et al., 2009). These results are consistent with a scenario where Bid mediated amplification of apoptosis signaling is required to overcome the caspase inhibition exerted by XIAP that is found exclusively in type II cells

following CD95 stimulation. In the apoptosis literature, thymocytes are considered prototypical type I cells (Jost et al., 2009). However, supporting evidence has only originated from experiments using total thymocytes. Thus it remains uncertain if smaller sub-populations, such as DN thymocytes, are true type I cells.

Regulation of survival during early T cell development and β-selection

During the early stages of T cell development, cell survival depends on cytokine mediated rather than TCR mediated signals. DN thymocytes deficient in IL-7 or IL-7Rα exhibit a survival defect that is restored in the presence of an exogenous source of Bcl-2, suggesting that IL-7 signaling suppresses apoptosis through the intrinsic pathway (Akashi et al., 1997; Maraskovsky et al., 1997; Peschon et al., 1994; von Freeden-Jeffry et al., 1997). Consistent with this notion, IL-7 signaling was found to induce the expression of both Bcl-2 and Mcl-1 in DN thymocytes (Fig. 1.6) (Opferman et al., 2003; von Freeden-Jeffry et al., 1997). However, only the phenotype of Mcl-1 deficient DN negative thymocytes mirror those deficient in IL-7 signaling, suggesting that Mcl-1 is the key physiological effector of IL-7 mediated survival during the cytokine dependent stage of DN thymocyte development (Opferman et al., 2003; Veis et al., 1993). DN3 thymocytes gradually down-regulate IL-7Rα expression and cell survival becomes contingent upon on the expression of a pre-TCR. A recent study demonstrated that BH3 only proteins, Bim and Bid, are highly expressed in pre-TCR deficient DN3 thymocytes and rapidly down-regulated upon pre-TCR signaling (Mandal et al., 2008). Moreover, the deletion of either Bim or Bid in $pT\alpha^{-/-}$ DN3 thymocytes suppresses cell death *in vivo* and *in vitro*,

indicating that both factors are physiological enforcers of the β-selection checkpoint (Fig. 1.6). Bcl2A1 is an anti-apoptotic member of the Bcl-2 family that is up-regulated upon pre-TCR signaling (Mandal et al., 2005). Unlike Bcl-2, Bcl-xL and Mcl-1, which carry a structural attribute that confers an anti-proliferative effect, induction of Bcl2A1 permits a robust proliferative burst following β-selection and is therefore an attractive mediator for pre-TCR mediated survival (Gonzalez et al., 2003; Mandal et al., 2005). However, reports demonstrating that siRNA mediated knock-down of Bcl2A1 had no apparent effect on T cell development renders the contributions of Bcl2A1 difficult to pin down (Mandal et al., 2005; Oberdoerffer et al., 2005). In addition to regulators of the intrinsic apoptotic pathway, the extrinsic apoptotic signaling pathway contributes significantly to life/death decisions in DN thymocytes. Transgenic expression of a dominant negative form of FADD (FADD-DN) is sufficient to override the requirement of a pre-TCR and drive differentiation of *Rag1*$^{-/-}$ DN thymocytes into the DP stage (Newton et al., 2000). Thus, the intrinsic and the extrinsic apoptotic pathways likely cooperate to regulate thymocyte survival during β-selection (Fig. 1.6).

Death by neglect

The objective of repertoire selection requires that survival of DP thymocytes rely solely on appropriate signaling through the αβ TCR. As previously discussed, thymocytes enter the DP stage as large proliferating cells and subsequently differentiate into a small and quiescent phenotype upon the initiation of *Tcrα* recombination (Egerton et al., 1990; Penit et al., 1995; Petrie et al., 1995; Shortman et al., 1990). Death by neglect represents

the spontaneous death of unsignaled DP thymocytes that takes place through the intrinsic apoptotic pathway and makes sure that only DP thymocytes with a potentially useful αβ-TCR are granted continued survival. In addition to being the only thymocyte compartment that does not express surface IL-7Rα, pre-selection DP thymocytes also uniquely express high levels of the suppressor of cytokine signaling (SOCS)-1 (Yu et al., 2006). The result is a complete absence of IL-7 signaling and down-regulation of the trophic factor glucose transporter-1 (Glut-1) and the anti-apoptotic factor Bcl-2 in pre-selection DP thymocytes. The net effect of these events is a drop in glucose metabolism and cell volume, and increased sensitivity towards death by neglect (Rathmell et al., 2001; Rathmell et al., 2000; Yu et al., 2003). To counteract premature death by neglect, expression of the critical survival factor Bcl-xL is greatly up-regulated in the pre-selection DP subset during T cell development (Grillot et al., 1995; Ma et al., 1995; Mick et al., 2004) (Fig. 1.6). DP thymocytes lacking Bcl-xL exhibit premature apoptosis and a limited *Tcrα* repertoire that is skewed towards the use of 5' located *Jα* segments (Guo et al., 2002; Sun et al., 2000). The mechanism underlying the rapid up-regulation of Bcl-xL expression in DP thymocytes is thought to involve the actions of RORγt and TCF-1, two essential transcription factors that are up-regulated following β-selection.

More recently, loss of Mcl-1 in DP thymocytes has also been linked to increased spontaneous cell death, suggesting that Mcl-1 may act synergistically with Bcl-xL to promote survival in pre-selection DP thymocytes (Dzhagalov et al., 2008). Balancing the effects of Bcl-xL and Mcl-1 to ensure death by neglect are the pro-apoptotic Bim, Bax and Bak. Deletion of Bim as well as the simultaneous deletions of Bax and Bak

dramatically suppresses spontaneous death of DP thymocytes *in vitro* (Bouillet et al., 1999; Rathmell et al., 2002) (Fig. 1.6). Interestingly, while forced Bcl-2 expression and deletion of *Bim* perturbed caspase mediated death by neglect, deletion of *Apaf1* or *Casp9* did not, suggesting that Bcl-2 family members activate effector caspases in an apoptosome independent fashion (Marsden et al., 2002).

In addition to Bcl-xL regulation, both transcription factors are also required for ISP to DP thymocyte development. Forced expression of Bcl-2 or Bcl-xL cannot rescue decreased DP development in mice lacking either RORγt or TCF-1 (Ioannidis et al., 2001; Sun et al., 2000), and forced IL-7 signaling prevents pre-TCR mediated up-regulation of RORγt and TCF-1. Thus, RORγt and TCF-1 function as a barrier rendering entry into the DP stage temporally distinct from residual IL-7 signals, ensuring that a qualified αβ-TCR signal is the sole remaining cue for continued DP thymocyte survival until positive selection. Positive selection leads to down-regulation of Bcl-xL and the re-expression of IL-7Rα and Bcl-2, marking yet another transition in the mode of survival regulation during T cell development.

Negative selection

Central tolerance of the T cell repertoire is imposed by negative selection induced apoptosis in the thymic medulla. Results demonstrating that deletion of Fas or TRAIL, and loss of FADD or caspase-8 function did not perturb negative selection *in vivo* make clear that the extrinsic apoptotic pathway does not play an essential role in this process (Salmena et al., 2003; Sidman et al., 1992; Smith et al., 1996; Yue et al., 2005). In

contrast, the requirement for intrinsic apoptotic signaling during thymocyte negative selection has been firmly established. *Bim*$^{-/-}$ thymocytes have profoundly perturbed negative selection and are resistant to anti-CD3 induced apoptosis both *in vitro* and *in vivo* (Bouillet et al., 1999; Villunger et al., 2004). The pro-apoptotic Bak and Bax are required to mediate the function of Bim and thymocytes doubly deleted for Bak and Bax display similar defects to *Bim*$^{-/-}$ thymocytes (Rathmell et al., 2002) (Fig. 1.6). The orphan steroid receptor Nur77 and the related Nur77 family member Nor-1 become highly expressed in post-selection thymocytes following a strong αβ-TCR signal (Woronicz et al., 1994). Expression of a dominant negative Nur77, that inactivates both Nur77-family members, impairs negative selection, consistent with a requirement of Nur77 and Nor-1 for negative selection (Cheng et al., 1997). It has been reported that Nur77 may facilitate negative selection in part by associating with Bcl-2 upon αβ-TCR stimulation to induce a conformational change converting Bcl-2 from an anti-apoptotic into a pro-apoptotic molecule (Lin et al., 2004). However, further work is required to establish this proposed mechanism for Nur77. Negative selection is caspase dependent as thymocytes that are doubly deficient for caspase-3 and -7 are resistant to αβ-TCR mediated apoptosis. However, it is unclear how the pro-apoptotic Bcl-2 family members mediate effector caspase activation as negative selection, like death by neglect, is not perturbed in thymocytes doubly deficient in *Apaf1* and *Casp9* (Villunger et al., 2004).

The life and death of a thymocyte must be precisely controlled for successful completion of T cell development and often rests on subtle differences in the level of TCR signaling. Aberrant regulation of apoptosis of developing T cells can lead to

autoimmunity, immunodeficiency and tumorigenesis. Thus, elucidation of the mechanisms that control cell survival during the different stages of T cell development is essential in our efforts to understand the generation of a diverse and self-tolerant T cell repertoire.

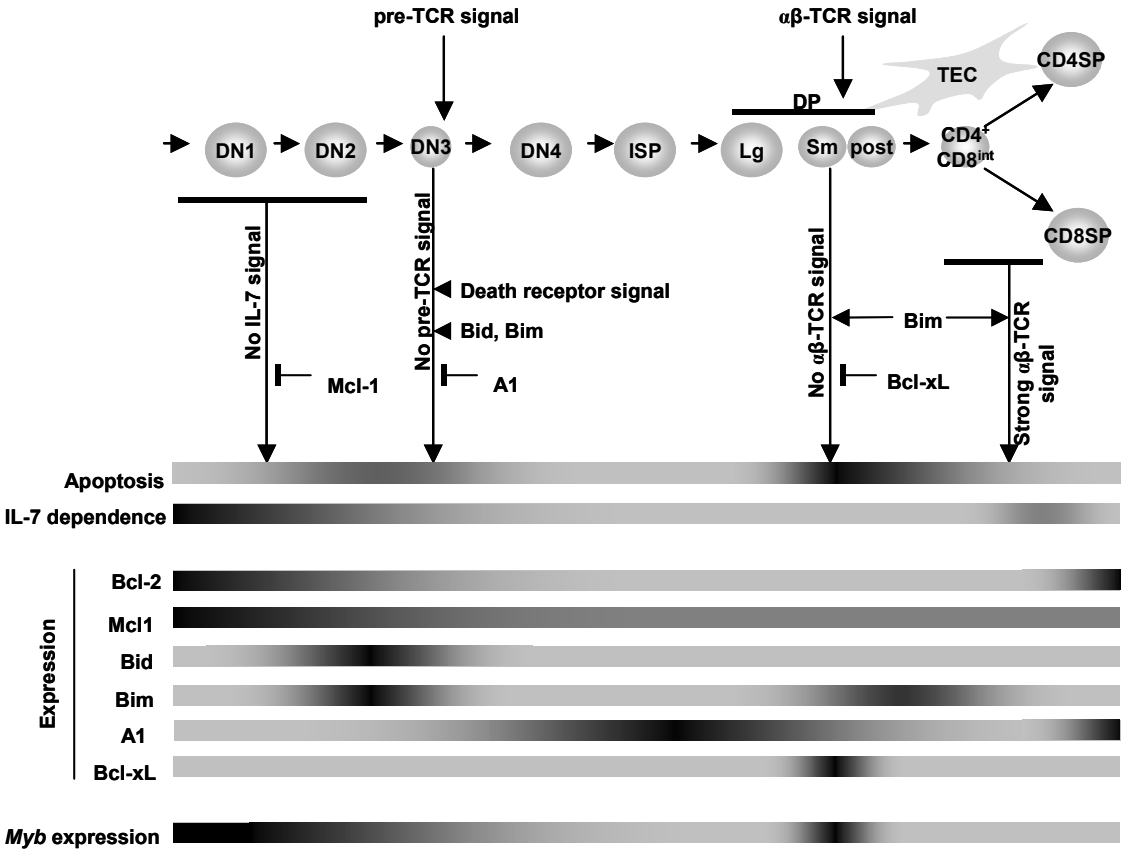

Figure 1.6 Apoptosis and survival during normal mouse T cell development. Thymocyte survival is regulated by different mechanisms involving both the intrinsic and the extrinsic apoptotic pathways during maturation. The survival during the DN1 and DN2 stages requires IL-7 signaling. Subsequent survival/apoptosis signals are predominantly dependent on the presence or absence of signals emanating from the pre-TCR and αβ-TCR as depicted. Bars indicate changes in apoptosis frequency, IL-7 dependency as well as the expression of relevant Bcl-2 family members and *Myb*.

1.3 c-Myb

The *Myb* proto-oncogene encodes the evolutionarily conserved transcription factor c-Myb, which can function to activate or repress transcription in a context dependent manner (Dai et al., 1996b; Nomura et al., 2004). *Myb* was originally identified as the cellular homologue of the transforming component in two avian retroviruses, AMV and E26, that cause leukemia in chickens (Lipsick and Wang, 1999). Compared to c-Myb, v-Myb contains N- and C-terminal truncations and point mutations which contribute to changes in protein activity and the oncogenic properties observed in v-Myb but not c-Myb (Lipsick and Wang, 1999). A large body of *in vitro* evidence implicates c-Myb in the regulation of developmental decisions affecting cell proliferation, differentiation and apoptosis in hematopoietic cells (Oh and Reddy, 1999). The embryonic lethality of $Myb^{-/-}$ mice on day E15 due to the severe anemia caused by failures of both erythroid and myeloid development further established its importance *in vivo* (Mucenski et al., 1991). In addition, aberrant over-expression of c-Myb has been linked with increased malignancy in several leukemias, colon and breast carcinomas. However, despite its discovery thirty years ago, we are only beginning to understand the physiological roles of c-Myb with the recent emergence of tissue specific deletion and hypomorphic mouse models (Carpinelli et al., 2004; Sandberg et al., 2005). To date, regulation and mechanism(s) of c-Myb function in normal development and oncogenesis remain poorly understood.

c-Myb expression

Myb expression is found in hematopoietic progenitors of all lineages, developing colonic crypts and breast epithelium. Expression decreases with increased level of cellular differentiation and forced *Myb* expression prevents terminal differentiation in cell lines of the erythroid, megakaryote and T lineages (Bender and Kuehl, 1987b; Duprey and Boettiger, 1985; Ess et al., 1999; Gonda et al., 1982; Sakamoto et al., 2006; Westin et al., 1982). *In vitro* evidence suggesting that c-Myb negatively regulates differentiation has found *in vivo* support in recent studies demonstrating that a differentiation block in a significant subset of human T cell acute lymphoblastic leukemia (T-ALL)s is caused by aberrant c-Myb expression and can be reversed upon c-Myb knock-down (Clappier et al., 2007; Lahortiga et al., 2007). The need for c-Myb protein expression to be strictly defined during distinct stages of normal hematopoiesis is evident in that small changes in dosage can bring about dramatic consequences in progenitor differentiation potential. The presence of c-Myb is required for the development of each hematopoietic lineage and suboptimal levels of c-Myb fail to support erythropoiesis and lymphopoiesis *in vivo*, but favored the differentiation of macrophages, megakaryocytes and the expansion of hematopoietic stem cells (HSC) (Emambokus et al., 2003; Garcia et al., 2009; Lu et al., 2008; Mukai et al., 2006). In addition, over-expression of c-Myb in a $Myb^{-/-}$ hematopoietic stem cell line prevented the terminal differentiation of erythrocytes and megakaryocytes and abolished B-lymphocyte development (Sakamoto et al., 2006). Collectively these findings demonstrate that precise control of c-Myb expression is crucial for cellular differentiation and lineage decision during hematopoiesis.

During normal hematopoiesis, c-Myb expression is strictly regulated at the level of transcriptional elongation, translation, and protein stability. Transcription of the full length *Myb* mRNA requires that RNA polymerase II overcome an attenuation sequence in the first intron of the *Myb* locus (Bender and Kuehl, 1987a; Yuan, 2000). This regulatory mechanism is commonly circumvented by a mutation in the attenuation sequence in human colon cancers (Hugo et al., 2006) and oestrogen receptor-α signaling in breast cancers (Drabsch et al., 2007). Proposed up-stream transcriptional regulators of *Myb* mRNA expression include NFkB (Toth et al., 1995), E2F (Sala et al., 1994), Ets-1 (Sullivan et al., 1997) and WT-1 (McCann et al., 1995), none of which have been confirmed *in vivo*. c-Myb expression is also regulated at the post-transcriptional level by several micro RNAs (Lu et al., 2008; Xiao et al., 2007; Zhao et al., 2009). Most notable is miR-150, which has been shown through loss and gain of function studies to significantly modulate c-Myb expression in developing lymphocytes and megakaryotes *in vivo* (Lu et al., 2008; Xiao et al., 2007). This control mechanism of c-Myb expression has also been shown to be frequently circumvented in breast, head and neck malignancies by mutations in the *Myb* 3' UTR containing conserved micro RNA target sites (Persson et al., 2009). Lastly, c-Myb expression is regulated at the post-translational level as reflected in its short half-life (< 60 min) (Bies and Wolff, 1997; Luscher and Eisenman, 1988). Phosphorylation, sumoylation and ubiquitylation have been reported to regulate c-Myb protein stability in a proteasome dependent fashion *in vitro* (Bies et al., 2002; Bies and Wolff, 1997; Kanei-Ishii et al., 2004). However, the regulation of c-Myb protein stability *in vivo* remains poorly studied.

MYB family of transcription factors

The discovery of c-Myb (*Myb)* paved the way for the discovery of two closely related transcription factors, A-MYB (*Mybl1*) and B-MYB (*Mybl2*). *Mybl1* expression is restricted to germinal center B-lymphocytes, spermatogenic tissue, the central nervous system and developing epithelium while *Mybl*2 is ubiquitously expressed in all replicating cells and is required for S-phase progression of the cell cycle. Possessing nearly identical DNA binding domains and similar overall structures, all MYB family members activate the same reporter gene constructs in transient co-transfection assays. However, despite overlapping expression, the three *Myb* proteins have distinct biological functions as illustrated by the different phenotypes of null mutations in mice. *Mybl2*$^{-/-}$ mice suffer early pre-implantation embryonic lethality around E4.5 to E6.5 (Tanaka et al., 1999) compared to the late embryonic lethality of *Myb*$^{-/-}$ mice on E15 (Mucenski et al., 1991), while *Mybl1*$^{-/-}$ mice are viable with defects in spermatogenesis and mammary gland development (Toscani et al., 1997). In addition, mRNA expression microarrays have demonstrated that ectopic expression of each protein activates distinct sets of human genes (Ness, 2003). Furthermore, the profile of genes that are activated by each protein is cell line specific, suggesting that MYB transcription factors are subject to context-dependent regulatory mechanisms.

c-Myb structure and function

c-Myb is a 75 kDa transcription factor that interacts with DNA, histones, co-activators and repressors to regulate transcription in a context dependent fashion. The 75 kDa c-Myb protein contains 636 amino acids and three major functional domains; an amino-terminal DNA-binding domain (DBD), an acidic transactivation domain (TAD) and a carboxyl-terminal negative regulatory domain (NRD) (Sakura et al., 1989) (Fig. 1.7). Alternatively spliced isoforms of c-Myb have been identified, including a highly conserved 89kDa isoform wherein an additional exon is inserted between the TAD and NRD (Woo et al., 1998). However, little physiological relevance has been attached t o this minor isoform to date.

The DBD consists of three consecutive helix-turn-helix motif repeats conserved through eukaryote evolution from humans to slime molds (Lipsick, 1996). NMR studies established the conformation of the DBD, which fits into the DNA major groove and mediates specific binding to the Myb response element (MRE) (PyAACG/TG) (Biedenkapp et al., 1988; Tahirov et al., 2002). Structural and biochemical studies demonstrate that the DBD also mediates interactions with several proteins including the CCAAT enhancer binding protein (C/EBPb) (Tahirov et al., 2002). This interaction was found to trans-activate a set of myeloid differentiation genes *in vitro*, possibly through recruitment of the SWI/SNF chromatin-remodeling complex (Kowenz-Leutz and Leutz 1999; Pedersen et al. 2001). Additionally, each of the DBD repeats carries the architectural signature of the chromatin-binding SANT domain found in a number of chromatin-regulating proteins (e.g., the Swi3, Ada2, TFIIIB, NcoR, and ISWI proteins)

(Aasland et al. 1996). Indeed, the DBD was found to interact with the N-terminal tail of histone H3 positioning K18 and K23 for acetylation in chicken bone marrow cells (Mo et al., 2005). Both histone tail binding and acetylation were prerequisites for the expression of myeloid c-Myb target genes, suggesting that c-Myb promotes tissue differentiation through modifying chromatin conformation. Perhaps the best characterized of these targets is the chicken *Mim1* gene, which is active in immature myeloid cells, where its activation requires c-Myb and C/EBPβ dependent chromatin opening of the promoter region (Plachetka et al., 2008). Interestingly, v-Myb lacks the ability to interact with C/EBPβ and histone H3 and to activate the endogenous, chromatin-embedded *Mim1* gene, suggesting that v-Myb is devoid of protein interactions that promote normal differentiation and possibly prevent tumorogenesis (Mo et al., 2005). More recently, the c-Myb DBD was found to mediate association with another transcriptional co-activator FLASH and co-localize with active RNA polymerase II transcription foci (Alm-Kristiansen et al., 2008). These findings highlight the multifaceted roles of the c-Myb DBD in conferring DNA sequence specificity, protein-protein interactions and chromatin organization.

The acidic TAD was initially identified as a 50-residue polypeptide fragment in v-Myb that is minimally required for transactivation (Bortner and Ostrowski, 1991; Weston and Bishop, 1989). The most important function of the TAD identified to date is its association with the histone acetyl transferase p300 (Dai et al., 1996a; Oelgeschlager et al., 1996). The structure of this complex was solved by NMR studies (Zor et al., 2004) and mice homozygous for a point-mutation $Myb^{M303V/M303V}$ that disrupts this complex

exhibit severe thrombocytosis, megakaryocytosis, anemia, lymphopenia, and the absence of eosinophils (Sandberg et al., 2005). The viable phenotype of *Myb*$^{M303V/M303V}$ mice as opposed to the embryonic lethal phenotype of *Myb*$^{-/-}$ mice suggests that c-Myb regulates hematopoiesis through both p300 dependent and independent mechanisms.

Further C-terminal is the loosely defined NRD, which includes a leucine zipper motif and a conserved EVES motif. C-terminal deletions correlates with increased c-Myb DNA binding, transcription transactivation and transforming activities (Gonda et al., 1989). This negative regulatory role is consistent with v-Myb lacking a large C-terminal portion of the NRD (Klempnauer et al., 1982) and has been postulated to be the combined function of several structural attributes including auto-inhibition (Nomura et al., 1993), and co-repressor recruitment (Nomura et al., 2004). Moreover, the NRD is heavily targeted by post-translational modifications including phosphorylation (Aziz et al., 1995), acetylation (Sano and Ishii, 2001), ubiquitylation (Bies and Wolff, 1997) and sumoylation (Bies et al., 2002). These modifications have been linked to changes in transcription activity and protein stability. However, a majority of these findings were made from deletion and mutation studies in transformed cell lines where the readout of c-Myb activity was typically artificial DNA binding and promoter reporter assays. To date, little is known about the physiological relevance of these structural features. Thus, despite the identification of multiple post-translational modifications, the lack of an *in vivo* model system to study c-Myb function greatly impeded our understanding of the physiological relevance of the structural attributes of c-Myb. Nonetheless, these studies did serve to highlight the important functional differences between c-Myb and v-Myb

reflected in the difference in their transforming potential. This notion was strengthened by mRNA microarray experiments showing that each of the mutations that distinguish v-Myb from c-Myb, including the N- and C-terminal truncations, and point mutations in the DBD and TAD affected the expression of different sets of target genes in human cell lines (Liu et al., 2006). Thus v-Myb appears to be more than just a de-repressed version of c-Myb but possesses unique activities that contribute to its transforming potential.

More recently, three *Myb* hypomorphs identified by ENU (ethylnitrosourea) mutagenesis screens were described, $Myb^{PLT3/PLT3}$, $Myb^{M303V/M303V}$ *and* $Myb^{PLT4/PLT4}$, each harboring a missense mutation in one of the three major domains DBD, TAD and NRD respectively (Fig. 1.7) (Carpinelli et al., 2004; Sandberg et al., 2005). Analysis of hematopoietic phenotypes in all three strains yielded the consensus that decreased c-Myb activity, much like suboptimal c-Myb expression, favor megakaryopoiesis and the expansion of HSC but severely impair the generation of lymphoid and erythroid cells. These *in vivo* results collectively suggest that the integrity of all three functional domains is required for c-Myb function in hematopoiesis. To date, around two-dozen c-Myb target genes have been validated by chromatin immunoprecipitation (ChIP) studies in various cell types, predominantly transformed cell lines derived from chicken, human and mouse. These include *Rag2* (Wang et al., 2000), *Ada*, *Mat2a, c-Myc* (Berge et al., 2007), *Bcl2, Ppp3ca, Cd53* (Lang et al., 2005), *Ca1* (Chen et al., 2006), *Gata3* (Maurice et al., 2007), chicken *Mim1* and *Lysozyme* (Mo et al., 2005) all of which play important roles in the regulation of differentiation, proliferation and survival. However, the identification

of these c-Myb targets was not based on *in vivo* functions of c-Myb and provides little insight into how c-Myb controls hematopoiesis.

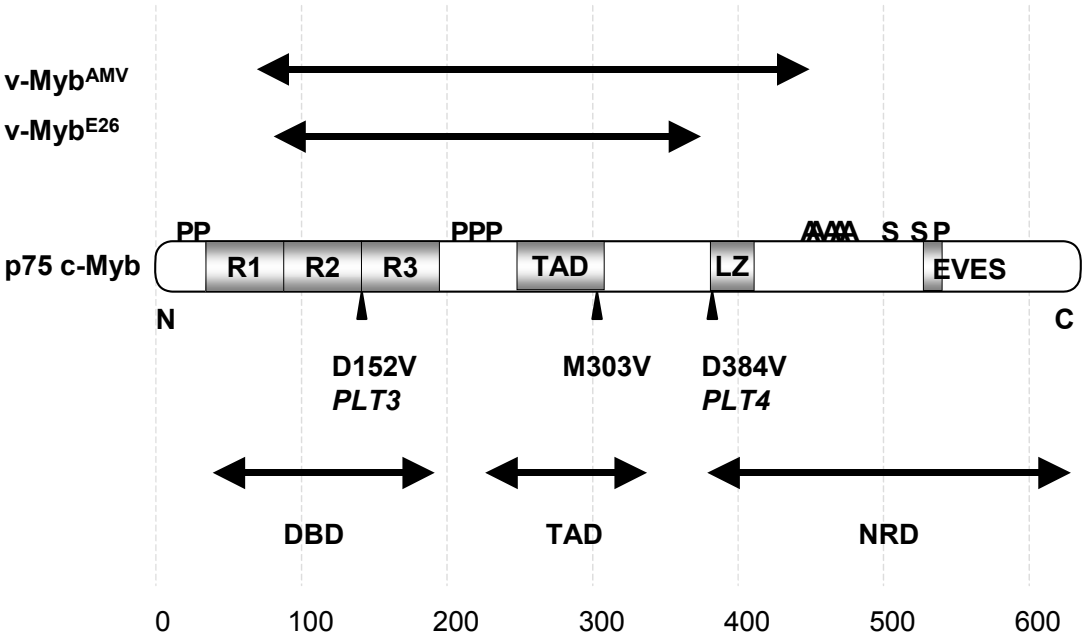

Figure 1.7 c-Myb protein structure. Diagram of the R1, R2, R3, regions of the DNA-binding domain (DBD), transcription activation domain (TAD), negative regulatory domain (NRD), leucine zipper motif (LZ), and the EVES motif. Known sites of post-translational modifications are indicated as P (phosphorylation), A (acetylation), and S (sumoylation). Dotted lines indicate amino acid residue number. Corresponding regions included in AMV and E26 v-Myb are indicated and mutations found in existing hypomorphic *Myb* alleles are annotated.

c-Myb and T cell development

During T cell development, *Myb* transcripts are most abundant in cortical thymocytes and expression decreases upon positive selection in the late DP stage (Ess et al., 1999; Hoffmann et al., 2003; Maurice et al., 2007; Mick et al., 2004). A physiological role for c-Myb in T cell development was first demonstrated by our laboratory in collaboration with Dr Gerald Siu (Amgen, Thousand Oaks, CA), using homozygous null c-*Myb/Rag1* (*Rag1*$^{-/-}$ ↔ c-*Myb*$^{-/-}$) chimeric mice (Allen et al., 1999). Thymocytes that originated from *Myb*$^{-/-}$ ES cells were blocked prior to initiation of V(D)J recombination and definitive T and B lineage commitment, suggesting that c-Myb is essential for early lymphopoiesis. However, this early developmental block precluded the elucidation of c-Myb function during later stages of T cell development. Some clues originated from forced expression of a dominant interfering protein MEnT *in vivo* (Badiani et al., 1994), which resulted in failure to enter cell cycle following β-selection (Pearson and Weston, 2000) and decreased survival of DP thymocytes (Taylor et al., 1996). However, ascribing the effects of MEnT specifically to c-Myb function was problematic since MEnT does not distinguish between the three MYB family members and likely interferes with both c-Myb and B-MYB in thymocytes. More recently, a partial block in DN3 to DN4 transition and a decrease in the DP thymocyte compartment were described again, this time in mice homozygous for the hypomorphic *Myb*^{M303V} allele (Sandberg et al., 2005). However, a caveat in this study was the lack of stage specific inactivation of c-Myb function/expression such that defective T cell development in these models could be due to defects in HSC or early progenitor stages.

To better address the physiological roles of c-Myb protein in the later stages of lymphocyte development, our laboratory employed the Cre/loxP conditional mutagenesis system to achieve tissue specific deletion at the *Myb* locus in mice. Using this model, we have made clear that c-Myb function is crucial during multiple stages of T cell development (Bender et al., 2004). First, c-Myb is required for DN thymocytes to transition into the DP stage, in part but not exclusively by to promoting efficient V(D)J recombination at the *Tcrβ* locus. Second, c-Myb is required for DP thymocyte survival in a *Tcrα* independent fashion. A survival defect in c-Myb deficient DP thymocytes has previously been attributed to decreased *Bcl2* transcription (Taylor et al., 1996). However, this scenario is unlikely as Bcl-2 is neither expressed nor required for DP thymocyte survival, and several groups including ours failed to detect significantly decreased amounts of Bcl-2 expression (Bender et al., 2004; Lieu et al., 2004). Thus, the mechanism underpinning the pro-survival role of c-Myb in DP thymocytes remains unclear. Finally, c-Myb is required for the efficient development of DP thymocytes towards the CD4SP lineage. Expression of the OT-II tg encoding a rearranged αβ-TCR specific for a class II MHC restricted OVA peptide cannot restore the CD4SP compartment in the absence of c-Myb (Bender et al., 2004). Since our initial observation, this finding has been confirmed by multiple laboratories (Lieu et al., 2004; Maurice et al., 2007), and implies that c-Myb plays multiple roles in regulating survival and differentiation within the DP stage. Several considerations for why the loss of c-Myb negatively affects CD4SP thymocyte development have been made. First, it is known that dysregulation of *Cd4* expression leads to the collapse of the normal, error-free lineage decision process (Locksley et al., 1993; Sarafova et al., 2009; Tyznik et al.,

2004), and c-Myb has been reported to both activate and repress *Cd4* gene expression in a context dependent manner (Allen et al., 2001; Siu et al., 1992). Although c-Myb deficiency does not dramatically affect *Cd4* expression in DP thymocytes and mature T cells *in vivo* (Bender et al., 2004), it is at present unclear if slight deviations in *Cd4* expression during T cell development might take place that contribute to the observed defect in CD4SP development. Second, it was recently reported that Gata3, a transcription factor important for CD4 lineage specification and Th-POK expression, is expressed at lower levels in c-Myb deficient post-selection DP thymocytes. c-Myb was found to bind to the *Gata3* promoter *in vivo*, consistent with *Gata3* being a direct target of c-Myb activity and thereby regulating CD4SP lineage development (Gallagher et al., 2005). However, the fact that c-Myb expression decreases while Gata3 expression increases following normal positive selection remains an unresolved discrepancy in this possible scenario. A major challenge facing the interpretation of the role of c-Myb in CD4SP development is that signals that dictate CD4/CD8 lineage decision is preceded by a severe *Tcrα* independent survival defect in c-Myb deficient DP thymocytes. This complicates the phenotype of post-selection DP and SP thymocytes lacking c-Myb. Hence, it will be important to elucidate the mechanism by which c-Myb promotes survival in DP thymocytes and deduce the contribution of c-Myb to CD4 lineage development without the secondary influence of impaired survival.

1.4 Thesis rationale

The thymic cortex consists largely of quiescent DP thymocytes that are in the process of *Vα-Jα* recombination at the *Tcrα* locus. At the time of this study, *Myb* mRNA was known to be abundantly expressed in cortical thymocytes while thymocytes in the medulla and peripheral T cells contained only about 10% as much *Myb* mRNA, suggesting that c-Myb may play an important role during the DP stage of thymopoiesis. Our laboratory had generated the first tractable genetic model to study c-Myb function *in vivo* using the Cre/loxP system in which tissue and stage specific deletion can be effectively achieved by crossing mice homozygous for the floxed Myb allele with different Cre expressing mouse strains. Initial studies using mice expressing an Lck-Cre tg mediating *Myb* deletion starting in the DN4 stage of T cell development clearly demonstrated that c-Myb plays multiple roles during DP to SP transition including the survival regulation of DP thymocytes and the ability of DP thymocytes to differentiate towards the CD4SP lineage. Further, our studies made clear that the observed survival defect is initiated prior to αβ-TCR engagement, severely confounding the interpretation of developmental events following αβ-TCR engagement. c-Myb has long been associated with pro-survival effects, most recently by our lab in pro-B cells and splenic B cells (Thomas et al., 2005). However, no *bona fide* down-stream mediator of c-Myb activity that is able restore survival in c-Myb deficient cells has been identified to date. The main purpose of this project was to elucidate the mechanism by which c-Myb promotes survival in pre-selection DP thymocytes.

Chapter II. Materials and Methods

2.1 Mice

Mice were weaned and genotyped by tail biopsy and polymerase chain reaction (PCR) at 3 weeks of age and used for experiments at 4-6 weeks of age. Mice with loxP sites flanking exon II of the *Myb* locus (Myb^{f}) were generated and as previously described (Bender et al., 2004) and listed in Table 2.1. $Myb^{f/f}$ mice were crossed with Cd4-Cre mice expressing the *Cre* recombinase under the control of the *Cd4* promoter/enhancer/silencer (obtained from Dr Christopher B. Wilson, University of Washington, Seattle, WA), which allows efficient expression of *Cre* as thymocytes enter the double positive stage (Lee et al., 2001). Presence of the Cd4-Cre transgene was assayed using generic PCR primers (Cre891 and Cre531) for *Cre*, which generate a fragment of 250 bp (Table 2.1). $Myb^{f/f}$ Cd4-Cre mice were crossed onto a $Tcr\alpha^{-/-}$ background (strain $Tcr\alpha^{tm1Mom}$, Jackson Labs, Bar Harbor, ME) to assess c-Myb function independently of αβ-TCR expression. *Tcrα* genotyping was performed using primers that detect intact endogenous *Tcrα* (imr0733 and imr0734) generating a product 164 bp as well as primers for the Neo cassette (imr0013 and imr0014) in the same PCR reaction generating an additional product of 280 bp when a *Tcrα* allele is inactivated. Finally, both $Myb^{f/f}$ Cd4-Cre mice and $Myb^{f/f}$ Cd4-Cre $Tcr\alpha^{-/-}$ mice were crossed with mice that express a Bcl-2tg (strain Bcl-2-25) under the control of the Eμ enhancer directed to the T cell lineage (Strasser et al., 1991) (gift of Dr Ellen V. Rothenberg, California Institute of Technology, Pasadena, CA). Genotyping the Bcl-2tg was performed using primers specific for the transgene

(IMR0550 and IMR0551) generating a product of 170 bp when transgene is present and primers for the endogenous *Il2* locus (IMR0042 and IMR0043) in the same PCR reaction generating a product of 324 bp as an internal control of the PCR reaction. All mice were maintained in accordance with the University of Virginia Animal Care and Use Committee guidelines. *Tcf1*$^{-/-}$ (Verbeek et al., 1995) and *RORγ*$^{-/-}$ mice (Sun et al., 2000) were gifts of Dr Zouming Sun, Beckman Research Institute of the City of Hope, Duarte, CA, and not maintained at the University of Virginia.

Tail biopsies for genotyping were digested in 500 µl tail lysis buffer [100 mM Tris-HCl pH 8.5, 5 mM EDTA pH 8, 200 mM NaCl, 0.2% SDS, 200 µg/ml proteinase K (Roche, Indianapolis, IN)] 55^{o}C over-night. Tissue debris was cleared by centriguation at 20000 RCF for 5 minutes at room temperature. DNA was precipitated with 500 µl isopropanol and washed once in 70% ethanol. DNA pellets were air dried and resuspended in 200 µl H_2O. 2 µl of DNA prep was used for each 25 µl genotyping PCR reaction. PCR reactions were performed using Apex Taq DNA Polymerase (Genessee Scientific, San Diego, CA) and run on a DNA engine Peltier Thermal Cycler (MJ research; Waltham, MA).

DNA extraction for Cd4-Cre mediated *Myb*$^{f/f}$ deletion efficiency analysis was performed by lysing electronically sorted thymocyte and splenocyte populations in 200 µl TSE lysis buffer (10 mM Tris, 150 mM NaCl, 10 mM EDTA, 0.2% SDS, 600 µg/ml proteinase K) followed by incubation at 55^{o}C over-night. DNA was precipitated using 200 µl of isopropanol in the presence of 1 µl glycogen and washed once in 70% ethanol. DNA was resuspended in H_2O and used for *Myb* genotyping PCR.

Table 2.1 Genotyping primers

Primer	Primer Sequence (5' to 3')	Cycling Conditions
N2	GCATGCCTCTGGAAAGTACCTTAAAC	94 °C 4 min, 30x(94 °C 1 min, 58 °C 1 min, 72°C 1 min), 72 °C 6 min, 4 °C soak.
N4	GTCTAGGAGCAAAGTTCTAACAGC	
N6	CAGACAGACAGAACGTGCATTC	
Cre531	CGATGCAACGAGTGATGAGG	94 °C 4 min, 30x(94 °C 1 min, 58 °C 1 min, 72°C 1 min), 72 °C 6 min, 4 °C soak.
Cre819	GCATTGCTGTCACTTGGTCCT	
Tcrα imr0733	ACTGTGCTGGACATGAAAGC	94 °C 3 min, 12x(94 °C 30 sec, 64 °C 30 sec*, 72°C 45 sec), 25x(94 °C 30 sec, 58 °C 30 sec, 72°C 45 sec), 72 °C 2 min, 4 °C soak. *-0.5°C per cycle
Tcrα imr0734	CCATAGATTTGAGCCAGGAGG	
Neo imr0013	CTTGGGTGGAGAGGCTATTC	
Neo imr0014	AGGTGAGATGACAGGAGATC	
Il2 Imr0042	CTAGGCCACAGAATTGAAAGATCT	94 °C 3 min, 35x(94 °C 30 sec, 54 °C 30 sec, 72°C 45 sec), 72 °C 2 min, 4 °C soak
Il2 Imr0043	GTAGGTGGAAATTCTAGCATCATCC	
Bcl2 imr0550	TGGATCCAGGATAACGGAGG	
Bcl2 imr0551	TGTTGACTTCACTTGTGGCC	

2.2 Flow cytometry and cell sorting assays

Isolation of single thymocyte suspension

Thymi were carefully removed and mashed through a 100 μm cell strainer (BD Scientific, San Jose, CA) into 10 ml ice cold DMEM harvest medium (DMEM supplemented with 5% FBS, 100 U /ml penicillin-streptomycin and 2 mM L-glutamine (Invitrogen / Gibco, Carlsbad, CA). Cells were pelleted at 700 RCF for 5 minutes at 4^{o}C (subsequent centrifugations were performed similarly) and viable cell count was determined by trypan blue exclusion on a hemacytometer.

Flow cytometry and fluorescence activated cell sorting (FACS)

$2x10^{6}$ cells were usually stained in 50 μl ice cold PBA [1x Phosphate Buffered Saline (PBS) (Invitrogen/Gibco), 0.01% NaN_3 and 0.5% Bovine Serum Albumin (BSA) (Roche)] using antibody concentrations indicated in Table 2.2 for 15 minutes on ice in the dark and washed once with ice cold PBA. Cells were then resuspended in 300 μl of PBA containing 1 μg/ml of the DNA dye 7-aminoactinomycin D (7AAD) (Invitrogen, Carlsbad, CA) and analyzed on a two laser FACSCalibur or Becton Dickinson FACSVantage SE Turbo Sorter with DIVA Option (BD Biosciences, San Jose, CA). Electronic cell sorting was done on a Becton Dickinson FACSVantage SE Turbo Sorter with DIVA Option. Data was analyzed using FlowJo (Tree Star) software.

Table 2.2 Flow cytometry antibodies

Antibody/Reagent	Clone	Dilution	Source
anti-CD4-APC	CT-CD4	1:100	Caltag (Burlingame, CA)
anti-CD8 APC-Alexa750	5H10	1:200	Caltag
anti-CD25 PE	PC61 5.3	1:100	Caltag
anti-CD44 FITC	1M7	1:100	eBioscience (San Diego, CA)
anti-CD53 (Rat IgM)	OX-79	1:100	BD Bioscience
anti-CD69 PE	H1.2F3	1:100	eBioscience
anti-CD90.2 PE	5a-853	1:800	eBioscience
anti-Tcrβ FITC	H57-597	1:75	eBioscience
anti-cKit APC	2B8	1:50	eBioscience
anti-CXCR4	2B11	1:200	eBioscience
Anti Rat IgM PE	HIS40	1:100	eBioscience
anti-Bcl-xL	54H6	1:50	Cell Signaling Technology (Beverly, MA)
anti-CCR7-APC	4B12	1:200	R&D Systems (Minneapolis, MN)
F(ab') Fragment Goat-anti-rabbit-IgG (H+L)-APC		1:400	Jackson ImmunoResearch (West Grove, PA)

Intracellular staining of Bcl-xL

Intracellular staining with anti-Bcl-xL (Cell Signaling) was performed according to manufacturer's recommendations. Briefly, 10^7 thymocytes per test sample were fixed with 2 % molecular grade formaldehyde (Invitrogen) in PBS at 37^{o}C for 10 minutes and washed twice in PBA. Subsequently, cells were permeabilized with 500 µl 90% ice cold methanol on ice for 30 minutes and washed twice with PBA. Cells were rehydrated in 100 µl PBA at room temperature for 10 minutes and separated into two tubes, one for anti-Bcl-xL staining and one for a secondary antibody alone staining control. Cells were incubated with rabbit anti-Bcl-xL or no antibody for 1 hr at room temperature and washed twice in PBA. Anti-CD8-FITC, anti-CD4-PE and the F(ab') Fragment Goat-anti-rabbit-IgG (H+L)-APC secondary antibody were incubated with test samples and secondary antibody alone staining controls for 30 minutes at room temperature in the dark. Cells were washed twice in PBS and analyzed for flow cytometry.

Measurement of Apoptotic Cell Death and DNA content

Annexin V staining was performed using the Annexin V-FITC or PE apoptosis detection kit (BD Biosciences, San Diego, CA) and according to manufacturer's recommendations. Briefly, cells were surface stained as usual and resuspended in 40 µl 1X Annexin V binding buffer and 2 µl Annexin V FITC or PE. Cells were incubated at room temperature for 30 minutes in the dark and analyzed for flow cytometry after the addition

of 260 µl 1X Annexin V Binding Buffer and 1 µg/ml 7AAD (Molecular probes). Live cells were defined as those negative for both Annexin V and 7AAD.

Detection of intracellular caspase 3 activation was performed using PE Active Caspase-3 Apoptosis Kit (BD Biosciences, San Jose, CA) per manufacturer's protocol. Briefly, thymocytes were surface stained for expression of CD4 and CD8, fixed and permeabilized using the Cytofix/Cytoperm kit (BD Pharmingen, San Diego, CA) per manufacturer's recommendations. Thymocytes were incubated with 25 µl BD Perm/Wash solution and 5µl anti-active caspase-3-PE per test sample for 30 minutes at room temperature in the dark. The cells were washed once with BD Perm/Wash solution, and resuspended in 300 µl PBA for flow cytometry analysis.

DNA fragmentation was measured by terminal dUTP labeling, using the *In Situ* Cell Death Detection Kit, TMR red (Roche) per manufacturer's protocol. Cells were surface stained as usual, fixed and permeabilized using the Cytofix/Cytoperm kit (BD Pharmingen) and resuspended in 25 µl of TMR red Tdt-incorporation solution. The cells were incubated for 1 hour at 37^{o}C, washed once in BD Perm/Wash solution and resuspended in PBA for flow cytometry analysis.

DNA content was analyzed using Draq5 (Alexis Biochemcials, Leicestershire, UK) per manufacturer's recommendations. Briefly, cells were surface stained as usual and resuspended in 300 µl of PBA with 5 µl of Draq5 and incubated at 37^{o}C for 20 minutes prior to flow cytometry analysis.

Magnet activated cell sorting (MACS)

Tcrα$^{-/-}$ thymocytes were depleted or selected for DP cells for RNA extraction and thymocyte cultures respectively by first resuspending $\leq 10^8$ toal thymocytes in 300 µl ice cold MACS buffer (PBS, 0.5% BSA with 2 mM EDTA filtered through a 0.2 µm filter and degassed). For positive selection of *Tcrα*$^{-/-}$ DP thymocytes, 100 µl CD4 MACS MicroBeads were added to thymocytes and incubated at 4^{o}C for 15 minutes. For negative selection, 50 µl of both MACS CD4 and CD8 MicroBeads were added to thymocytes and incubated as above. After bead incubation, thymocytes were washed with 10 ml of ice cold MACS buffer, resuspended in 1 ml of ice cold MACS buffer and selected over LS MACS columns per manufacturer's instructions. Briefly, columns were primed with 3 ml of MACS buffer and the cell suspensions were added without letting the columns run dry. Columns were washed with 3 x 3 ml of MACS buffer. For positive selection of *Tcrα*$^{-/-}$ DP thymocytes, columns were taken off the magnet and gently eluted using 5 mls of ice cold MACS buffer and the provided plunger. For negative selection to enrich for *Tcrα*$^{-/-}$ DN thymocytes, 10 ml of flow through were caught in a 15 ml conical tube. Cells were counted and pelleted as previously described.

2.3 Molecular biology

RNA extraction and reverse transcription (RT)

Thymocytes were lysed and homogenized over Qiashredder columns (Qiagen, Valencia, CA). Total RNA was extracted using the RNeasy Mini kit (Qiagen) including on-column DNase digestion (RNase-free DNase Set: Qiagen) following the manufacturer's recommendations. RNA was converted into cDNA using Superscript II First strand cDNA synthesis system with oligo(dT) primers (Invitrogen, Carlsbad, CA) following manufacturer's recommendations.

Quantitative real-time PCR (qPCR)

qPCR was performed using Titanium Taq DNA polymerase (Clonetech, Mountain View, CA) and 1× SYBR Green (Invitrogen) in an Opticon DNA engine (MJ research; Waltham, MA). qPCR conditions are as follows, 3 minutes at 95°C, followed by 40 cycles of 95°C for 40s, 66°C for 20s, and 72°C for 30s. After a final extension step (72°C for 1 min), melting curve analysis was executed. Primers sequences were designed using Primer3 software (http://primer3.sourceforge.net/) to have a melting temperature of around 64 ^{o}C and generate fragments of ~50-150 bp unless otherwise cited (Table 2.3 and 2.4). Relative signal was calculated using the $2^{-\Delta\Delta CT}$ method as previously described (Pfaffl, 2001). For mRNA expression assays, primers were designed to span two adjacent exons and cDNA levels were normalized to *Hprt1* expression.

Table 2.3 qRT-PCR Primers

Target gene	Orientation	Primer Sequence (5' to 3')
Myb	F	AACGAGCTGAAGGGACAGCA
	R	TGGCATGGTGTTCTCCCAAA
Bcl2l (Verschelde et al., 2006)	F	TACAGCATTGCGGAGGAAGTAGAC
	R	TTAGTTACACCGAACACTTGATTCTGG
Rorγ (Ivanov et al., 2006)	F	CCGCTGAGAGGGCTTCAC
	R	TGCAGGAGTAGGCCACATTACA
Tcf1 (Goux et al., 2005)	F	CGCTGCATAACAAGCC
	R	CCAGCTCACAGTATG GG
Ccnd3	F	GCGTCCCCACCCGAAAGGCG
	R	CCAGGAAGTCGTGCGCAATC
Gadd45b	F	GGGGGATTTTGCAATCTTCT
	R	CGGTGAGGCGATCCTGA
Gimap4	F	CGGGGTTCATCCCAGAAAGT
	R	CCCTGTTGAACTCTTTCCTGCT
Maf	F	GCAACGGCTTCCGAGAAAA
	R	GGAGTCCCTTGGGTACATGA
Fosl2	F	TCCCGGGAACTTTGACACCT
	R	GCGTTGATTGTGGGGATGAA
Socs3	F	AAGGCCGGAGATTTCGCTTC
	R	GGGAAACTTGCTGTGGGTGA
Sh2d1a	F	TGGAAGCTATCTGCTGCGAGAC
	R	CGGCACTCCAAGAACCTGTTT
Smarce1	F	TGCGGAAGCTGCATTAGAGG
	R	GCAGTGGCTGTGTGCTTCATT

Klf2	F	CGTGTTGGACTTCATCCTCTC
	R	CGGCTCCGGGTAGTAGAAG
Foxo1	F	CAAGGATAAGGGCGACAGCA
	R	TGGATTGAGCATCCACCAAG
Dtx1	F	ATGCATCAGTTCCGGCAAGA
	R	TCTCCCATTCCCACACGATG
Camk4	F	TATGCAACTCCAGCCCCTGA
	R	TAGGCACAGCCTCGGAGAAT
Gfi1	F	ACTTTTGGAGGCCCCCTTCT
	R	GGCTTGAAAGGCAGCGTGTA
Hprt1	F	TGCCGAGGATTTGGAAAAAGTG
	R	CACAGAGGGCCACAATGTG

mRNA expression microarray analysis

DP thymocytes from four *Myb*$^{f/w}$ Cd4-Cre *Tcrα*$^{-/-}$ and four *Myb*$^{f/f}$ Cd4-Cre *Tcrα*$^{-/-}$ mice were positively selected using MACS CD4 MicroBeads (Miltenyi Biotec, Auburn, CA) as previously described. Positive selection yielded populations of 91-99% purity as determined by flow cytometry. Total RNA (3-15 μg) was extracted and assessed for its integrity by analysis on an Agilent Bioanalyzer. Generation of double stranded cDNA and biotin-labeled cRNA was synthesized according to Affymetrix (Santa Clara, CA) recommendations. Biotin-labeled cRNA from each mouse was individually hybridized to Mouse Genome 430 2.0 (Affymetrix) Gene Chip for 16 h, and scanned with the Affymetrix Gene-Array Scanner as previously described (Gallagher et al., 2005). c-RNA

synthesis, hybridization and data collection were performed at the University of Virginia Gene Chip analysis Core Facility.

Pairwise analysis of control and mutant sample groups was performed using the GeneSifter microarray data analysis system (http://www.genesifter.net/) (VizX Labs LLC, Seattle, WA) to identify genes with statistically significant ($p<0.01$ Student's *t*-test) >2 fold change in expression within the Gene Ontology group GO:0043067:regulation of programmed cell death (Ashburner et al., 2000).

_Jα_ segment profiling

Total cellular RNA from electronically sorted DP thymocytes was subjected to reverse transcription. PCR amplified fragments using primers specific for the Vα3 and Cα gene segments (Table 2.4) were separated on a 1.5% agarose gel. The agarose gel was incubated for 30 minutes under gentle shaking in 0.4 M NaOH and immobilized to GeneScreen Plus hybridization membrane (PerkinElmer, Waltham, MA) over-night by capillary transfer. Membrane was baked for 1 hr at 80^{o}C and southern blotted for usage of the indicated *Jα* segments sequentially as previously described (Guo et al., 2002; Villey et al., 1996). Probes for southern blotting were previously described (Riegert and Gilfillan, 1999; Villey et al., 1996) (Table 2.4) and end labeled with [α-^{32}P]dATP (Perkin Elmer) using T4 polynucleotide kinase (New England Biolabs, Ipswich, MA) per manufacturer's instructions and cleaned up using G25 Microspin columns (GE Healthcare). Membranes were hybridized with the labeled probe in oligo hybridization solution (0.6 M NaCl, 10 mM NaH_2PO_4 H_2O, 1 mM ETDA, 5x Denhardt's solution and

1% SDS) for 4 hrs at 65°C with rotation and washed twice in wash buffer (0.6 M NaCl, 60 mM NaCitrate $2H_2O$, 0.1 % SDS) for 15 minutes at room temperature. Labeled membranes were exposed to Kodak Biomax MS films, stripped using boiling stripping buffer (0.6 M NaCl, 60 mM NaCitrate $2H_2O$, 0.5 % SDS) and subjected to hybridization with the next probe.

Table 2.4 *Jα* profile typing oligonucleotides

***Tcrα* segment**	**Oligo type**	**Sequence 5'-3'**	**Reference**
Va3	PCR	ACCCAGACAGAAGGCCTGGTCACT	(Levin et al., 1993)
Ca1	PCR	ACTGGGGTAGGTGGCGTTGGTCTCT	Villey, I 1996 Immunity 5:331
Ja58	Probe	AGACCCAGTGCCTTGCTGCA	(Villey et al., 1996)
Ja57	Probe	CGCAGACCCTCCTTGATTCA	(Villey et al., 1996)
Ja42	Probe	TGCATTGCTTCCTCCAGAAT	(Villey et al., 1996)
Ja39	Probe	GGCACCTGCATTATTATTCA	(Villey et al., 1996)
Ja32	Probe	GTTGCCACTGCTCCCATA	(Villey et al., 1996)
Ja31	Probe	CTGCGTCCCATCACCAAAGAAGAT	(Riegert and Gilfillan, 1999)
Ja12	Probe	GAGGCTATAAAGTGGTCTTTG	(Riegert and Gilfillan, 1999)
Ja2	Probe	ACCACTTAGTCCTCCAGTAT	(Villey et al., 1996)
Ca5	Probe	CAAAGTCGGTGAACAGGCAGAG	(Villey et al., 1996)

Retroviral constructs

pLitmus28-HA-c-Myb. The pLitmus28-FL-c-Myb expression vector contains N-terminally FLAG-tagged wildtype c-Myb cDNA. However, the FLAG-tag was not detectable on the expressed protein and was therefore replaced with a N-terminal triple HA-tag as follows. NdeI sites were added onto the 5' (4540-3920 bp) portion of mouse c-Myb by PCR amplification from the 5' ATG to the internal EcoR1 site using pLitmus28-FL-c-Myb as template. Forward: 5' CAT ATG GCC CGG AGA CCC CGA CAC AGC ATC TAC AGT A 3' Reverse: 5' CAT ATG CGT CTG GCT GGC TTT GGA AGG CTC CTG CAG 3'. The PCR product was subcloned into the PCR2.1-TOPO vector using the TOPO TA cloning kit (Invitrogen), and then sequenced. The NdeI flanked 623 bp fragment was cloned into the NdeI site of pEBB-triple-HA (Gift of Dr Kodi S. Ravichandran, University of Virginia, Charlottesville, VA), positioning a 5' triple HA-tag in frame of the c-Myb ATG. The BamH1-EcoR1 677 bp fragment containing the triple-HA tagged portion of c-Myb was then cloned back into the pLitmus28-FL-c-Myb plasmid BamH1-EcoR1, replacing the original FLAG-tagged 589 bp portion to create a complete pLitmus28-HA-c-Myb expression plasmid.

MIGR1-c-Myb. HA-c-Myb was subcloned from pLitmus28-HA-c-Myb into the BamHI/BglII site of the previously described pMIGR1 (Pear et al., 1998) (gift from Dr Warren S. Pear, University of Pennsylvania, Philadelphia, PA).

The MIGR1-Bcl-xL vector was a kind gift from Dr. Thomas J. Braciale (University of Virginia, Charlottesville, VA). The RetroMax packaging vector pCL-Eco was from Imgenex, San Diego, CA. Plasmids were amplified using OneShot Top10

competent cells (Invitrogen) and extracted using Qiagen Maxi prep kits (Qiagen, Valencia, CA).

2.4 Protein biochemistry

Table 2.5 Western blotting antibodies

Antibody	Clone	Band size	Dilution	Manufacturer
Anti-c-Myb	C 1-1	75 kDa	1:1000	Millipore (Bedford, MA)
Anti-Mcl-1	600-401-394	35 kDa	1:1000	Rockland (Gilbertsville, PA)
Anti-Tcf-1	C63D9	48, 50 kDa	1:1000	Cell signaling
Anti-RORγ		58 kDa	1:200	Gift of Dr Dan Littman, NYU, NY
Rabbit anti-Bcl-xL	54H6	30 kDa	1:1000	Cell Signaling Technology (Beverly, MA)
Mouse anti-βactin HRP	AC-15	42 kDa	1:20000	Sigma (St Louis, MO)
Anti Rabbit HRP			1:10000	GE Healthcare (Piscataway, NJ)
Anti Mouse HRP			1:10000	GE Healthcare (Piscataway, NJ)
Anti-armenian hamster HRP			1:5000	Santa Cruz Biotechnology (Santa Cruz, CA)

Western blotting

Electronically sorted DP thymocytes were lysed in (20 mM Tris, 7.4; 100 mM NaCl, 10 mM EDTA; 1 mM EGTA, 1% Triton X-100) (Emambokus et al., 2003) containing EDTA-free protease inhibitor cocktail (Roche) and 1 mM PMSF. Fifteen milligrams of

protein was fractionated on 10% SDS-polyacrylamide gels and transferred to Protran nitrocellulose transfer membranes (Whatman, Dassel, Gernmany). Membranes were blocked in PBS-T (PBS, 0.05% Tween-20) with 5% non-fat dry milk for 1 hr and incubated with the appropriate primary antibody over-night at 4°C in PBS-T at the concentrations listed in Table 2.5. Membranes were washed three times in PBS-T and probed wtih the appropriate secondary antibody in PBS-T for 1 h at room temperature (Table 2.5). Membranes were washed three times and proteins were detected by enhanced chemiluminescence (Amersham, Piscataway, NJ) on HyBlot CL film (Denville Scientific, Saint-Laurent, Canada).

Chromatin Immunoprecipitation (ChIP)

Preparation of chromatin. Thymocytes were harvested in ice cold DMEM harvesting medium, counted and pelleted at 340 RCF for 7 min at 4 degrees, and resuspend in cold PBS (Invitrogen/Gibco) at 10^7 cells per ml. Protein was crosslinked to chromatin by adding 1/10 volume of buffered formaldehyde [11% molecular grade formaldehyde (Invitrogen), 0.1 M NaCl, 1 mM EDTA, 0.5 mM EGTA, 50 mM Hepes pH8 (Invitrogen/Gibco)] and incubated on ice for 10 minutes with occational mixing. The reaction was stopped by the addition of 125 mM glycine followed by a 5-minute incubation at room temperature with rocking. Cells were pelleted at 700 RCF, washed once in ice cold PBS and subsequently resuspended in cold cytoplasmic lysis buffer [10 mM Tris-HCl pH8, 85 mM KCl, 0.5% NP40, 1 mM PMSF and EDTA-free protease inhibitor cocktail (Roche)] at 10^7 cells/ml and incubated on ice for 10 minutes. Nuclei

were pelleted at 1800 RPM for 5 minutes at 4°C and resuspended at 10^7 cells/ml in ice cold sonication buffer [10 mM Tris-HCl pH8, 0.1 mM EDTA, 1% NP40, 1 mM PMSF, EDTA-free protease inhibitor cocktail (Roche)]. Sonication was performed using the W-375 cell disruptor (Ultrasonics Inc, Plainview, NY) in 1 ml aliquots in eppendorf tubes that are placed on a chilled cold block. Sonicate thymocyte chromatin 15 x 10 1 second pulses at output 3, duty cycle 90. Cold block was re-chilled on ice every five minutes to keep samples cool throughout the sonication procedure. Sonication conditions were optimized to generate chromatin fragments 200-500 bp in size. Debris was cleared by centrifugation at max speed for 10 minutes at 4°C and chromatin prep was supplemented with 5% glycerol and 127 mM NaCl and snap-frozen using liquid N2 before storing at –80°C until ready for immunoprecipitation.

Immunoprecipitation. Chromatin was thawed on ice, supplemented with fresh PI and PMSF and cleared by centrifugation at max speed for 5 minutes at 4°C. Chromatin was transferred into new tubes and pre-cleared with 100 µl 50% protein A agarose/salmon sperm DNA slurry (Upstate #16-157) per 1 ml chromatin prep for 1 hour at 4 degrees with rotation. Non-specific binding to beads was pelleted by centrifugation at 900 RCF for 3 minutes at 4°C and pre-cleared chromatin was transferred into new tubes. 0.5 ml of chromatin was used per RNA Pol2 or AcH3 ChIP sample and 1 ml was used for per c-Myb ChIP sample. Chromatin was incubated with the appropriate amount of antibodies over-night with rotation at 4°C (Table 2.6). Immune complexes were collected with 100 ml of salmon sperm DNA/protein A agarose slurry for 1 hour with rotation at 4°C. Beads were pelleted at 3000 RPMs for 3 minutes at 4°C while

supernatants were saved as input controls. Beads were washed for 5 minutes with rotation at 4°C with low salt buffer (10 mM Tris-HCl pH8, 2 mM EDTA, 0.1% SDS, 1% NP40, 150 mM NaCl), high salt buffer (10 mM Tris-HCl pH8, 2 mM EDTA, 0.1% SDS, 1% NP40, 500 mM NaCl), LiCl buffer (10 mM Tris-HCl pH8, 1mM EDTA, 1% Deoxycholate, 1% NP40, 250 mM LiCl) and twice in TE (10mM Tris pH 7.4, 1mM EDTA). All wash buffers were ice cold and supplemented with protease inhibitors and PMSF. Bound complexes were eluted twice with 250 µl elution buffer (0.1 M, 1% SDS) at room temperature for 15 minutes with rotation. The two eluates from the same sample were combined and approximately 500 µl in volume.

Extraction of immunoprecipitated genomic DNA. Formaldehyde crosslinking of precipitated chromatin and chromatin input was reversed in the presence of 200 mM NaCl at 65°C overnight. Chromatin was treated with 200 µg/ml RNase A at 37°C for 30 minutes. Subsequently, protein was digested at 55°C for 1 hour by adding 40 mM Tris pH 6.5, 10 mM EDTA and 40 µg/ml Proteinase. DNA was phenol chloroform extracted and precipitated by adding 1 µl of glycogen, 277 mM nuclease free sodium acetate pH 5.5 (Ambion, Austin, TX) and 2 volumes of 100% ETOH at –20°C for 30 minutes. DNA was pelleted at max speed for 30 minutes at 4°C and washed twice with 500 µl 70% ETOH. DNA pellets were air-dried and generally resuspended in 70 µl H2O. 10 µl of 10% input DNA was separated by agarose gel electrophoresis to assess the efficacy of DNA shearing. Quantities of precipitated genomic DNA was determined by qPCR or conventional semi-quantitative PCR (Table 2.7). In both cases, Titanium Taq DNA polymerase (Clonetech) and 5 µl of precipitated DNA was used in each PCR reaction.

Table 2.6 ChIP Antibodies

Antibody	Clone	Amount	Source
Anti-c-Myb	EP769Y	3µg	Epitomics
RNA polymerse II	4H8	3µg	Abcam (Cambridge, MA)
Rabbit IgG		3µg	Santa Cruz Biotechnology

Table 2.7 ChIP PCR Primers

Primer ID	Primer Sequence (5' to 3')	Reference
Bcl2l1 1F	TTGGACACCGACATCGAAAG	
Bcl2l1 1R	CGCGTGGAACGTTTATGGTT	
Bcl2l1 2F	TCTCGATGCCAGTCCCTTT	
Bcl2l1 2R	GTTTTGCGGCTGGGAAGTAT	
Bcl2l1 3F	TCCTTCCAGAGAGGTCTAGG	
Bcl2l1 3R	TGGAGACCTCGTTTTTCCTGAG	
Bcl2l1 4F	ATTCCTCTGTCGCCTTCTGA	
Bcl2l1 4R	CCCCGGAAGGTCTTTTGTAT	
Bcl2l 3.5F	ATTCCTCTGTCGCCTTCTGA	
CD53 F	CAGACCCACGGGTATTTTGT	
Cd53 R	AACCCAAGCGAGAAGAGTGA	
Oct2 5	TGGAGGAGCTGGAACAGTTT	(McMurry., 2000)
Oct2 6	TGTTTGGACCTTGGCATCTTTG	
Cd3e 5	TTCATCCTTATGGGAAGGC	(Rajkamal Tripathi, 2002
Cd3e 6	ACACAGGAAGTGTAGAGG	

2.5 Cell culture

Incubator conditions

All cells were cultured at 37°C for the indicated times in a humidified chamber with an atmosphere of 5% CO_2.

Thymocyte survival assays

Freshly isolated total thymocytes were cultured in RPMI-1640 growth medium supplemented with 10% FBS, 100 U/ml penicillin-streptomycin, 2 mM L-glutamine (Gibco, Carlsbad, CA) and 50 μM 2-mercaptoethanol (Sigma-Aldrich, St. Louis, MO) at $2x10^6$ cells/ml with no treatment, 40 μM Z-VAD(OMe)-FMK (ICN Pharmaceuticals, Aurora, OH) or Z-IETD (R&D systems, Minneapolis, MN). To monitor the synchronized differentiation of large and small pre-selection DP thymocytes *in vitro*, total thymocytes were negatively selected over MACS CD4 MicroBeads (Miltenyi Biotec, Auburn, CA). Flow-through was >95% DN and ISP thymocytes as determined by flow cytometry and placed in culture for the indicated amounts of time.

Cell lines

The 293T fibroblast cell line was grown in DMEM supplemented with 10% FBS, 100 U /ml penicillin-streptomycin and 2 mM L-glutamine (Invitrogen/Gibco). The NIH3T3 cell line was grown in IMDM supplemented with 10% FBS, 100 U/ml penicillin-streptomycin and 2 mM L-glutamine. The OP9-DL1 stromal cells were obtained from Dr Juan Carlos Zuniga-Pflucker (Schmitt and Zuniga-Pflucker, 2002) and cultured in αMEM

supplemented with 20% FBS, 100 U/ml penicillin-streptomycin and 2 mM L-glutamine. The 16610D9 and FA2C1 *p53*$^{-/-}$ thymoma lines were obtained from Dr Barabara L. Kee (University of Chicago, Chicago IL) and cultured in RPMI-1640 supplemented with 10% FBS, 100 U/ml penicillin-streptomycin 2 mM L-glutamine and 50 μM 2-mercaptoethanol (Bain et al., 1999; Reschly et al., 2006).

Production of retroviral supernatants

Retroviral supernatants were produced by transient $CaPO_4$ co-transfection of 293T cells with the appropriate MIGR1 based expression vector and the RetroMax packaging vector pCL-Eco (Imgenex, San Diego, CA). This procedure was based on Current Protocols in Molecular Biology, 9.11.2, Basic protocol 1. 293T cells were seeded at 2 x 10^6 cells / 60 mm plate/4 ml 293T medium on day 1. On day 2, transfection cocktail was prepared by combining 10 μg of the MIGR1 expression plasmid, 10 μg of pCL-Eco, 50 μl of 2.5 M $CaCl_2$ solution pH 7.2 (10 mM HEPES, 2.5 M $CaCl_2$) and TE pH 7.3 (10 mM Tris-HCl, 1 mM EDTA) to a final volume of 500 μl / plate to be transfected. This solution was subsequently combined with 500 μl of 2X HEBS pH 7.2 [50 mM HEPES, 10 mM KCl, 0.28 M NaCl, 1.2 mM Dextrose, 1.5 mM Na_2HPO_4 ($7H_2O$)] in a dropwise fashion under mechanical aeration produced by bubbling air through a Pasteur pipette. The transfection cocktail was vortexed for 5 seconds and gently added to 293T cells at 1 ml / 60 mm plate on top of the existing 4 ml 293T medium and incubated under standard conditions over-night. On day 3, old medium (~5 ml/plate) was replaced with 3 ml/plate of fresh OP9 medium and incubated over-night. On day 4 viral supernatant was filtered through 0.45

μm Whatman syringe filters (GE Healthcare), snap frozen with 1 ml aliquots with liquid N_2 and stored at –80°C until ready for use. 3 ml of fresh pre-warmed OP9 medium was gently added back to the 293T monolayer and a second batch of retroviral supernatants was harvested on day 5.

Determining viral titer

This procedure was loosely based on Current protocols in molecular biology, 9.10.5 and 9.11.9. 3 wells of NIH3T3 were seeded at 2 x 10^5 / 2 ml / p6 well for each viral batch to be titred. The following day, the 3 wells of exponentially growing NIH3T3 cells were infected by spinfection with 100, 10 and 1 μl viral supernatant respectively as follows. Each p6 well was supplemented with an additional 2 ml of NIH3T3 medium and 4 μg/ml polybrene (Sigma). Cells were centrifuged at 872 RCF for 90 minutes at RT and returned to the incubator. 24 hours after completion of spinfection, single cell suspension was obtained by trypsinization and flow cytometry was performed to assess percent GFP^+, transduced cells. A viral concentration that produced linear dilution of GFP^+ cells was used to calculate the approximate viral concentration as follows:

(proportion of GFP+ cells) x (8 x 10^5) x dil / 4 = Infectious particles / ml

Proportion of GFP+ cells = %GFP+/100

8 x 10^5 ≈ cell number on the day of flow cytometry analysis

NIH3T3 replication factor = 4

dilution factor: 100 μl supernatant =10, 10 μl supernatant =100, 1 μl supernatant =1000

Transduction of thymocyte / OP9-DL1 co-cultures

Enriched DN thymocytes were allowed to differentiate on OP9-DL1 cells (generous gift from J.C. Zuniga-Pflucker, University of Toronto, Toronto, Canada) (Schmitt and Zuniga-Pflucker, 2002). OP9-DL1 cells were seeded at $2.5x10^4$ / well on a p24 plate one day prior to co-culture. 10^8 total thymocytes were depleted for DP thymocytes as described. Flow-through was counted and seeded onto OP9-DL1 monolayers at 5 x 10^5 thymocytes /ml /24 well plate and cultured over-night in the presence of 5 ng/ml recombinant murine IL-7 (PeproTech, Rocky Hill, NJ). The following day, co-cultures were transduced by adding 1 ml of infection cocktail pre-warmed to 37^{o}C onto the existing 1 ml of OP9 media in each well and spinfected at 872 RCF for 90 minutes at RT. 1 ml of infection cocktail includes freshly thawed retroviral supernatant, 5 ng recombinant IL-7, 16 μg polybrene (Sigma-Aldrich) and OP9 medium if needed. The amount of virus used for different wells was balanced according to the volume limit of the most dilute viral stock, which was usually pMIGR1-c-Myb (~2-5 x 10^6 infectious particles / ml). Following spinfection, co-cultures were returned to the incubator for 4 hours after which the 2 ml/p24 well of virus containing medium was replaced with 1 ml fresh OP9 medium supplemented with 5 ng/ml recombinant IL-7. The greatest number of transduced DP thymocytes was detectable at 72 hrs post transduction. Co-cultures were therefore harvested at this time by forceful pipetting for flow cytometry or electronic cell sorting. Live, transduced DP thymocytes were defined as GFP^+, $CD90.2^+$, $CD4^+$, $CD8^+$ and $7AAD^-$.

2.6 Statistics

Differences between data sets were analyzed with two-tailed Student's *t*-test and a confidence level of 99% for the mRNA expression microarray and 95% for all other experiments.

Chapter III. c-Myb promotes the survival of $CD4^+CD8^+$ DP thymocytes through the up-regulation of Bcl-xL.

3.1 Introduction

DP thymocytes undergoing *Vα-Jα* recombination at the *Tcrα* locus have an intrinsic survival window of 3-4 days. During this time, they undergo multiple rounds of rearrangements at the *Tcrα* locus, testing further distally located *Vα* and *Jα* segments in order to maximize the chances of assembling a selectable αβ-TCR (Brandle et al., 1992; Huang and Kanagawa, 2001a; Petrie et al., 1993; Villey et al., 1996; Wang et al., 1998). This mechanism is known as receptor editing and is terminated by positive selection signals or death by neglect (Borgulya et al., 1992; Brandle et al., 1992; Turka et al., 1991), ensuring only thymocytes that express a productive αβ-TCR will survive to constitute the peripheral T cell repertoire. Thus, the survival window of pre-selection DP thymocytes limits the progression of *Tcrα* rearrangements and thereby influences opportunities for positive selection and the generation of a diverse peripheral T cell repertoire (Huang et al., 2005; Xi and Kersh, 2004b). The lifespan of pre-selection DP thymocytes must therefore be precisely tuned to balance mechanisms that enforce death by neglect and those that enable sufficient receptor editing.

The onset of *Vα-Jα* rearrangements at the *Tcrα* locus during the DP stage is accompanied by cessation of the post β-selection proliferative burst and cell division is

not observed again until the SP stage of T cell development (Egerton et al., 1990; Penit et al., 1995; Petrie et al., 1993). Hypo-responsiveness to cytokine-mediated survival signaling in pre-selection DP thymocytes has been reported to cause a decrease in Bcl-2 expression, glucose metabolism and cell volume, as well as increased sensitivity to death by neglect (Gratiot-Deans et al., 1994; Rathmell et al., 2001; Yu et al., 2006). To counteract premature death by neglect, expression of the critical survival factor Bcl-xL is greatly up-regulated in the DP stage of T cell development (Grillot et al., 1995; Ma et al., 1995). Bcl-xL is one of five alternatively spliced gene products encoded by the *Bcl2l1* locus and the predominant isoform expressed in the thymus (Gonzalez-Garcia et al., 1994). *Bcl2l1* expression is high in DP thymocytes but low in DN and SP thymocytes (Grillot et al., 1995; Ma et al., 1995). Up-regulation of Bcl-xL during the DP stage has been attributed to the actions of the essential transcription factors RORγt and TCF-1 (Ioannidis et al., 2001; Sun et al., 2000). Bcl-xL deficient DP thymocytes undergo premature apoptosis and produce a *Tcrα* repertoire that is skewed to preferential use of proximal 5' *Jα* segments (Guo et al., 2002; Ma et al., 1995).

We have previously used conditional mutagenesis to demonstrate that c-Myb plays a crucial and complex role during the DP stage of T cell development. c-Myb deficient DP thymocytes undergo increased cell death in an αβ-TCR independent fashion and impaired development into CD4 SP thymocytes (Bender et al., 2004). At the time of this thesis study, the survival defect in c-Myb deficient pre-selection DP thymocytes was poorly understood and interpretations of c-Myb function in αβ-TCR dependent processes were severely confounded by the αβ-TCR independent survival defect. Thus, it was

important to gain better understanding in the mechanism by which c-Myb promotes the survival of pre-selection DP thymocytes. Here, I demonstrate that *Myb* mRNA expression is dynamically regulated during T cell development and specifically up-regulated in the small, quiescent pre-selection DP thymocytes. During this stage, premature apoptosis occurs in the absence of c-Myb via the intrinsic apoptotic pathway and restricts the 3' progression of *Jα* segment usage during *Tcrα* recombination. An exogenous source of Bcl-2 is able to restore the observed survival defect but not the decreased CD4SP thymocyte representation in c-Myb deficient thymocytes, demonstrating that the role of c-Myb in the development of CD4SP thymocytes is independent of its effect on the intrinsic apoptotic pathway. Bcl-2 is sparsely expressed in normal pre-selection DP thymocytes and this study makes clear that Bcl-xL is the physiological Bcl-2 family member that mediates c-Myb function in pre-selection DP thymocytes. Forced Bcl-xL expression is able to rescue impaired survival caused by c-Myb deficiency and re-introduction of c-Myb restores both Bcl-xL expression and the small pre-selection DP compartment. Importantly, c-Myb stimulates Bcl-xL expression at the level of transcription, through a novel pathway independent of RORγt and TCF-1 expression. Finally, our results demonstrate that survival is regulated differently in large and small pre-selection DP thymocytes, and that only the latter depend on c-Myb and Bcl-xL for their survival. In conclusion, this study provides new insight into the regulation of survival during T cell development and establishes Bcl-xL as a novel effector of c-Myb activity.

3.2 Results

Myb expression in T cell development

Myb mRNA is abundantly produced by DN and DP thymocytes compared to SP thymocytes and naïve CD4 and CD8 T cells (Bender et al., 2004; Ess et al., 1999; Hoffmann et al., 2003). To better resolve changes in *Myb* mRNA expression during αβ T cell development, we performed quantitative reverse-transcription (qRT) PCR analysis on mRNA extracted from electronically sorted populations ranging from DN2 thymocytes (Godfrey et al., 1993) to mature, naïve T cell subsets in the spleen (Fig. 3.1A). The greatest amount of *Myb* mRNA was detected in DN2 and DP thymocytes. Interestingly, the amount of *Myb* mRNA detected decreased in DN3, DN4 and ISP thymocytes compared to DN2 and DP thymocytes, suggesting that *Myb* mRNA expression decreases as developing thymocytes transit through the DN3, DN4 and ISP stages and then increases approximately 4-fold in the DP subset. *Myb* mRNA expression is greatly decreased in CD4 and CD8 SP thymocytes and naïve CD4 and CD8 T cells compared to DP thymocytes.

The DP compartment consists of a heterogeneous population of cells. Thymocytes enter the DP stage as large cells still cycling from the post β-selection proliferative burst. After a few rounds of division, withdrawal from cell cycle coincides with the onset of *Vα-Jα* recombination at the *Tcrα* locus (Egerton et al., 1990; Penit et al., 1995; Petrie et al., 1995). Quiescent thymocytes awaiting positive selection are

characterized by their small cell volume and can be distinguished from early DP blasts based on cell size. Positive selection during the DP stage can be readily monitored by the induction of surface CD69 expression (Testi et al., 1994). Thus, to further resolve the rise and fall of *Myb* expression, the DP compartment was further sorted into $CD69^{-}FSC^{hi}$, $CD69^{-}FSC^{lo}$ and $CD69^{+}FSC^{lo}$ subsets, referred to here as large pre-selection, small pre-selection and post-selection DP thymocytes respectively (Fig. 3.1B). The largest amount of *Myb* mRNA was detected in the small pre-selection DP subset (Fig. 3.1B). Moreover, a corresponding peak in expression was readily detectable in $Tcr\alpha^{-/-}$ mice (Fig. 3.1C), demonstrating that increased *Myb* mRNA expression occurs in small pre-selection thymocytes in an αβ-TCR independent manner. Consistent with previous reports (Ess et al., 1999; Hoffmann et al., 2003; Maurice et al., 2007; Mick et al., 2004), a sharp decrease of *Myb* mRNA level was observed in the post-selection DP subset, suggesting that down-regulation of *Myb* mRNA expression is a consequence of αβ-TCR mediated selection signals (Fig. 3.1B). In further support of this notion, mimicking positive selection by *in vitro* stimulation of $Tcr\alpha^{-/-}$ DP thymocytes with phorbol 12-myristate 13-acetate (PMA) and $Ca2^{+}$ ionophore A23187 (Ohoka et al., 1996; Takahama and Nakauchi, 1996) resulted in induction of surface CD69 expression accompanied by a rapid decrease in *Myb* mRNA content (Fig. 3.2). These results demonstrate that *Myb* expression is dynamically regulated during T cell development. The abundance of *Myb* mRNA expression detected in the small pre-selection DP subset suggests that c-Myb may play a particularly important role at this critical stage during thymocyte development.

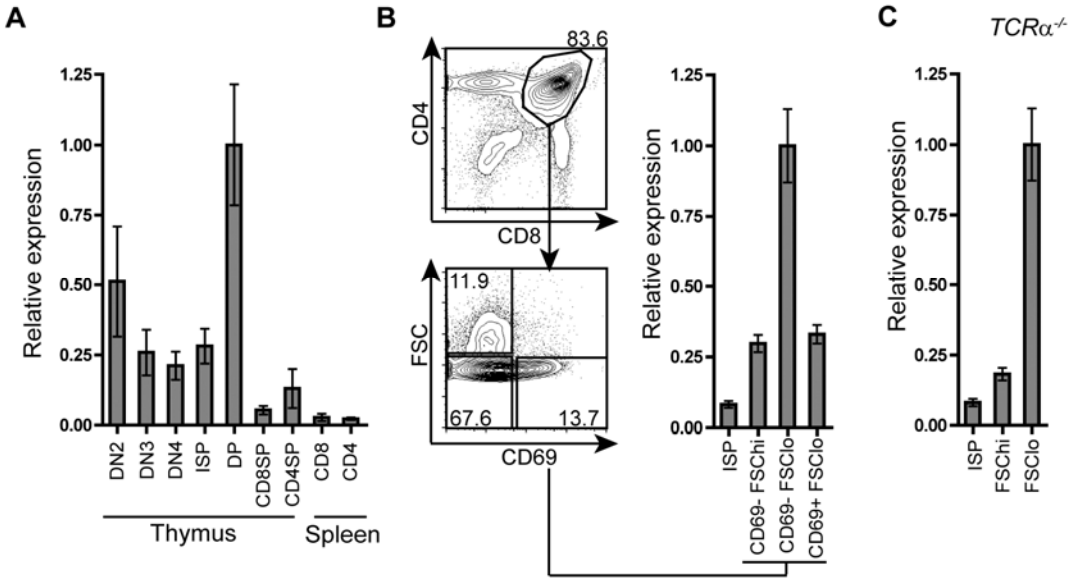

Figure 3.1 Expression of *Myb* mRNA during αβ-T cell development. *Myb* mRNA expression was analyzed by quantitative real-time PCR and normalized to the expression of *Hprt1* mRNA. The peak of relative *Myb* mRNA levels in each experiment is indicated as 1. Data are presented as mean +/- SEM and are representative of two mice. (A) Relative *Myb* mRNA levels in DN2 ($CD4^-CD8^-$c-$Kit^+CD44^+CD25^+$), DN3 ($CD4^-CD8^-$c-$Kit^-CD44^-CD25^+$), DN4 ($CD4^-CD8^-$c-$Kit^-CD44^-CD25^-$) thymocytes (Godfrey et al., 1993), ISP ($TCR\beta^{lo}CD4^-CD8^+$) and thymic and splenic CD4SP ($TCR\beta^{hi}CD4^+CD8^-$) and CD8SP ($TCR\beta^{hi}CD8^+CD4^-$) populations. (B) Relative *Myb* mRNA in ISP ($TCR\beta^{lo}CD4^-CD8^+$), large pre-selection DP ($FSC^{hi}CD69^-CD4^+CD8^+$), small pre-selection DP ($FSC^{lo}CD69^-CD4^+CD8^+$) and post-selection DP subsets ($FSC^{lo}CD69^+CD4^+CD8^+$). (C) Relative *Myb* mRNA expression in *Tcrα*$^{-/-}$ ISP ($CD4^-CD8^+$), large pre-selection DP ($CD4^+CD8^+FSC^{hi}$) and small pre-selection DP ($CD4^+CD8^+FSC^{lo}$) subsets.

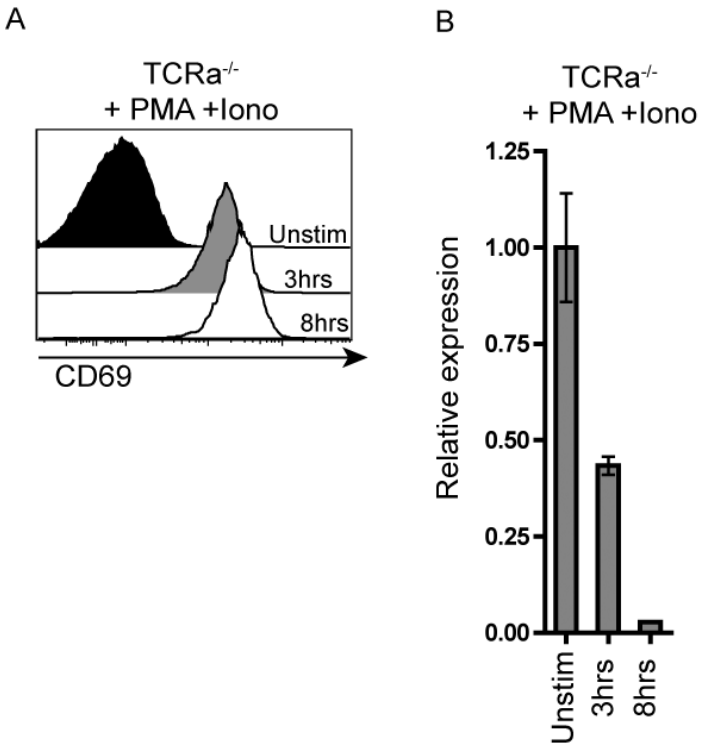

Figure 3.2 The amount of *Myb* mRNA contained in pre-selection DP thymocytes decreases upon *in vitro* stimulation. Total *Tcrα*$^{-/-}$ thymocytes were stimulated in liquid cell culture with 10 ng/mL PMA and 10 ng/mL A23187. Cells were harvested for flow cytometry and RNA extraction at the indicated time points. Results are representative of two independent experiments. (A) Thymocytes were surface stained for CD4, CD8 and CD69 and analyzed by flow cytometry. Histogram shows expression of the positive selection marker CD69 on DP thymocytes following stimulation. (B) Relative *Myb* mRNA levels were measured by quantitative real-time PCR and normalized to *Hprt1* mRNA expression.

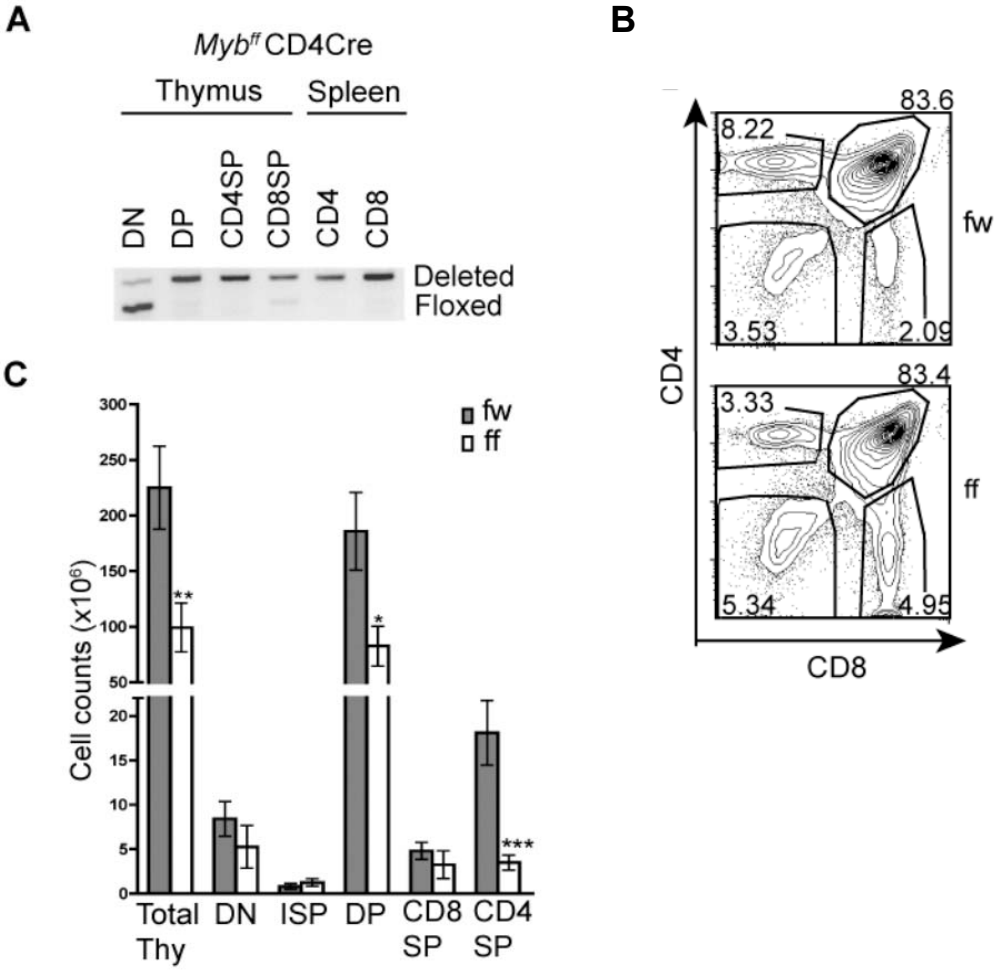
A
Mybff CD4Cre
Thymus
Spleen
DN
DP
CD4SP
CD8SP
CD4
CD8
Deleted
Floxed
B
83.6
8.22
fw
3.53
2.09
83.4
3.33
ff
5.34
4.95
CD4
CD8
C
fw
ff
Cell counts (x10⁶)
300
250
200
150
100
50
20
15
10
5
0
**
*
***
Total Thy
DN
ISP
DP
CD8 SP
CD4 SP

Figure 3.3 *Myb*$^{f/f}$ Cd4-Cre DP thymocytes display impaired survival. (A) Deletion efficiency at the floxed *Myb* locus in a *Myb*$^{f/f}$ Cd4-Cre mouse**.** Genomic DNA was extracted from electronically sorted DN ($CD4^-CD8^-$), DP ($CD4^+CD8^+$), CD4SP ($CD4^+CD8^-$) and CD8SP ($CD8^+CD4^-$) thymocyte populations and naïve CD4 and CD8 splenic T cells. The presence of the floxed and deleted *Myb* alleles was analyzed by PCR (Bender et al., 2004). (B) *Myb*$^{f/w}$ (fw) Cd4-Cre and *Myb*$^{f/f}$ (ff) Cd4-Cre thymocytes were analyzed for surface expression of CD4 and CD8. Numbers next to gates represent the percentage of cells through a live lymphocyte gate. Data is representative ≥10 mice of each genotype. (C) Bar graph shows mean +/- SEM of the absolute number of total, DN ($CD4^-CD8^-$), ISP ($TCR^{lo}CD4^-CD8^+$), DP ($CD4^+CD8^+$), CD8SP ($TCR^{hi}CD4^-CD8^+$) and CD4SP ($TCR^{hi}CD4^+CD8^-$) thymocyte populations of 4-6-week-old *Myb*$^{f/w}$ Cd4-Cre and *Myb*$^{f/f}$ Cd4-Cre mice. n≥6, *p = 0.0019, **p = 0.0011, ***p < 0.0001 (Student's *t*-test).

Tissue specific deletion of *Myb* in DP thymocytes

We have previously demonstrated that Lck-Cre mediated deletion in mice homozygous for the loxP targeted allele of *Myb* ($Myb^{f/f}$) results in a *Tcrα* independent survival defect in DP thymocytes and impaired development of CD4SP thymocytes (Bender et al., 2004). We obtain the same phenotype with Cd4-Cre mediated deletion (Fig. 3.3). However, deletion of the Myb^{f} allele is more efficient and mainly restricted to the DP and subsequent stages in the thymus and the spleen. We do not detect altered DN4:DN3 ratio or counter selection for the Myb^{f} allele in CD4SP thymocytes as we did using Lck-Cre (Fig. 3.3A) (Bender et al., 2004) indicating minimal deletion at the *Myb* locus prior to the DP stage. $Myb^{w/w}$ and $Myb^{f/w}$ mice that carry a Cd4-Cre allele displayed no difference in phenotype at 4-6 weeks of age (data not shown) and $Myb^{f/w}$ Cd4-Cre thymocytes were used as experimental controls in the present work.

Absolute number analysis of $Myb^{f/f}$ Cd4-Cre thymocytes from 4-6 week-old mice resulted in several interesting observations. The absolute number of thymocyte subsets were calculated based on total thymus cellularity counted by trypan blue exclusion and the representation of each thymocyte population was analyzed by flow cytometry (Fig. 3.3B). The number of $Myb^{f/f}$ Cd4-Cre DP thymocytes was decreased by 50% compared to $Myb^{f/w}$ Cd4-Cre controls (Fig. 3.3C). Furthermore, the number of the CD4SP thymocytes was decreased by 75% while the number of CD8SP thymocytes remained unaltered. The resulting shift in the CD4:CD8 ratio (Fig. 3.3B) is consistent with previous reports suggesting that c-Myb plays a role in the regulation of CD4 versus CD8 lineage decision (Bender et al., 2004; Lieu et al., 2004; Maurice et al., 2007).

Collectively, these results confirm our previous findings and establish *Myb*$^{f/f}$ Cd4-Cre mice as a superior model over Lck-Cre to address the functions of c-Myb in DP thymocytes. All *Myb*$^{f/f}$ and *Myb*$^{f/w}$ mice used in this thesis work carry the Cd4-Cre transgene and will hereon be referred to simply as *Myb*$^{f/f}$ and *Myb*$^{f/w}$.

c-Myb prevents pre-mature apoptotic cell death in small pre-selection DP thymocytes.

To determine if the decreased number of *Myb*$^{f/f}$ DP thymocytes is a result of apoptotic cell death we measured the ability of *Myb*$^{f/w}$ and *Myb*$^{f/f}$ DP thymocytes to survive in the presence or absence of the pan-caspase inhibitor Z-VAD in liquid culture. After both 6 and 24 hrs in culture, the percentage of live thymocytes was defined as those negative for both 7AAD and Annexin 5 staining as detected by flow cytometry. Consistent with previous findings, we measured a statistically significant decrease in DP thymocyte survival in the absence of c-Myb after both 6 and 24 hrs in culture (Fig. 3.4A). A different analysis of the same experiment comparing the surface distribution of CD4 and CD8 between *Myb*$^{f/f}$ and *Myb*$^{f/w}$ thymocytes through a 7AAD and Annexin 5 double negative gate revealed a decrease in the percentage of *Myb*$^{f/f}$ DP thymocytes accompanied by a corresponding increase in the percentage of *Myb*$^{f/f}$ DN and SP thymocytes at 24 hrs post-culture (Fig. 3.4B), indicative of a DP specific survival defect. Survival of *Myb*$^{f/f}$ DP thymocytes was restored to a level equivalent to controls after treatment with Z-VAD, suggesting that the decreased number of cells detected in c-Myb deficient DP thymocytes

was due to apoptotic cell death. This result was further confirmed by TUNEL assay and caspase-3 activation in cultured c-Myb deficient DP thymocytes (Fig. 3.4C).

Apoptotic cell death occurs during the DP stage most commonly through αβ-TCR independent death by neglect, but also through αβ-TCR dependent negative selection. We crossed *Myb*$^{f/f}$ mice onto a *Tcrα*$^{-/-}$ background to confirm the αβ-TCR independent nature of the previously observed survival defect (Bender et al., 2004). T cell development in *Tcrα*$^{-/-}$ mice is arrested at the small DP thymocyte stage and ends in death by neglect due to the absence of αβ-TCR mediated survival. Absolute cell number analysis of large and small pre-selection DP thymocytes was calculated. Strikingly, while no significant difference was observed in the large DP compartment, a severe reduction was observed in the small DP compartment of c-Myb deficient thymi (Fig. 3.5A). This result is consistent with a functional relevance of the abundant c-Myb expression in the small pre-selection DP subset (Fig. 3.1B). In addition, the ability of *Myb*$^{f/f}$ CD4Cre *Tcrα*$^{-/-}$ DP thymocytes to survive *in vitro* was significantly impaired after 6 and 24 hrs (Fig. 3.5B). In accordance with the selective decrease in the number of small DP thymocytes detected in *Myb*$^{f/f}$ *Tcrα*$^{-/-}$ mice, the same population was selectively depleted from the pool of live DP thymocytes after 24 hrs in liquid culture while the large DP compartment remained largely intact in comparison to *Myb*$^{f/w}$ *Tcrα*$^{-/-}$ cultures (Fig. 3.5C). The presence of Z-VAD restored the observed survival defect as well as the live small pre-selection DP compartment (Fig. 3.5B and C). Thus, our results demonstrate that the previously observed αβ-TCR independent survival defect in c-Myb deficient DP

thymocytes is a consequence of accelerated apoptotic cell death occurring preferentially in the small pre-selection DP thymocyte subset where *Myb* is highly expressed.

A relative increase in the proportion of large pre-selection DP thymocytes has previously been linked to decreased survival due to an inability to withdraw from cell cycle (Sun et al., 2000). The DP compartment in *Rorγt*$^{-/-}$ mice is drastically decreased due to increased cell death and contains mainly proliferating large pre-selection DP thymocytes (Sun et al., 2000). The *in vitro* survival of *Rorγt*$^{-/-}$ DP thymocytes was demonstrated to be significantly restored by the presence of the pan cyclin-dependent kinase inhibitor, roscovitine (5μM), suggesting that the observed survival defect is at least in part caused by a failure to withdraw from cell cycle (Sun et al., 2000). To investigate if c-Myb deficient DP thymocytes undergo increased apoptosis due to hyper proliferation, we compared the percentage of *Myb*$^{f/f}$ *Tcrα*$^{-/-}$ and *Myb*$^{f/w}$ *Tcrα*$^{-/-}$ DP thymocytes with >2n DNA content. Despite the over-representation of large pre-selection DP thymocytes in *Myb*$^{f/f}$ *Tcrα*$^{-/-}$ mice, we did not detect an increase in the percentage of cycling cells in this compartment compared to *Myb*$^{f/w}$ *Tcrα*$^{-/-}$ thymocytes (Fig. 3.6A). In addition, the presence of roscovitine had no protective effect on the survival of *Myb*$^{f/f}$ *Tcrα*$^{-/-}$ thymocytes (Fig. 3.6B). These results demonstrate that impaired survival caused by the lack of c-Myb is not a consequence of hyper proliferation and that the nature of the survival defect in *Myb*$^{f/f}$ *Tcrα*$^{-/-}$ DP thymocytes is fundamentally different from that in *Rorγ*$^{-/-}$ mice. While *Rorγ*$^{-/-}$ DP thymocytes fail to assume the small, quiescent phenotype, *Myb*$^{f/f}$ *Tcrα*$^{-/-}$ DP thymocytes are able to enter but fail to sustain the small pre-selection DP thymocyte compartment.

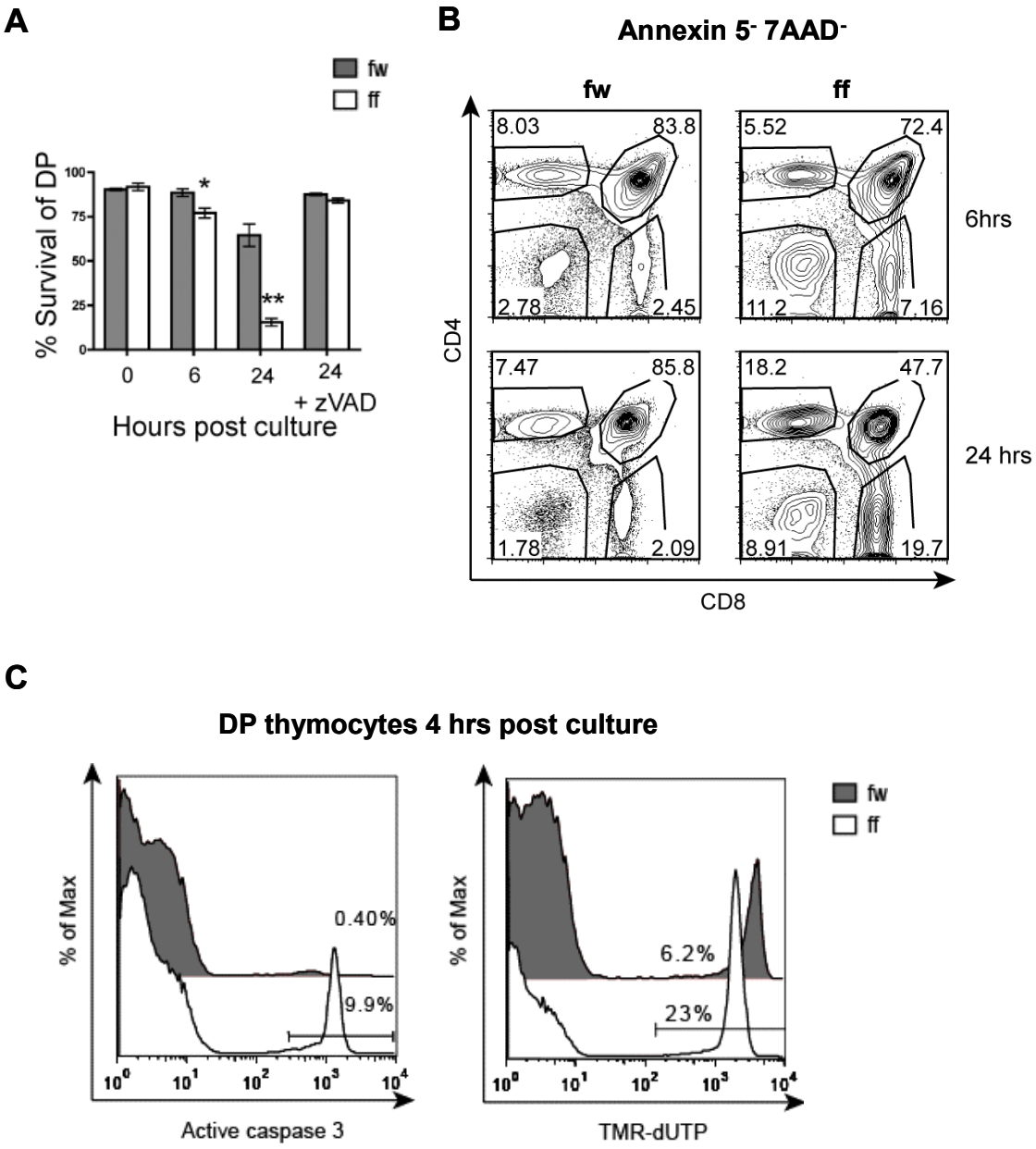
A
fw
ff
% Survival of DP
100
75
50
25
0
*
**
0
6
24
24
+ zVAD
Hours post culture
B
Annexin 5- 7AAD-
fw
ff
8.03
83.8
2.78
2.45
5.52
72.4
11.2
7.16
6hrs
7.47
85.8
1.78
2.09
18.2
47.7
8.91
19.7
24 hrs
CD4
CD8
C
DP thymocytes 4 hrs post culture
% of Max
0.40%
9.9%
Active caspase 3
% of Max
6.2%
23%
TMR-dUTP
fw
ff

Figure 3.4 *Myb*$^{f/f}$ Cd4-Cre mice undergo premature apoptotic cell death. (A) Survival assessment of *Myb*$^{f/w}$ Cd4-Cre and *Myb*$^{f/f}$ Cd4-Cre DP thymocytes after 6 and 24 hrs in culture. Where indicated, thymocytes were cultured in the presence of 40 μM of the pan-caspase inhibitor Z-VAD (ICN Pharmaceuticals, Aurora, OH). Cultures were stained for CD4, CD8, 7AAD, and Annexin 5. Percent survival of DP was defined as the percentage of 7AAD$^-$Annexin 5$^-$ cells through a CD4$^+$CD8$^+$ gate. n≥5, *p = 0.045, **p < 0.0001. (B) The same *in vitro* survival assay was analyzed for the distribution of CD4 and CD8 surface expression through a 7AAD$^-$Annexin 5$^-$ live gate. (C) Total *Myb*$^{f/w}$ Cd4-Cre and *Myb*$^{f/f}$ Cd4-Cre thymocytes were placed in liquid culture for 4 hrs and harvested for analysis by flow cytometry. Thymocytes were stained for surface expression of CD4 and CD8 followed by either (left) intracellular staining for active caspase 3 using PE Active Caspase-3 Apoptosis Kit (BD Biosciences, San Jose, CA) or (right) terminal dUTP labeling, using the In Situ Cell Death Detection Kit, TMR red (Roche, Indianapolis, IN).

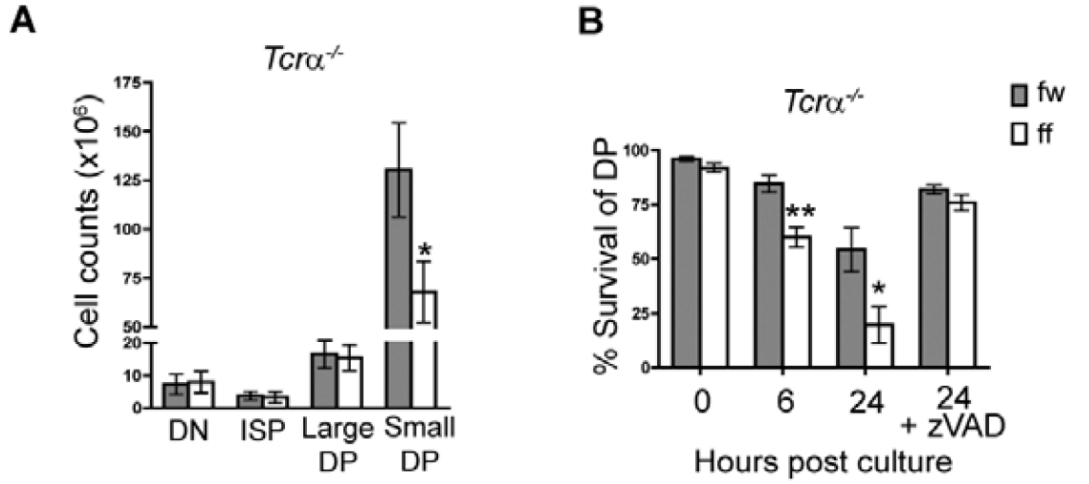

C

***Tcrα*$^{-/-}$**
Annexin 5^{-}, 7AAD^{-}, DP
24 hrs post culture

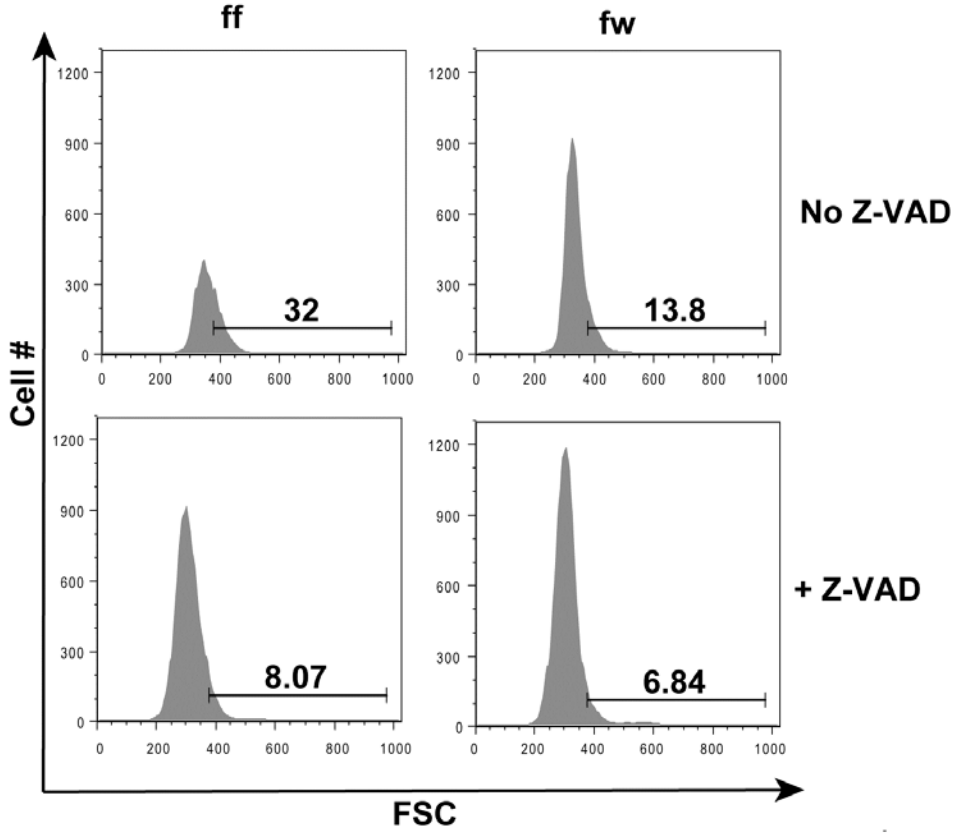

Figure 3.5 *Myb*$^{f/f}$ Cd4-Cre DP thymocytes undergo increased apoptotic cell death in a *Tcrα* independent fashion. (A) The absolute number of 4-6-week-old *Myb*$^{f/w}$ (fw) Cd4-Cre *Tcrα*$^{-/-}$ and *Myb*$^{f/f}$ (ff) Cd4-Cre *Tcrα*$^{-/-}$ thymocyte subsets was calculated based on total thymic cellularity and the percentage of DN ($CD4^-CD8^-$), ISP ($CD4^-CD8^+$), large pre-selection DP ($CD4^+CD8^+FSC^{hi}$) and small pre-selection DP ($CD4^+CD8^+FSC^{lo}$) thymocytes. Data are presented as mean +/- SEM. n≥5, *p = 0.0068 (Student's *t*-test). (B) Assessment of *Tcrα*$^{-/-}$ DP thymocyte survival after 6 and 24 hrs in culture. Where indicated, thymocytes were cultured in the presence of 40 μM Z-VAD. Cultures were stained for CD4, CD8, 7AAD, and Annexin 5. Percent survival of DP was defined as the percentage of $7AAD^-$Annexin 5^- cells through a $CD4^+CD8^+$ gate. n≥5, *p = 0.011, **p = 0.0023. (C) Cultured DP thymocytes were analyzed for FSC distribution through a $7AAD^-$Annexin 5^- live gate.

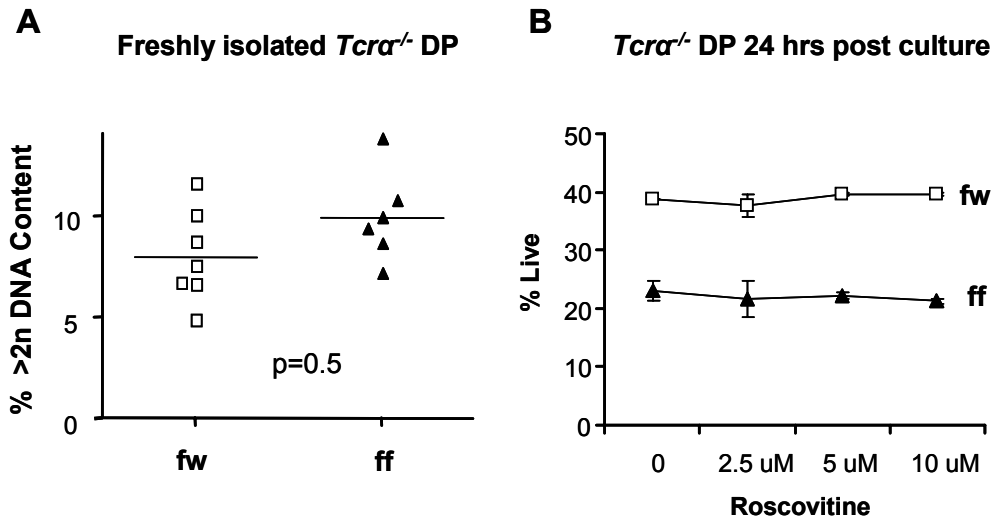

Figure 3.6 Premature apoptosis is not a result of an inability of *Myb*$^{f/f}$ pre-selection DP thymocytes to withdraw from cell cycle. (A) DNA content analysis of *Myb*$^{f/f}$ Cd4-Cre *Tcrα*$^{-/-}$ and *Myb*$^{f/w}$ Cd4-Cre *Tcrα*$^{-/-}$ DP thymocytes was analyzed by flow cytometry for CD4, CD8 and Draq5 staining. The percentage DP thymocytes harboring >2n DNA content were plotted. (B) *Myb*$^{f/f}$ Cd4-Cre *Tcrα*$^{-/-}$ and *Myb*$^{f/w}$ Cd4-Cre *Tcrα*$^{-/-}$ thymocytes cultured for 24 hrs in liquid culture in the presence of the indicated concentrations of the cyclin dependent kinase inhibitor, roscovitine, were assayed for survival by CD4, CD8, Annexin 5 and 7AAD staining. Line graph shows mean percent survival of DP +/- SEM for experimental replicates. Results are representative of 3 separate experiments.

c-Myb suppresses the intrinsic apoptotic pathway in pre-selection DP thymocytes.

Secreted proteins and cell-cell contacts has the potential to either enhance or impede survival. To begin investigating the cause of premature apoptosis in c-Myb deficient pre-selection DP thymocytes, we designed an assay to test if c-Myb sufficient thymocytes might provide survival enhancing signals that are absent in c-Myb deficient thymocytes, and *vice versa* if c-Myb deficient DP thymocytes might aberrantly provide death inducing signals. *Myb*$^{f/f}$ *Tcrα*$^{-/-}$ and *Myb*$^{f/w}$ *Tcrα*$^{-/-}$ thymocytes were co-cultured at a 1:1 ratio, and assessed survival after 24 hrs. Donor origin was distinguished by labeling thymocytes from either *Myb*$^{f/f}$ *Tcrα*$^{-/-}$ or *Myb*$^{f/w}$ *Tcrα*$^{-/-}$ thymocytes with CFSE (Fig. 3.7A). Flow cytometric analysis demonstrated that co-cultures had no effect on the ability of either *Myb*$^{f/f}$ *Tcrα*$^{-/-}$ or *Myb*$^{f/w}$ *Tcrα*$^{-/-}$ DP thymocytes to survive *in vitro*, ruling out the presence of death inducing, or the absence of survival enhancing soluble factors and/or thymocyte cell-cell contacts as a potential cause of increased spontaneous cell death in *Myb*$^{f/f}$ *Tcrα*$^{-/-}$ pre-selection DP thymocytes.

Spontaneous apoptosis of normal DP thymocytes in liquid culture is believed to mimic death by neglect, which occurs through the intrinsic apoptotic pathway in a cytochrome c/Apaf-1/caspase-9 apoptosome independent fashion (Marsden et al., 2002). To examine a possible contribution by the extrinsic apoptotic pathway, we cultured *Myb*$^{f/f}$ *Tcrα*$^{-/-}$ and *Myb*$^{f/w}$ *Tcrα*$^{-/-}$ thymocytes in the presence or absence of the caspase-8 specific inhibitor Z-IETD. While Z-IETD effectively inhibited apoptosis of anti-CD95 treated C57BL/6j DP thymocytes (Fig. 3.7B), it did not prevent premature apoptosis of *Myb*$^{f/f}$

Tcrα$^{-/-}$ DP thymocytes *in vitro* (Fig. 3.7C), arguing against a major role for the extrinsic apoptotic pathway in the observed survival defect.

To investigate if c-Myb promotes the survival of pre-selection DP thymocytes by suppressing the activity of the intrinsic apoptotic pathway, we turned our attention to members of the Bcl-2 family. Bcl-2 family members are key effectors of the intrinsic apoptotic pathway and the over-expression or abrogation of several Bcl-2 family proteins has been associated with dramatic effects on the lifespan of pre-selection DP thymocytes (Bouillet et al., 1999; Rathmell et al., 2002; Strasser et al., 1991; Sun et al., 2000; Verschelde et al., 2006). To determine if forced expression of a pro-survival Bcl-2 family member could rescue survival, *Myb*$^{f/f}$ mice were crossed with Bcl-2tg mice where transgene expression is directed to the T cell lineage (Strasser et al., 1991). The Bcl-2tg restored both cellularity (Fig. 3.8A) and *in vitro* survival of c-Myb deficient DP thymocytes (Figure 3.8B), suggesting that c-Myb suppresses the intrinsic apoptotic pathway to promote the survival of pre-selection DP thymocytes.

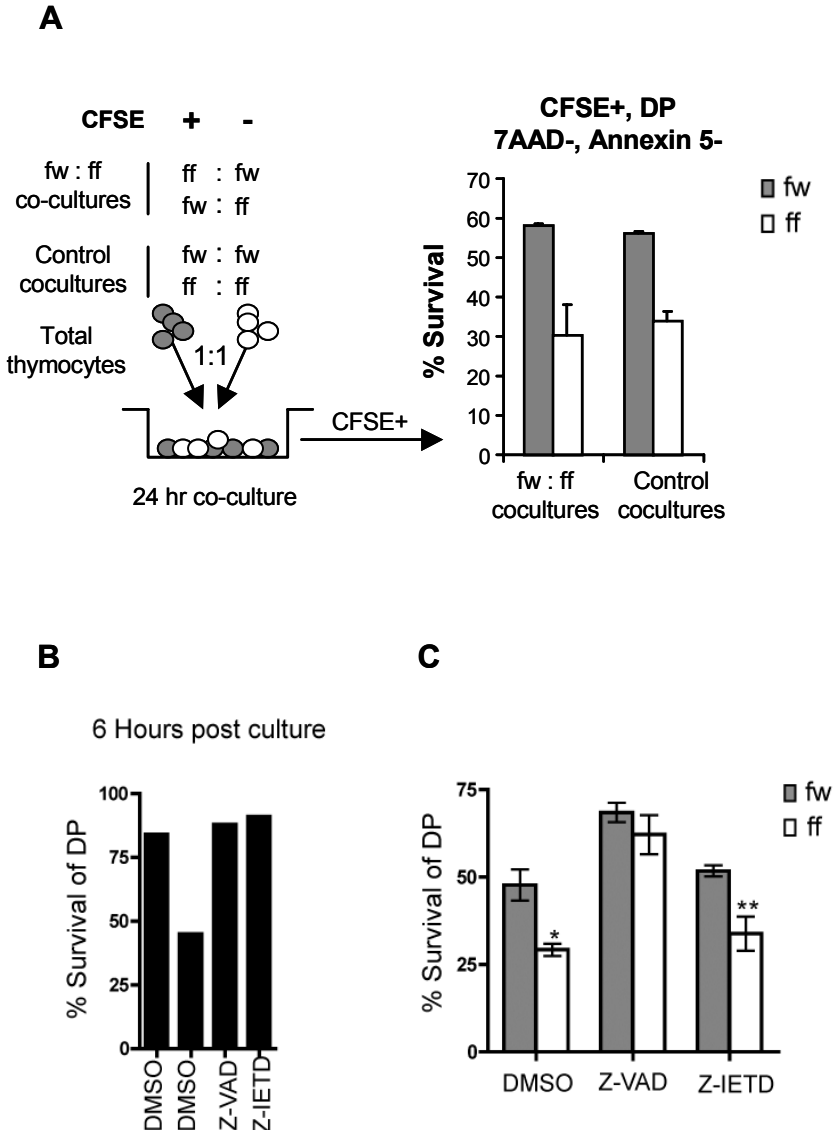
A
CFSE + -
fw : ff co-cultures
ff : fw
fw : ff
Control cocultures
fw : fw
ff : ff
Total thymocytes
1:1
CFSE+
24 hr co-culture
CFSE+, DP
7AAD-, Annexin 5-
% Survival
70
60
50
40
30
20
10
0
fw
ff
fw : ff cocultures
Control cocultures
B
6 Hours post culture
% Survival of DP
100
75
50
25
0
DMSO
DMSO
Z-VAD
Z-IETD
C
% Survival of DP
75
50
25
0
fw
ff
*
**
DMSO
Z-VAD
Z-IETD

Figure 3.7 The survival defect of *Myb*$^{f/f}$ Cd4-Cre *Tcrα*$^{-/-}$ DP thymocytes is not a result of cell extrinsic factors. (A) Co-culture of thymocytes from *Myb*$^{f/f}$ Cd4-Cre *Tcrα*$^{-/-}$ and *Myb*$^{f/w}$ Cd4-Cre *Tcrα*$^{-/-}$ mice does not affect the ability of thymocytes from either donor to survive in liquid culture. Thymocytes of the indicated genotypes were placed in co-culture at a 1:1 ratio after cells from the indicated donor (gray cells) in each co-culture were loaded with 10 μM CFSE. CFSE labeled and unlabeled thymocytes from the same donor were co-cultured as controls. Cells were harvested for survival assessment by flow cytometry 24 hrs post culture. Percentage live (Annexin 5$^-$, 7AAD$^-$) cells through a CFSE$^+$ gate are plotted to the right. Bar graph shows mean +/- SEM of 2 experimental replicates. Results are representative of two separate experiments. (B) Validation of the efficacy of Z-IETD. Total thymocytes from *Tcrα*$^{-/-}$ mice were placed in liquid culture for 6 hrs in the presence of 40 μM of the caspase-8 inhibitor Z-IETD (R&D systems, Minneapolis, MN) or Z-VAD (ICN Pharmaceuticals, Aurora, OH). In addition, 2 μg/mL of anti-mouse CD95 (BD Biosciences, San Jose, CA) was added to the culture where indicated. Survival graph shows that Z-IETD and Z-VAD are equivalent in their ability to prevent CD95 receptor-mediated apoptosis in control DP thymocytes. (C) Thymocytes were cultured in the presence of 40 μM of the indicated caspase inhibitor or 2 μl/ml of DMSO for 24 hrs. Z-VAD but not Z-IETD significantly prevents accelerated apoptosis in *Myb*$^{f/f}$ Cd4-Cre *Tcrα*$^{-/-}$ DP thymocytes. *p = 0.0056, **p = 0.0050 (Student's *t*-test).

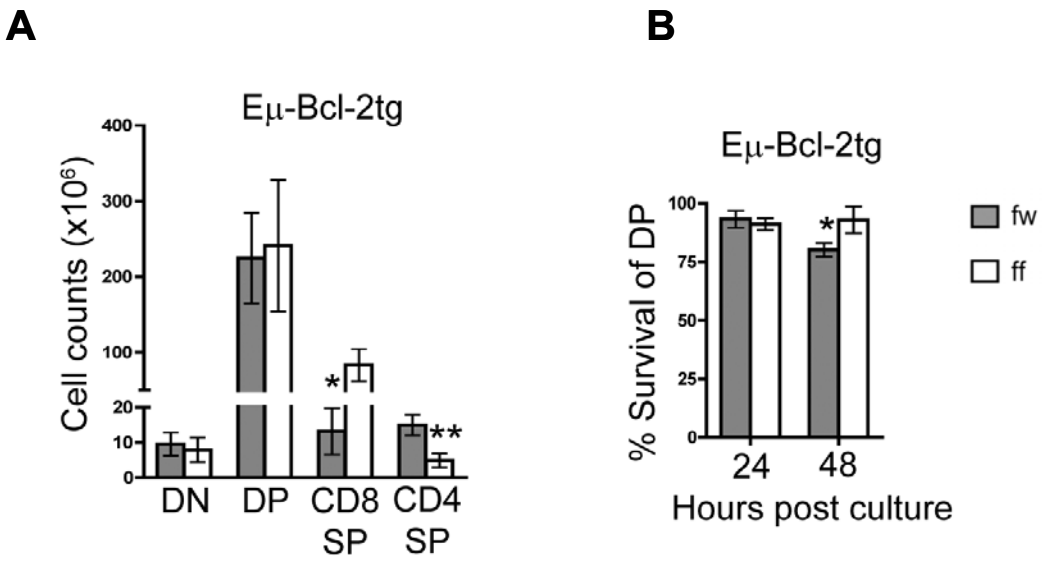

Figure 3.8 The survival defect in of *Myb*$^{f/f}$ *Tcrα*$^{-/-}$ DP thymocytes is restored by constitutive Bcl-2tg expression. (A) Absolute number of Bcl-2tg DN ($CD4^-CD8^-$), DP ($CD4^+CD8^+$), CD8SP ($CD4^-CD8^+$) and CD4SP ($CD4^+CD8^-$) thymocyte populations of 4-6-week-old *Myb*$^{f/w}$ Cd4-Cre and *Myb*$^{f/f}$ Cd4-Cre mice. Data are presented as mean +/- SEM. n=3, *p = 0.022, **p = 0.011. (B) Assessment of total Bcl-2tg DP thymocyte survival after 24 and 48 hrs in culture. n=3, *p = 0.030.

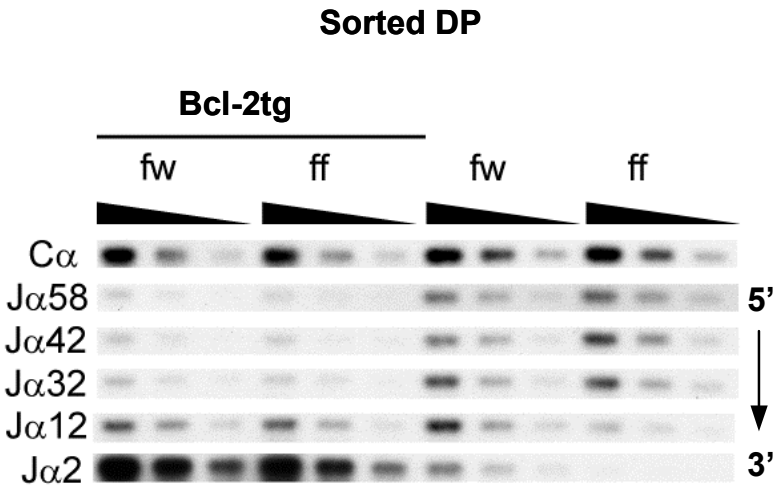

Figure 3.9 *Myb*$^{f/f}$ thymocytes exhibit decreased 3' *Jα* segment usage due to impaired survival *in vivo*. cDNA was generated from sorted *Myb*$^{f/w}$ Cd4-Cre and *Myb*$^{f/f}$ Cd4-Cre DP thymocytes in the presence and absence of Bcl-2tg expression. PCR amplification was performed with serially (1/3) diluted cDNA samples using primers specific for *Vα3* and *Cα*. PCR products were sequentially probed using oligonucleotide probes specific for the indicated *Jα* segments as previously described (Riegert and Gilfillan, 1999; Villey et al., 1996). An internal *Cα* probe was used to normalize input cDNA. Data is representative of two independent experiments.

c-Myb deficient DP thymocytes exhibit skewed *Jα* segment usage due to pre-mature cell death.

An important manifestation of decreased pre-selection DP thymocyte survival *in vivo* is the predominant usage of 5' proximal *Tcrα Jα* segments due to limited 3' progression of rearrangements along the *Jα* locus (Guo et al., 2002). To assess the effect of our observed *in vitro* survival defect on c-Myb deficient pre-selection DP thymocytes *in vivo*, we compared *Jα* segment usage in DP thymocytes from $Myb^{f/w}$ and $Myb^{f/f}$ mice, with or without Bcl-2tg expression. cDNA generated from sorted DP thymocytes was subjected to a PCR-based assay (Villey et al., 1996) in which products amplified by *Vα3* and *Cα* segment specific primers were sequentially probed for a selection of *Jα* segments ranging from 5' (proximal) to 3' (distal) in location (Riegert and Gilfillan, 1999; Villey et al., 1996). A probe against the *Cα* segment demonstrates equal loading. Comparison of *Jα* segment profiles revealed a severe decrease in the usage of the distally located *Jα12* and *Jα2* gene segments by $Myb^{f/f}$ DP thymocytes compared to controls (Fig. 3.9). In contrast, both $Myb^{f/w}$ and $Myb^{f/f}$ DP thymocytes displayed preferential usage of the distal *Jα2* segment in the presence of Bcl-2tg expression, consistent with prolonged survival independent of c-Myb. Thus, c-Myb deficient DP thymocytes do not progress to distal *Jα* segment usage as a direct consequence of premature apoptosis *in vivo*.

Bcl-2tg expression restores the DP but not the CD4SP thymocyte compartment in the absence of c-Myb

We analyzed the distribution of CD4 and CD8 surface expression on *Myb*$^{f/f}$ Bcl-2tg thymocytes to characterize the effect of c-Myb deficiency on CD4 lineage representation without the influence of impaired survival (Fig. 3.10A). Bcl-2tg expression did not restore but rather exacerbated the skewed CD4SP:CD8SP ratio as a result of a lingering 75% decrease in the number of CD4SP thymocytes and a previously undetectable increase in the representation and absolute number of CD8SP thymocytes in *Myb*$^{f/f}$ mice (Fig. 3.10A and 3.8A). Consistent with a case of augmented positive selection, we observed a novel ~4 fold increase in the percentage of post-selection (CD69^{+}TCRβ^{hi}) DP thymocytes in *Myb*$^{f/f}$ Bcl-2tg mice in comparison to *Myb*$^{f/w}$ Bcl-2tg mice (Fig. 3.10A). Normal DP to SP thymocyte differentiation is not accompanied by cellular proliferation. To investigate if aberrant proliferation might contribute to the observed increase in *Myb*$^{f/f}$ Bcl-2tg CD8SP thymocytes we carried out analysis of DNA content. Essentially no cycling cells were observed in either *Myb*$^{f/f}$ Bcl-2tg or *Myb*$^{f/w}$ Bcl-2tg CD8SP thymocytes, likely due to the documented anti-proliferative effect of Bcl-2 over-expression (Linette et al., 1996), thus ruling out increased proliferation as a possible explanation for the observed increase in the *Myb*$^{f/f}$ Bcl-2tg CD8SP thymocyte compartment (Fig. 3.10B). Thus, Bcl-2tg expression appears to reveal manifestations of c-Myb deficiency that were previously masked by premature death. Taken together, our observations demonstrate that the role of c-Myb in CD4SP thymocyte differentiation is not a secondary effect of accelerated apoptosis in pre-selection DP thymocytes that lack c-Myb. In addition, Bcl-2tg expression revealed new phenotypic differences between *Myb*$^{f/f}$ and *Myb*$^{f/w}$ thymocytes consistent with increased positive selection and development of CD8SP

thymocytes, suggesting that c-Myb may be a negative regulator of both processes. Our observations call for the previously proposed role for c-Myb in DP to SP thymocyte differentiation focused solely on differentiation to the CD4SP lineage (Maurice et al., 2007) be re-evaluated in a system where premature apoptosis is corrected.

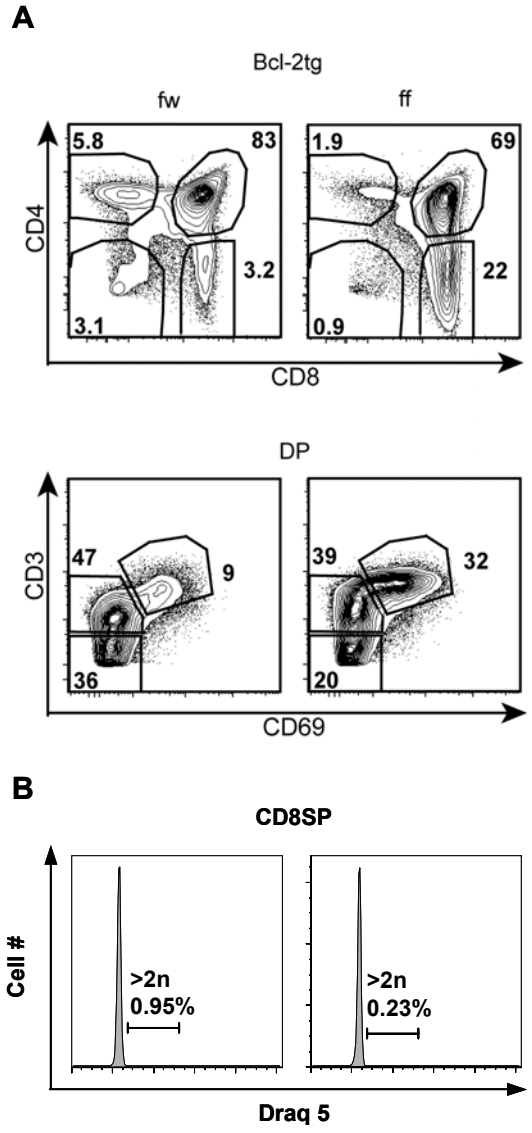

Figure 3.10 Bcl-2tg expression reveals increased development of CD8SP thymocytes by c-Myb deficient mice. (A) Total thymocytes from *Myb*$^{f/f}$ Cd4-Cre Bcl-2tg and *Myb*$^{f/w}$ Cd4-Cre Bcl-2tg mice were stained for CD4, CD8, CD3, CD69 and 7AAD surface expression and analyzed by five-color flow cytometry. CD4 versus CD8 distribution is seen through a live lymphocyte gate, and CD3 versus CD69 is seen through a $CD4^+CD8^+$ thymocyte gate. (B) DNA content analysis of CD8SP thymocytes was performed by flow cytometric analysis of CD4, CD8 and Draq5 staining. Through a CD8SP gate, the percentage of cells harboring >2n DNA content are shown. Results represent two separate experiments.

Bcl-xL expression is decreased in c-Myb deficient pre-selection DP thymocytes

To identify candidate c-Myb target genes that mediate protection from apoptosis through the intrinsic pathway, we performed mRNA expression microarray analysis and compared gene expression profiles of *Myb*$^{f/w}$ *Tcrα*$^{-/-}$ and *Myb*$^{f/f}$ *Tcrα*$^{-/-}$ DP thymocytes (See Appendix 2). A focused analysis of the ontology group Regulation of programmed cell death (GO: 0043067) identified a statistically significant 2.4 fold decrease in *Bcl2l1* (Bcl-xL) transcript levels (Table A3). In addition, while no pro-apoptotic members were clearly up-regulated, *Bcl2l1* was the only anti-apoptotic family member significantly down-regulated in *Myb*$^{f/f}$ *Tcrα*$^{-/-}$ DP thymocytes (Fig. 3.11A). The expression of *Bcl2l1*, like that of *Myb*, is specifically up-regulated in DP thymocytes (Grillot et al., 1995; Ma et al., 1995), making *Bcl2l1* an attractive candidate down-stream target of c-Myb.

The decrease in *Bcl2l1* mRNA level identified in the microarray experiment held true in sorted small DP thymocytes as measured by qRT-PCR (Fig. 3.11B). Surprisingly, we did not detect decreased expression of Bcl-xL protein by western blotting, despite undetectable levels of residual c-Myb protein in sorted small *Myb*$^{f/f}$ *Tcrα*$^{-/-}$ DP thymocytes (Fig. 3.12A). However, since the protein half-life of Bcl-xL (~18 hrs) greatly exceeds that of c-Myb (<1 hr) (Bies and Wolff, 1997; Klempnauer et al., 1986; Luscher and Eisenman, 1988; Mason et al., 2007) we reasoned that c-Myb deficient thymocytes that lack expression of Bcl-xL might die rapidly leaving mainly cells that maintain sufficient expression of Bcl-xL to survive. To address this possibility, Bcl-xL protein expression was examined in *Myb*$^{f/w}$ *Tcrα*$^{-/-}$ and *Myb*$^{f/f}$ *Tcrα*$^{-/-}$ DP thymocytes that either carried a Bcl-2tg or were treated with Z-VAD in liquid culture. Strikingly, both approaches revealed a

marked decrease in the Bcl-xL protein expression of c-Myb deficient DP thymocytes (Fig. 3.12A and B), suggesting that impaired survival masked the reduction in Bcl-xL protein in freshly isolated pre-selection DP thymocytes lacking c-Myb. We also compared Mcl-1 protein expression in *Myb*$^{f/f}$ *Tcrα*$^{-/-}$ and *Myb*$^{f/f}$ *Tcrα*$^{-/-}$ DP thymocytes with or without Bcl-2tg expression. Mcl-1 is another pro-survival member of the Bcl-2 family recently reported to play a role in the survival of DP thymocytes (Dzhagalov et al., 2008). Consistent with our mRNA expression microarray result (Fig. 3.11A), we did not detect a decrease in amount of Mcl-1 protein in *Myb*$^{f/f}$ *Tcrα*$^{-/-}$ DP thymocytes with or without Bcl-2tg expression (Fig. 3.12A). Thus, the reduced amount of Bcl-xL protein in *Myb*$^{f/f}$ *Tcrα*$^{-/-}$ Bcl-2tg DP thymocytes is protein specific among anti-apoptotic Bcl-2 family members.

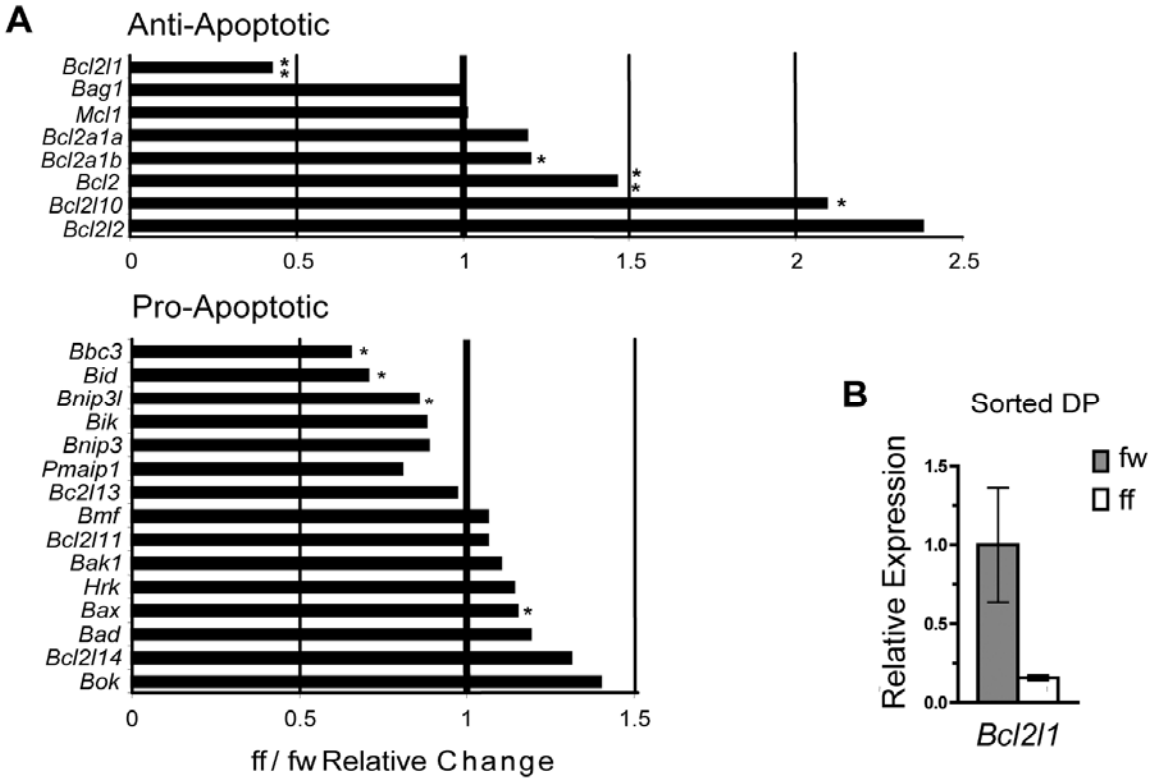

Figure 3.11 Decreased *Bcl2l1* mRNA expression in *Myb*$^{f/f}$ *Tcr*$\alpha^{-/-}$ DP thymocytes. (A) Changes in mRNA expression of Bcl-2 family members in c-Myb deficient pre-selection DP thymocytes detected by mRNA expression microarray analysis. mRNA expression microarray analysis was performed comparing DP thymocytes from *Myb*$^{f/w}$ Cd4-Cre *Tcr*$\alpha^{-/-}$ and *Myb*$^{f/f}$ Cd4-Cre *Tcr*$\alpha^{-/-}$ mice. Bar graphs represent mean of relative mutant:control mRNA expression of anti- and pro-apoptotic Bcl-2 family members in DP thymocytes. Genes of the Bcl-2 super family were manually selected from the complete GO:0043067:regulation of programmed cell death ontology list (Ashburner et al., 2000). n=4, *$p < 0.05$, **$p < 0.01$ (Student's *t*-test). (B) *Bcl2l1* mRNA expression was analyzed by quantitative real-time PCR in electronically sorted *Myb*$^{f/w}$ Cd4-Cre *Tcr*$\alpha^{-/-}$ and *Myb*$^{f/f}$ Cd4-Cre *Tcr*$\alpha^{-/-}$ DP thymocytes and normalized to *Hprt1* mRNA expression. Results are representative of 3 separate experiments.

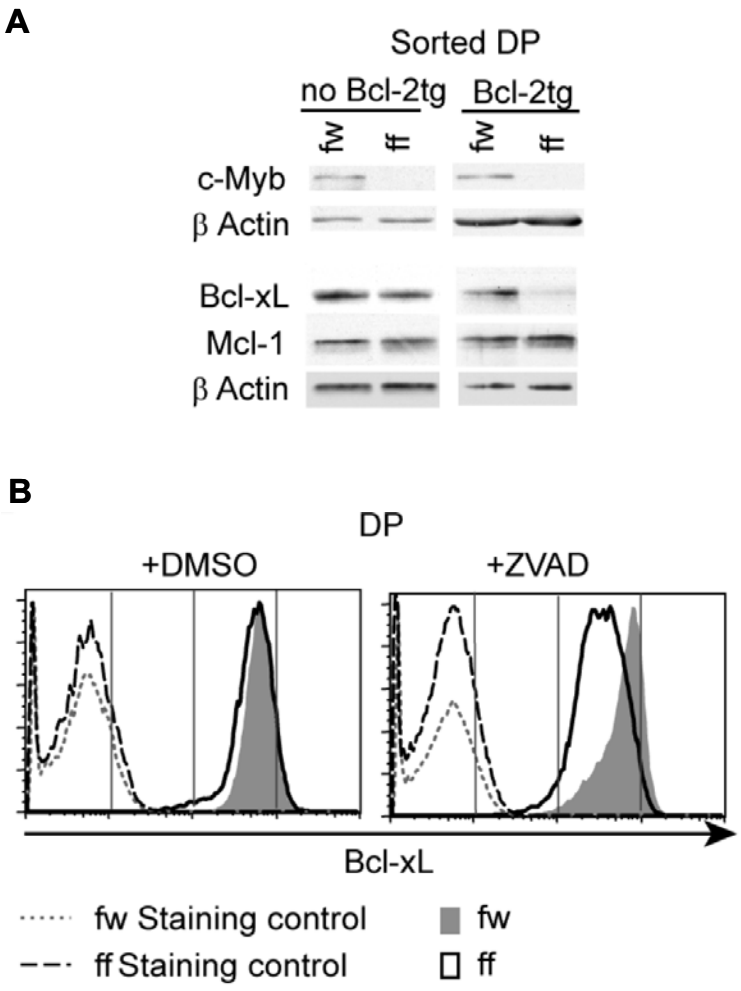

Fig 3.12 Decreased Bcl-xL protein expression in *Myb*$^{f/f}$ *Tcrα*$^{-/-}$ DP thymocytes. (A) Western blot of whole cell lysates from electronically sorted *Myb*$^{f/w}$ Cd4-Cre *Tcrα*$^{-/-}$ and *Myb*$^{f/f}$ Cd4-Cre *Tcrα*$^{-/-}$ DP thymocytes with and without Bcl-2tg expression probed for c-Myb, Bcl-xL, Mcl-1 and β-actin. (B) Intracellular staining for Bcl-xL, CD4 and CD8 in *Myb*$^{f/w}$ Cd4-Cre *Tcrα*$^{-/-}$ and *Myb*$^{f/f}$ Cd4-Cre *Tcrα*$^{-/-}$ DP thymocytes 24 hrs post culture with either 2 µl/ml DMSO or 40 µM Z-VAD. All antibodies except the anti-Bcl-xL primary antibody were used in the staining controls.

Exogenous c-Myb restores the expression of Bcl-xL in c-Myb deficient pre-selection DP thymocytes

To confirm that Bcl-xL is a down-stream effector of c-Myb mediated survival in DP thymocytes, we determined if an exogenous source of c-Myb could restore Bcl-xL expression and cell survival in *Myb*$^{f/f}$ *Tcrα*$^{-/-}$ DP thymocytes. We utilized an *in vitro* system in which thymocytes from *Myb*$^{f/w}$ *Tcrα*$^{-/-}$ and *Myb*$^{f/f}$ *Tcrα*$^{-/-}$ mice were allowed to differentiate in co-culture with OP9-Delta-like 1 (DL1) stromal cells (Schmitt and Zuniga-Pflucker, 2002), where the expression of genes could then be manipulated through retroviral transduction. After verifying that the survival defect previously observed in c-Myb deficient pre-selection DP thymocytes in liquid culture can be recapitulated in the OP9-DL1 co-culture system (Fig. 3.13), we designed an experimental scheme in which DN thymocytes, enriched by negative selection over anti-CD4 and anti-CD8 magnetic beads, were placed in co-culture, transduced with a c-Myb cDNA containing retrovirus (MIGR1-c-Myb) and allowed to differenitate into DP thymocytes (Fig. 3.14A). Transduced live DP thymocytes (7AAD^{-}, Thy1.2^{+}, GFP^{+}, CD4^{+}CD8^{+}) were electronically sorted 72hrs post-infection and subsequently either analyzed for *Bcl2l1* mRNA expression or cultured for an additional 24 hrs to assess survival. A decreased percentage of MIGR1 transduced *Myb*$^{f/f}$ *Tcrα*$^{-/-}$ DP thymocytes was observed on day 4 of co-culture compared to MIGR1 transduced control DP thymocytes (Fig. 3.14B), consistent with impaired survival in pre-selection DP thymocytes that lack c-Myb. Importantly, decreased survival upon additional culture of MIGR1 transduced *Myb*$^{f/f}$ *Tcrα*$^{-/-}$ DP thymocytes confirmed that the defect is intrinsic to the DP compartment and

not a consequence of impaired DN to DP transition (Fig. 3.14C). By the same criteria, MIGR1-c-Myb transduced *Myb*$^{f/f}$ *Tcrα*$^{-/-}$ thymocytes displayed complete restoration of survival. Importantly, qRT-PCR and intracellular flow cytometric analysis revealed restored expression of *Bcl2l1* mRNA and protein in MIGR1-c-Myb transduced *Myb*$^{f/f}$ *Tcrα*$^{-/-}$ DP thymocytes compared to MIGR1-c-Myb transduced control DP thymocytes (Fig. 3.14D and E), suggesting that c-Myb regulates *Bcl2l1* expression in pre-selection DP thymocytes. In addition, we repeatedly observed increased accumulation of *Myb*$^{f/f}$ *Tcrα*$^{-/-}$ FSC^{lo} DP thymocytes when transduced with MIGR1-c-Myb (Fig. 3.14F). This observation is consistent with increased survival and accumulation of the small pre-selection DP compartment. In accordance with the notion that Bcl-xL is a downstream effector of c-Myb in DP thymocytes, MIGR1-Bcl-xL transduced thymocytes also restored *Myb*$^{f/f}$ *Tcrα*$^{-/-}$ DP thymocyte survival (Figure 3.14G and H]. Taken together, these findings demonstrate that Bcl-xL acts as a physiological effector of c-Myb function in small pre-selection DP thymocytes to prolong a critical survival window. Importantly, an experimental system has been established through which we can interrogate the functional effect of over-expression or knockdown of genes potentially regulated by c-Myb during T cell development as well as verify putative c-Myb regulated genes. In addition to Bcl-xL, we took advantage of this system to demonstrate the restoration of several other candidate targets identified by the mRNA microarray screen to be either up- or down-regulated in pre-selection DP thymocytes that lack c-Myb (See Appendix Fig. A3), thereby confirming their regulation by c-Myb. Moreover, transduction of *Myb*$^{f/f}$ thymocytes using retroviruses containing structural c-Myb mutants provides an ideal

assay to test the requirement of c-Myb structural features and post-translational modifications in promoting DP thymocyte survival.

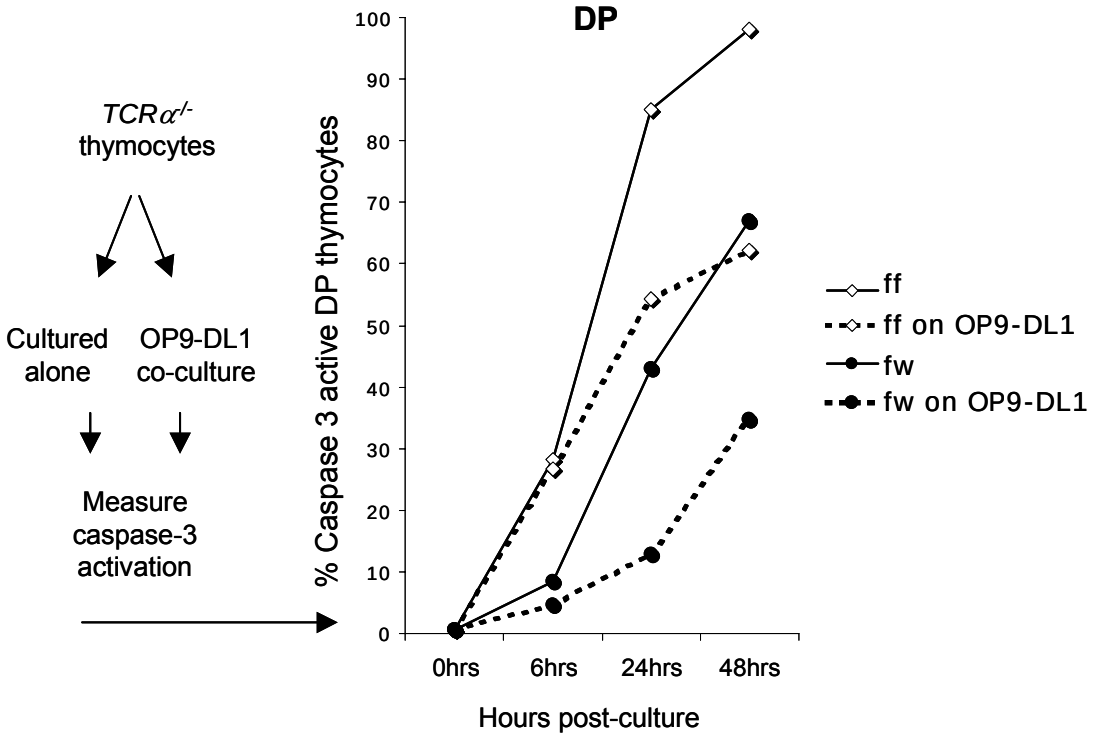

Figure 3.13 OP9-DL1 co-cultured *Myb*$^{f/f}$ Cd4-Cre *Tcrα*$^{-/-}$ DP thymocytes recapitulate the survival defect observed in *Myb*$^{f/f}$ Cd4-Cre *Tcrα*$^{-/-}$ single cultures. Total *Myb*$^{f/w}$ Cd4-Cre *Tcrα*$^{-/-}$ and *Myb*$^{f/f}$ Cd4-Cre *Tcrα*$^{-/-}$ thymocytes were co-cultured with OP9-DL1 stromal cells or alone for the indicated times and analyzed by flow cytometry for CD4, CD8 and active caspase-3. Results are representative of one experiment.

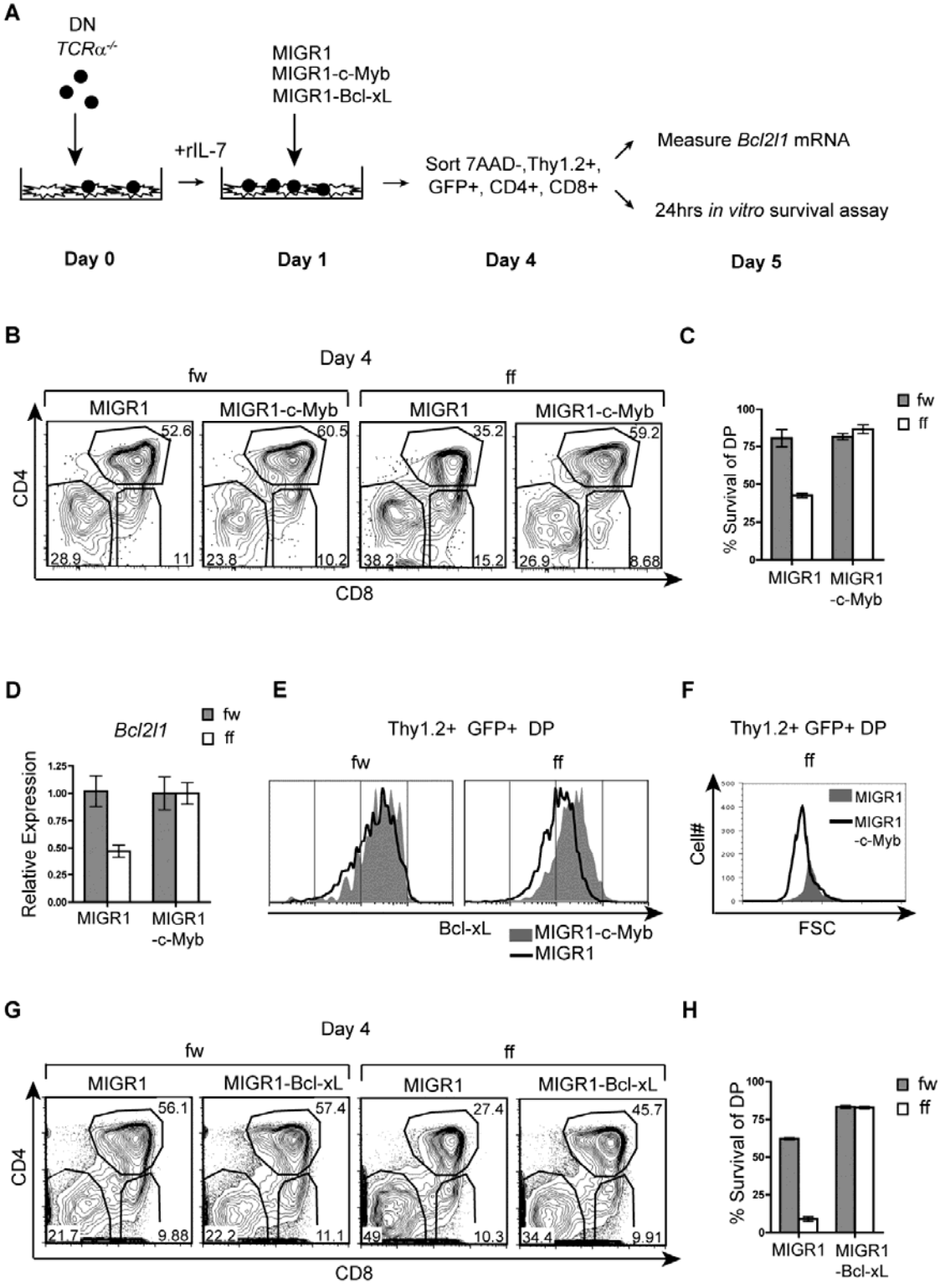
A
DN
TCRα-/-
+rIL-7
MIGR1
MIGR1-c-Myb
MIGR1-Bcl-xL
Sort 7AAD-,Thy1.2+,
GFP+, CD4+, CD8+
Measure Bcl2l1 mRNA
24hrs in vitro survival assay
Day 0
Day 1
Day 4
Day 5
B
Day 4
fw
ff
MIGR1
MIGR1-c-Myb
52.6
60.5
35.2
59.2
28.9
11
23.8
10.2
38.2
15.2
26.9
8.68
CD4
CD8
C
% Survival of DP
fw
ff
MIGR1
MIGR1 -c-Myb
D
Bcl2l1
Relative Expression
E
Thy1.2+ GFP+ DP
Bcl-xL
MIGR1-c-Myb
MIGR1
F
Thy1.2+ GFP+ DP
Cell#
FSC
G
Day 4
MIGR1-Bcl-xL
56.1
57.4
27.4
45.7
21.7
9.88
22.2
11.1
49
10.3
34.4
9.91
H
MIGR1 -Bcl-xL

Figure 3.14 An exogenous source of c-Myb restores Bcl-xL expression and survival in *Myb$^{f/f}$ Tcrα$^{-/-}$* DP thymocytes. (A) Experimental plan to rescue survival of DP thymocytes by retroviral transduction in OP9-DL1 stromal cell cultures. (B) Day 4 co-cultures transduced with MIGR1-c-Myb or MIGR1 were analyzed by flow cytometry for CD4 and CD8 surface expression through a Thy1.2^{+}7AAD^{-}GFP^{+} gate. Results are representative of 4 separate experiments. (C) DP thymocytes transduced with MIGR1-c-Myb or MIGR1 were electronically sorted on day 4 of co-culture and cultured for an additional 24hrs to assess spontaneous apoptosis as measured by Annexin 5 and 7AAD staining. Results are presented as mean +/- SEM and are representative of 4 separate experiments. (D) Transduced DP thymocytes from 4B were electronically sorted and *Bcl2l1* mRNA expression was analyzed by quantitative real-time PCR. Data is normalized to *Hprt1* mRNA expression. Results are presented as mean +/- SEM and are representative of 3 separate experiments. (E) Intracellular staining for Bcl-xL of MIGR1-c-Myb or MIGR1 transduced *Myb$^{f/w}$ Tcrα$^{-/-}$* and *Myb$^{f/f}$ Tcrα$^{-/-}$* DP thymocytes. To retain *Myb$^{f/f}$ Tcrα$^{-/-}$* DP thymocytes with reduced Bcl-xL protein, 40 μM Z-VAD was added to the co-cultures 48 hrs prior to intracellular staining on day 5. Results are representative of 3 separate experiments. (F) Forward light scatter profiles of MIGR1-c-Myb or MIGR1 transduced *Myb$^{f/f}$* DP thymocytes on day 4 of co-culture measured by flow cytometry. Results are representative of 3 separate experiments. (G) Day 4 co-cultures transduced with either MIGR1-Bcl-xL or MIGR1 were analyzed for CD4 and CD8 expression by flow cytometry through a Thy1.2^{+}7AAD^{-}GFP^{+} gate. Results are representative of 3 separate experiments. (H) DP thymocytes transduced with either MIGR1-Bcl-xL or MIGR1 were sorted on day 4 of co-culture and cultured for an

additional 24hrs to assess spontaneous apoptosis as measured by Annexin 5 and 7AAD staining. Results are presented as mean +/- SEM and are representative of 3 separate experiments.

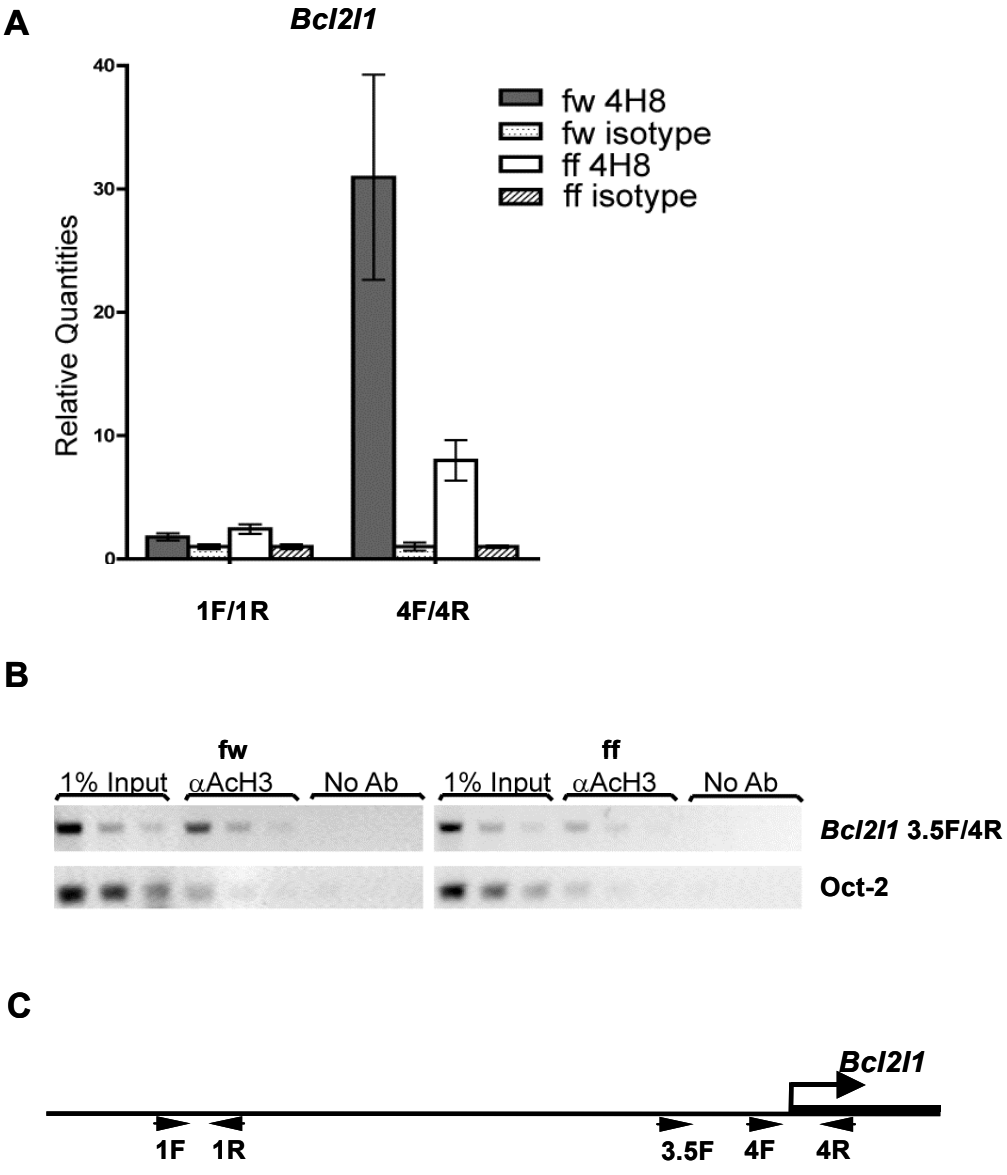

Figure 3.15 c-Myb promotes *Bcl2l1* expression at the level of transcription. (A) RNA polymerase II ChIP in *Myb*$^{f/w}$ Cd4-Cre *Tcrα*$^{-/-}$ and *Myb*$^{f/f}$ Cd4-Cre *Tcrα*$^{-/-}$ total thymocytes. Precipitated genomic DNA was amplified using primer sets (4F and 4R) specific to either the transcription initiation site (+1) or a negative control site approximately 1kb upstream (-1000bp) (1F and 1R) by qRT-PCR. Results are normalized to IgG control samples and presented as mean +/- SEM and are representative of 2 independent experiments. (B) Anti-acetylated histone H3 ChIP in *Myb*$^{f/w}$ Cd4-Cre *Tcrα*$^{-/-}$ and *Myb*$^{f/f}$ Cd4-Cre *Tcrα*$^{-/-}$ total thymocytes. Precipitated genomic DNA was amplified using primer sets (F3.5 and R4) surrounding the transcriptional start site by semi quantitative PCR. Primers for the *Oct-2* promoter were used as a negative control (McMurry and Krangel, 2000). ChIP Results are representative of 2 independent experiments. (C) Orientations and approximate positions of ChIP PCR primers.used are indicated in relationship to the *Bcl2l1* transcriptional start site in thymocytes.

A

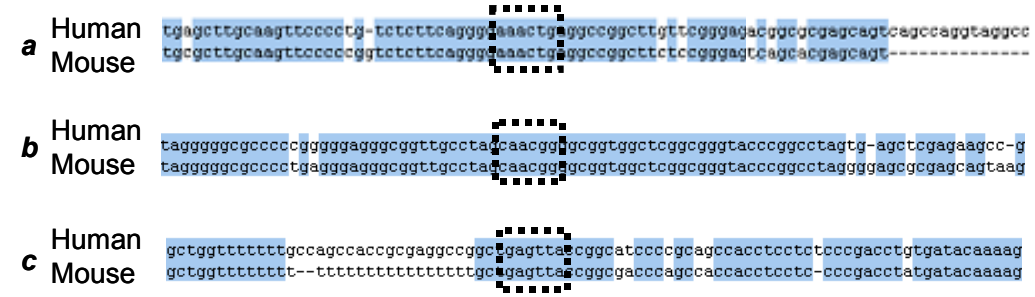
a
Human
Mouse
b
Human
Mouse
c
Human
Mouse

B

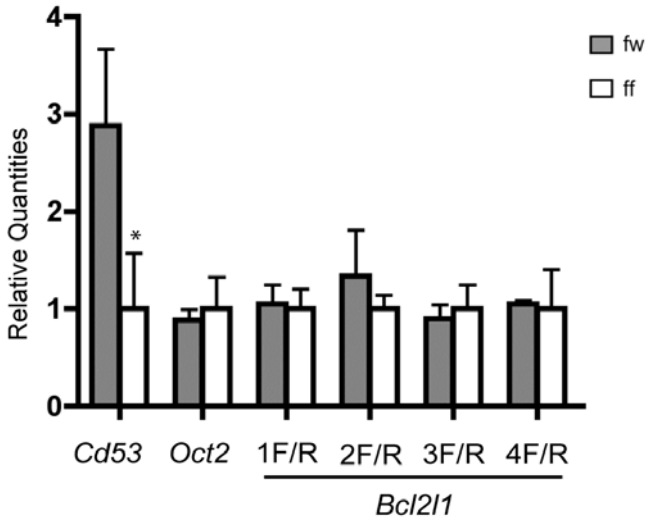
fw
ff
Relative Quantities
0
1
2
3
4
*
Cd53
Oct2
1F/R
2F/R
3F/R
4F/R
Bcl2l1

C

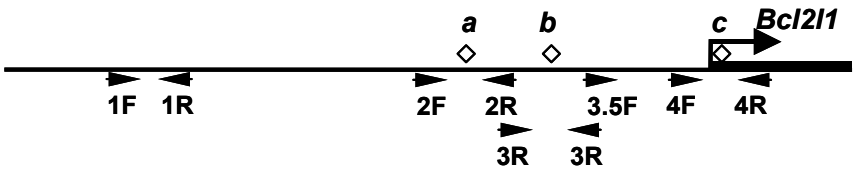
a
b
c
Bcl2l1
1F
1R
2F
2R
3R
3R
3.5F
4F
4R

Figure 3.16 No enrichment of c-Myb was detectable at three potential c-Myb binding sites of the *Bcl2l1* promoter by ChIP. (A) Sequence alignment of the human and mouse *Bcl2l1* promoter region was performed using Clone Manager (Sci-Ed Software, Cary, NC). Grey area highlights sequence conservation. Three conserved MRE sequences (a-c) were identified as indicated. (B) Anti-c-Myb (Epitomics, Burlingame, CA) precipitated DNA from $Myb^{f/w}$ Cd4-Cre $Tcr\alpha^{-/-}$ and $Myb^{f/f}$ Cd4-Cre $Tcr\alpha^{-/-}$ total thymocytes was amplified using primers surrounding the three potential c-Myb binding sites as follows. Primers 2 F/R surrounds MRE a, 3 F/R surrounds MRE b and 4 F/R surrounds MRE c. Primers surrounding a validated c-Myb binding site in the *Cd53* promoter was used as positive control (Lang et al., 2005). Primers surrounding an arbitrary site in the *Oct2* promoter (McMurry and Krangel, 2000) as well as primers surrounding a site upstream of the putative c-Myb binding sites (1 F/R) in the *Bcl2l1* promoter were used as negative controls. Quantitative real-time PCR results are presented as the mean and SEM of relative fw/ff signal from three sets of mice. (C) Map of *Bcl2l1* promoter region. Diamonds represent MRE consensus sites. Horizontal arrows represent primer localization and orientation.

c-Myb regulates transcription at the *Bcl2l1* locus independent of RORγt and TCF-1 expression

To determine if the decrease in Bcl-xL expression in c-Myb deficient DP thymocytes is indeed a consequence of reduced transcription at the *Bcl2l1* locus we measured RNA pol2 localization at the previously identified transcriptional start site (primers F4 and R4) (Grillot et al., 1997) by chromatin immunoprecipitation (ChIP). Primers that amplify a site approximately 1kb up-stream of the transcriptional start site (primers F1 and R1) were used as negative control. qPCR of DNA precipitated with anti-RNA pol2 revealed a 31-fold enrichment of over isotype control at the transcriptional start site in total $Myb^{f/w}$ $Tcr\alpha^{-/-}$ thymocytes compared to an 8-fold enrichment in $Myb^{f/f}$ $Tcr\alpha^{-/-}$ thymocytes (Fig. 3.15A). No enrichment was detected in either sample using the negative control primer set F1/R1 (Fig. 3.15A), demonstrating that c-Myb regulates Bcl-xL expression in pre-selection DP thymocytes by promoting transcription at the *Bcl2l1* locus. Histone H3K9 acetylation is an active mark of transcription that is highly enriched at transcriptional start sites and has been found to correlate with increased transcription at the *Bcl2l1* locus (Ezzat et al., 2006; Wang et al., 2008). To investigate if the extent of this modification is altered in c-Myb deficient thymocytes, we performed chromatin immunoprecipitation using an anti-acetyl-H3K9/K14 antibody predominantly recognizing acetyl H3K9 (Wang et al., 2008), and detected an approximate 3-fold decrease in acetylation at the *Bcl2l1* promoter region in $Myb^{f/w}$ $Tcr\alpha^{-/-}$ compared to $Myb^{f/f}$ $Tcr\alpha^{-/-}$ thymocytes by semi-quantitative PCR amplification (Fig. 3.15B). This result suggests that c-Myb is able to

directly or indirectly influence the chromatin structure at the *Bcl2l1* promoter to facilitate transcription activation.

DNA sequence analysis identified three potential c-Myb binding sites in the *Bcl2l1* promoter region that are conserved between humans and mice (Fig. 3.16A). To investigate if any of these sites are occupied by c-Myb *in vivo* we performed anti-c-Myb ChIP. In recent years, the success of c-Myb ChIP has been severely limited by the availability of good antibodies for immunoprecipitation. We achieved best success using a rabbit monoclonal antibody directed at the N-terminal of the c-Myb polypeptide. The efficacy of the anti-c-Myb ChIP was verified in $Myb^{f/w}$ $Tcr\alpha^{-/-}$ thymocytes by a statistically significant enrichment at a previously identified c-Myb binding site in the promoter region of *Cd53* (Lang et al., 2005), a gene that is normally induced during positive selection and prematurely de-repressed in c-Myb deficient pre-selection DP thymocytes (See Appendix Fig. A5). However, anti-c-Myb ChIP in $Myb^{f/w}$ $Tcr\alpha^{-/-}$ thymocytes did not reveal enrichment of c-Myb at any of the three potential binding sites compared to $Myb^{f/f}$ $Tcr\alpha^{-/-}$ thymocytes (Fig. 3.16B). These results suggest that c-Myb regulates *Bcl2l1* expression at the level of transcription, but likely not through direct binding to the three conserved c-Myb binding sites in the proximal *Bcl2l1* promoter.

Deficiency of TCF-1 or RORγt results in the premature apoptosis of DP thymocytes due to decreased Bcl-xL expression (Ioannidis et al., 2001; Sun et al., 2000). To determine if the absence of c-Myb results in altered expression of TCF-1 or RORγt, we examined their mRNA and protein expression in sorted $Myb^{f/w}$ $Tcr\alpha^{-/-}$ and $Myb^{f/f}$ $Tcr\alpha^{-/-}$ DP thymocytes. To reveal potential changes in protein expression that might be masked

by impaired survival we also measured the amount of TCF-1 and RORγt protein in *Myb*$^{f/w}$ *Tcrα*$^{-/-}$ and *Myb*$^{f/f}$ *Tcrα*$^{-/-}$ DP thymocytes that carry a Bcl-2tg. mRNA expression detected by mRNA expression microarray and qRT-PCR in sorted small pre-selection DP thymocytes did not reveal statistically significant changes in the expression of *Tcf1* and *Rorγ* (Fig. 3.17A and Appendix Table A2). Moreover, western blot analysis using electronically sorted DP thymocytes did not reveal differences in protein expression of TCF-1 or RORγt between *Myb*$^{f/w}$ *Tcrα*$^{-/-}$ and *Myb*$^{f/f}$ *Tcrα*$^{-/-}$ mice with or without Bcl-2tg expression (Fig. 3.17B). Thus, decreased expression of Bcl-xL in c-Myb deficient DP thymocytes is not the result of impaired TCF-1 or RORγt expression.

To determine if TCF-1 or RORγt promote Bcl-xL expression indirectly through modulating c-Myb expression, we compared c-Myb protein expression in *Tcf1*$^{-/-}$ and *Rorγt*$^{-/-}$ to wildtype total thymocytes (Lee et al., 2001; Strasser et al., 1991). We also detected no difference in the amount of c-Myb contained in *Tcf1*$^{-/-}$, *Rorγt*$^{-/-}$ and B6 thymocytes by western blot (Fig. 3.17C), suggesting that TCF-1 and RORγt do not control c-Myb expression during T cell development. Interestingly, we observed an apparent decrease in the amount of RORγt protein in *Tcf1*$^{-/-}$ thymocytes but no change in the amount of TCF-1 protein in *Rorγt*$^{-/-}$ thymocytes (Fig. 3.17C), suggesting that TCF-1 may indirectly stimulate Bcl-xL expression by up-regulating RORγt expression during T cell development. Taken together, our results demonstrate that c-Myb promotes transcription at the *Bcl2l1* locus in DP thymocytes via a distinct genetic pathway, independent of RORγt and TCF-1 expression.

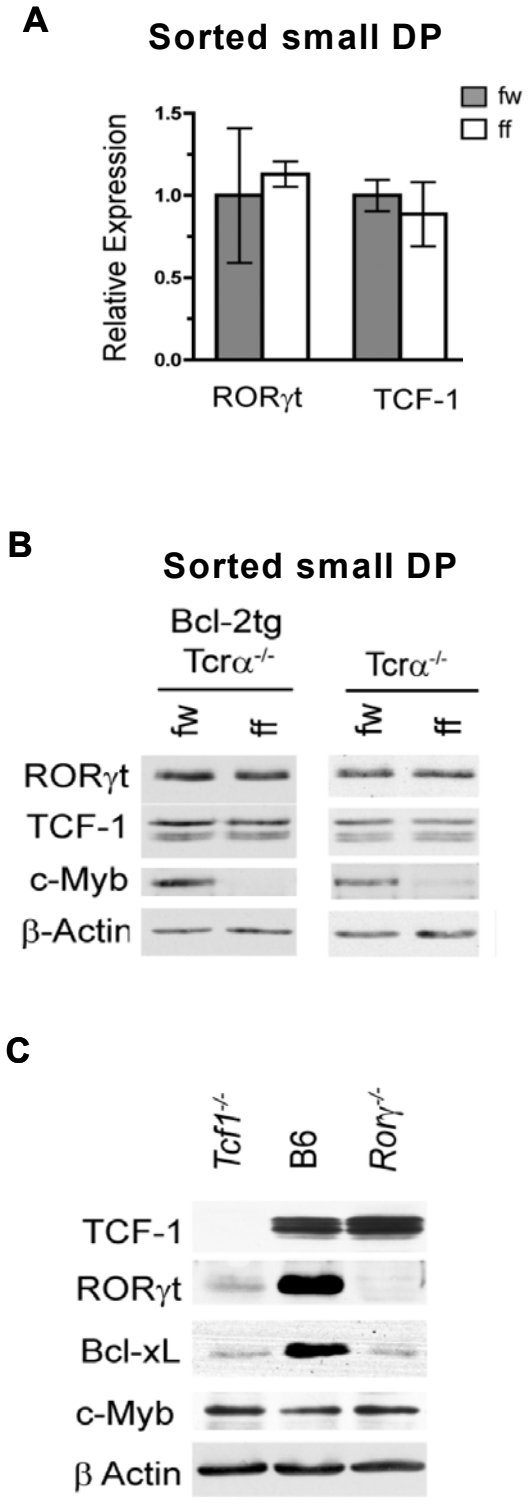

Figure 3.17 c-Myb promotes Bcl-xL expression via a novel genetic pathway independent of TCF-1 and RORγt expression (A) *Rorγ* and *Tcf1* mRNA levels in sorted *Myb*$^{f/w}$ Cd4-Cre *Tcrα*$^{-/-}$ and *Myb*$^{f/f}$ Cd4-Cre *Tcrα*$^{-/-}$ DP thymocytes measured by quantitative real-time PCR and normalized to *Hprt1* mRNA expression. Data are presented as mean +/- SEM and representative of 2 independent experiments. (B) Western blot of whole cell lysates from sorted *Myb*$^{f/w}$ Cd4-Cre *Tcrα*$^{-/-}$ and *Myb*$^{f/f}$ Cd4-Cre *Tcrα*$^{-/-}$ DP thymocytes with and without of Bcl-2tg expression probed for TCF-1, RORγt, c-Myb and β-actin. (C) Western blot of whole cell lysates from *Rorγ*$^{-/-}$, C57BL/6j, and *Tcf1*$^{-/-}$ total thymocytes probed for TCF-1, RORγt, c-Myb, Bcl-xL and β-actin.

Small but not large pre-selection DP thymocytes are dependent on Bcl-xL for survival

It has been well established that Bcl-xL is a crucial survival factor in DP thymocytes (Grillot et al., 1995; Ma et al., 1995). Our observation that the number of small but not large DP thymocytes was reduced in *Myb*$^{f/f}$ *Tcrα*$^{-/-}$ compared to *Myb*$^{f/w}$ *Tcrα*$^{-/-}$ mice suggested that c-Myb and Bcl-xL are obligatory only for the survival of small pre-selection DP thymocytes (Fig. 3.5A). However, this notion was based on the assumption that large *Myb*$^{f/f}$ *Tcrα*$^{-/-}$ DP thymocytes contained significantly less Bcl-xL protein than *Myb*$^{f/w}$ *Tcrα*$^{-/-}$, and it remained possible that these cells may have retained sufficient amounts of Bcl-xL made prior to mediated deletion at the *Myb* locus. To clarify this point, we monitored Bcl-xL protein expression and cell survival as *Myb*$^{f/w}$ *Tcrα*$^{-/-}$ and *Myb*$^{f/f}$ *Tcrα*$^{-/-}$ thymocytes differentiated from the large to the small pre-selection DP stage *in vitro* based on a previously described assay (Yu et al., 2004). Thymocytes were depleted of the DP population on magnetic beads and placed in liquid culture, allowing DN and ISP thymocytes that have received preTCR signals *in vivo* to differentiate into the large and small pre-selection DP stage followed by death by neglect in a synchronous manner. After 20 and 36 hrs, *in vitro* differentiated DP thymocytes from both *Myb*$^{f/f}$ *Tcrα*$^{-/-}$ and *Myb*$^{f/w}$ *Tcrα*$^{-/-}$ mice consisted predominantly of large and small pre-selection DP thymocytes respectively (Fig. 3.18A). At 20 hrs post culture, reduced intracellular Bcl-xL protein was readily detectable without Z-VAD treatment in *Myb*$^{f/f}$ *Tcrα*$^{-/-}$ DP thymocytes compared to *Myb*$^{f/w}$ *Tcrα*$^{-/-}$ DP thymocytes (Fig. 3.18B) while no significant difference was detected in their ability to survive (Fig. 3.18C). This result demonstrates

that Bcl-xL protein expression is significantly reduced in *Myb*$^{f/f}$ *Tcrα*$^{-/-}$ large DP thymocytes without a negative impact on their survival and is consistent with a model where c-Myb and Bcl-xL are not required for the survival of large pre-selection DP thymocytes. This is in contrast to 36 hrs post culture, when we observed no difference in Bcl-xL protein expression (Fig. 3.18B) but significantly impaired survival in *Myb*$^{f/f}$ *Tcrα*$^{-/-}$ DP thymocytes (Fig. 3.18C), indicative of a survival defect in DP thymocytes harboring reduced Bcl-xL protein. This phenotype closely resembles our observations in total thymocytes without Z-VAD treatment, likely because the DP compartment is largely composed of small pre-selection DP thymocytes *in vivo* both in *Myb*$^{f/w}$ *Tcrα*$^{-/-}$ (~90%) and *Myb*$^{f/f}$ *Tcrα*$^{-/-}$ (~80%) mice (Fig. 3.5A). Collectively, these results support a model where thymocyte survival becomes dependent on Bcl-xL at a point near the end of the proliferative large pre-selection DP stage or as developing thymocytes enter the quiescent small pre-selection stage.

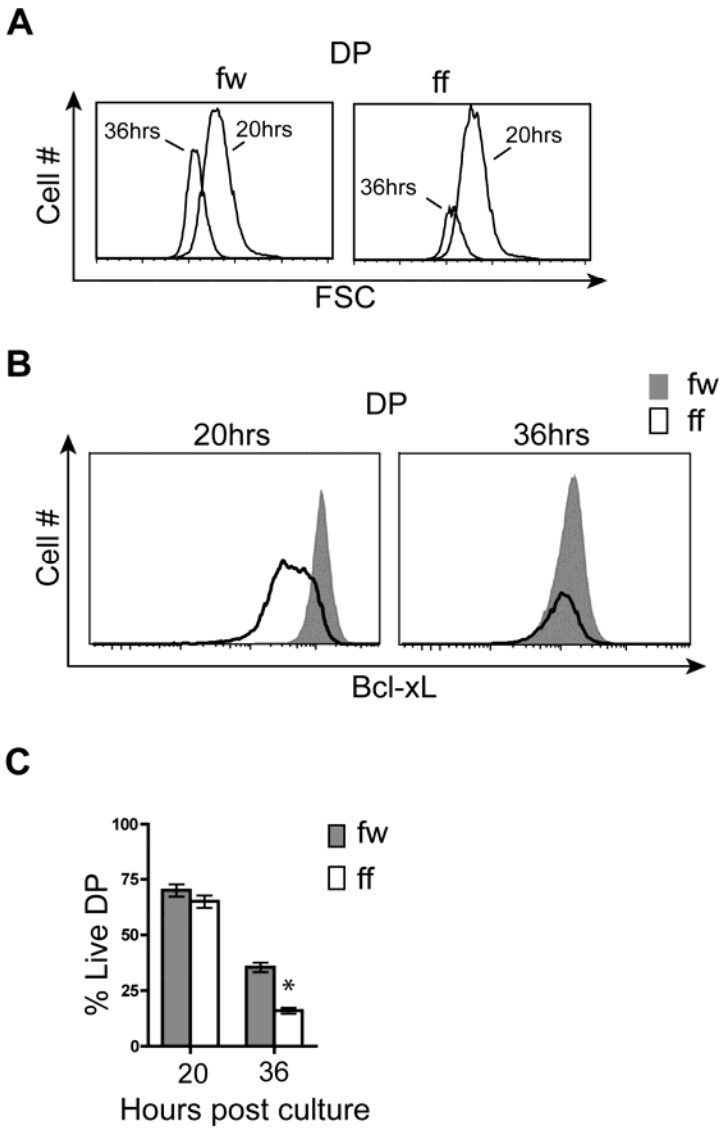

Figure 3.18 Small but not large pre-selection DP thymocytes are acutely sensitive to reduced intracellular Bcl-xL. Total *Myb*$^{f/w}$ *Tcrα*$^{-/-}$ and *Myb*$^{f/f}$ *Tcrα*$^{-/-}$ thymocytes were depleted of DP thymocytes using MACS CD4 MicroBeads. Negatively selected cells were subsequently cultured for 20 or 36 hrs and analyzed by flow cytometry. (A) Histogram overlays present the change in FSC of *Myb*$^{f/w}$ *Tcrα*$^{-/-}$ and *Myb*$^{f/f}$ *Tcrα*$^{-/-}$ DP thymocytes from 20 to 36 hrs post culture. (B) Intracellular staining for Bcl-xL measured by flow cytometry at 20hrs and 36 hrs post culture through a live DP thymocyte gate. (C) Assessment of DP thymocyte survival after 20 hrs and 36 hrs in culture by staining for CD4, CD8, 7AAD and Annexin 5. Results are presented as mean +/- SEM. n≥3, *p < 0.005 (Student's *t*-test).

3.3 DISCUSSION

Apoptosis is an essential process underlying normal lymphocyte development and dysregulated control of apoptosis can lead to autoimmune disease or immunodeficiency. The intrinsic lifespan of pre-selection DP thymocytes regulates the composition and diversity of the *Tcrα* repertoire and is therefore critical to normal T cell development (Guo et al., 2002). Thymocytes enter the DP stage as large proliferating cells and initiation of *Tcrα* recombination coincides with the transition of large pre-selection DP thymocytes into a small, quiescent subset that is prone to death by neglect (Petrie et al., 1995; Rathmell et al., 2000; Yu et al., 2006). We previously reported that c-Myb is required for the survival of DP thymocytes in an αβ-TCR independent fashion (Bender et al., 2004). We now demonstrate that c-Myb expression is up-regulated in small, pre-selection DP thymocytes where it promotes survival by controlling the expression of Bcl-xL. Thymocytes have developed a mechanism to efficiently increase Bcl-xL expression in the pre-selection DP compartment to promote survival and increase the opportunity for assembling an αβ-TCR (Grillot et al., 1995; Guo et al., 2002; Ma et al., 1995). Our observation that c-Myb deficient DP thymocytes exhibit a *Tcrα* repertoire that is skewed toward the use of 5' located *Jα* segments demonstrates that c-Myb plays a crucial role in determining the window of time that is available for developing thymocytes to produce a diverse *Tcrα* repertoire.

Spontaneous apoptosis of DP thymocytes in liquid culture mimics death by neglect and is thought to be controlled by the balanced functions of Bcl-xL and the pro-apoptotic Bcl-2 family members Bax, Bak and Bim in a cytochrome c/Apaf-1/caspase-9

apoptosome independent fashion (Bouillet et al., 1999; Guo et al., 2002; Marsden et al., 2002; Rathmell et al., 2002). Our mRNA expression microarray experiments identified a unique decrease in *Bcl2l1* mRNA expression among the anti-apoptotic Bcl-2 family members but no obvious changes in the expression of pro-apoptotic Bcl-2 family members in c-Myb deficient DP thymocytes. This finding, combined with our ability to rescue survival in c-Myb deficient DP thymocytes with exogenously supplied Bcl-xL, is consistent with previous work that described a non-redundant role for Bcl-xL in DP thymocyte survival (Ma et al., 1995; Sun et al., 2000). A recent report examined the synergy of Bcl-xL and Mcl-1 in promoting DP thymcyte survival implying functional redundancy *in vivo* (Dzhagalov et al., 2008). To clarify this point, we carefully analyzed Mcl-1 expression and detected no difference in the level of Mcl-1 mRNA or protein in c-Myb deficient DP thymocytes. Thus, our results demonstrate that reduced expression of Bcl-xL alone is sufficient to have a significant impact on pre-selection DP thymocyte survival.

Few effectors of c-Myb activity have been identified and tested in physiologically relevant models to date. We demonstrate that the efficient up-regulation of Bcl-xL expression in pre-selection DP thymocytes is controlled at least in part at the level of transcription by c-Myb as RNA polymerase II localization at the *Bcl2l1* transcription start site was decreased in c-Myb deficient thymocytes. Consistent with a direct role for c-Myb in promoting *Bcl2l1* transcription, we identified three consensus MREs in the mouse *Bcl2l1* promoter (Grillot et al., 1997) that are conserved in humans. However, we were unable to directly localize c-Myb to these sites by ChIP assay. Thus, c-Myb may

promote Bcl-xL transcription through an indirect mechanism, although it remains possible that c-Myb may tether to the *Bcl2l1* promoter through protein-protein interactions independently of its DNA binding domain through several scenarios (Fig. 3.19), or interact with as yet unidentified regulatory regions that control *Bcl2l1* transcription. Indeed, atomic force microscopy has visualized the ability of c-Myb to participate in long range transcriptional regulation through protein-protein interaction and DNA looping (Tahirov et al., 2002). Thus, despite the importance of *Bcl2l1* in DP thymocytes, direct binding of a transcription factor to its promoter region remains to be discovered. Irrespective of the precise mode of regulation, we demonstrate that c-Myb controls transcription at the *Bcl2l1* locus in small pre-selection DP thymocytes and that Bcl-xL is a down-stream effector of c-Myb activity during normal T cell development. The implications of this finding may reach beyond normal T cell development to the association of duplication events at the *Myb* locus in over eight percent of human T-ALL and attendant defects in the control of survival, proliferation and differentiation in these tumors (Clappier et al., 2007; Lahortiga et al., 2007).

With this study, we have made clear that c-Myb, RORγt and TCF-1 are all necessary components in the developmental program responsible for the critical up-regulation of Bcl-xL expression in the pre-selection DP compartment. The expression of all three transcription factors is up-regulated in DP thymocytes. The induction of both RORγt and TCF-1 expression is known to require signaling through the preTCR (Goux et al., 2005; Xi and Kersh, 2004b) as well as cessation of IL-7 receptor signaling during T cell development (Yu et al., 2004). Our finding that RORγt protein expression is

diminished in thymocytes that lack TCF-1 supports a model where TCF-1 indirectly promotes Bcl-xL expression by regulating RORγt expression (Fig. 3.20). Signals that mediate the up-regulation of c-Myb during the DP stage remain elusive. However, western blot analysis demonstrates that c-Myb protein expression does not control nor is itself controlled by RORγt or TCF-1 protein expression. Thus, our data demonstrate that c-Myb is a component of a novel genetic pathway that promotes transcription at the *Bcl2l1* locus in DP thymocytes independent of TCF-1 and RORγt expression.

Our studies have identified a previously unrecognized difference in the requirement for Bcl-xL in the maintenance of the small but not the large pre-selection DP thymocyte compartment. c-Myb deficient small pre-selection DP thymocytes are rapidly eliminated from the thymus upon loss of Bcl-xL protein expression, but no significant decrease in the cellularity or survival of large preselection DP thymocytes was detectable despite the loss of Bcl-xL in the absence of c-Myb. In addition, the continued survival of large pre-selection DP thymocytes after the loss of Bcl-xL protein offers a likely explanation to why reduced Bcl-xL protein is readily detectable in freshly isolated $Ror\gamma^{-/-}$ and $Tcf1^{-/-}$ thymocytes but not $Myb^{f/f}$ $Tcr\alpha^{-/-}$ thymocytes. $Ror\gamma^{-/-}$ DP thymocytes are blocked in the large pre-selection stage due to an inability to withdraw from cell cycle (Sun et al., 2000; Xi et al., 2006). The $Tcf1^{-/-}$ DP compartment is also mainly composed of large pre-selection DP thymocytes (data not shown), possibly due to insufficient amounts of RORγt. In contrast, the $Myb^{f/f}$ DP compartment consists of mainly small pre-selection DP thymocytes. Since only the small pre-selection DP thymocytes appear to undergo increased apoptosis after the loss of Bcl-xL expression, only those cells remain

that produce sufficient amounts of Bcl-xL to survive. The developmental block observed at the large pre-selection stage in *Rorγ*$^{-/-}$ but not *Myb*$^{f/f}$ mice suggests that RORγt is required for both transition to as well as the survival of the small pre-selection DP compartment while c-Myb is mainly important for the latter (Table 3.1).

Table 3.1 Compare and contrast the pro-survival roles of RORγt and c-Myb in DP thymocytes

	***Rorγ*$^{-/-}$ DP**	***Myb*$^{f/f}$ Cd4-Cre DP**
Large to small transition	X	√
Withdrawal from cell cycle	X	√
DP thymocyte survival defect	X	X
Roscovitine induced survival rescue	√	X
Decrease in Bcl-xL expression	√	√
Ease in detecting decreased Bcl-xL protein	√	X
	Failure to enter (and maintain) the smDP compartment	Failure to maintain the smDP compartment

Previously, we reported that representation of the CD4SP thymocyte compartment is decreased in the absence of c-Myb. However, interpretation of this data was confounded by premature cell death and a limited *Tcrα* repertoire among DP thymocytes deficient in c-Myb. Here we demonstrate that a Bcl-2tg can correct premature cell death but not decreased CD4SP representation in the thymus. This finding demonstrates that c-Myb regulates the development of CD4SP thymocytes independent of premature apoptosis. In addition, Bcl-2tg expression revealed a previously unrecognized increase in

the percentage of positively selected DP thymocytes and mature CD8SP thymocytes in c-Myb deficient mice, suggesting that c-Myb may be a negative regulator of positive selection and CD8SP thymocyte development. These observations demonstrate that the αβ-TCR independent survival defect of c-Myb deficient DP thymocytes masks important αβ-TCR dependent manifestations of c-Myb deficiency during T cell development. The latter is likely to be addressed using a model such as *Myb*$^{f/f}$ Bcl-2 tg mice where DP to SP differentiation is not convoluted by a impaired survival.

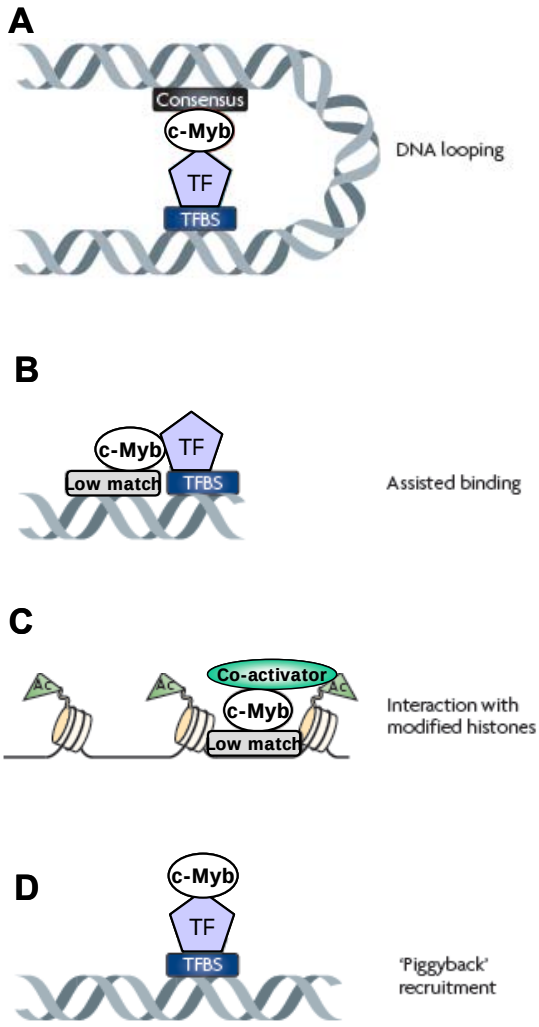

Figure 3.19 Possible scenarios for c-Myb binding to sites that lack the consensus MRE. (A) c-Myb could bind to its consensus motif and loop, as a result of protein–protein interactions, to interact with another transcription factor (TF) that is bound to a distant site (TFBS) of the chromosome. (B, C) c-Myb could bind to a sequence that has a low match to its MRE (Low match) and be anchored onto the DNA by protein–protein interactions with a transcription factor (B) or a co-activator recruited to a modified, for example acetylated (Ac), histone. D) c-Myb could be recruited to a DNA sequence by protein-protein interactions with another transcription factor independent of its DBD. Figure adapted from (Farnham, 2009).

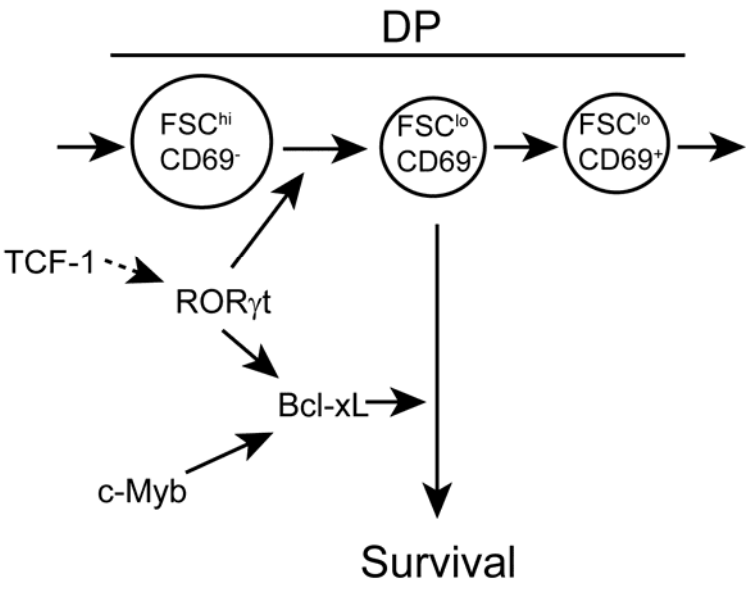

Figure 3.20 A model depicting the regulatory network that controls Bcl-xL expression in pre-selection DP thymocytes. Bcl-xL is necessary for the survival of small pre-selection DP thymocytes during αβ-T cell development. c-Myb, RORγt and TCF-1 are all required to efficiently up-regulate Bcl-xL expression in DP thymocytes. RORγt also promotes the large to small pre-selection DP transition. Increased c-Myb expression in small pre-selection DP thymocytes promotes the expression of Bcl-xL by a genetic pathway independent of RORγt and TCF-1. Expression of RORγt appears to be TCF-1 dependent.

Chapter IV General discussion and future directions

We have previously used conditional mutagenesis at the *Myb* locus to demonstrate that c-Myb plays a multifaceted role during the DP stage of T cell development, including promoting the survival of pre-selection DP thymocytes and development of CD4SP thymocytes (Bender et al., 2004). However, the survival defect was poorly understood and it was therefore impossible to asses its impact on impaired CD4SP development. Work in this thesis used mouse genetics to isolate the separate roles of c-Myb within DP thymocytes in survival and differentiation, and identified Bcl-xL as a *bona fide* down-stream mediator of the former. This thesis has established that c-Myb controls Bcl-xL expression at the level of transcription by a novel genetic pathway and that only small but not large pre-selection DP thymocytes are dependent on c-Myb and Bcl-xL for survival. This represents the first study to identify a physiological mediator of the long recognized pro-survival function of c-Myb in lymphocytes and sheds light on the regulatory network that controls DP thymocyte survival. Going forward, many questions remain to be answered pertaining the regulation and mechanism of c-Myb function. This chapter will discuss the rationale and strategies applicable for pursuing these questions.

What is the precise mechanism by which c-Myb regulates *Bcl2l1* transcription in pre-selection DP thymocytes?

In this study, *Bcl2l1* was identified as a c-Myb target in a genome-wide comparison of the mRNA expression profiles between pre-selection DP thymocytes sufficient and deficient for c-Myb. The list of differentially expressed genes identified by this approach (See Appendix Table A4 and A5) reflects a snapshot pre-selection DP thymocytes with or without c-Myb at steady-state and likely includes direct and indirect c-Myb transcriptional targets, changes in gene expression caused by developmental and cellular compensatory mechanisms in response to loss of c-Myb as well as altered mRNA stability. Given the importance of defining T cell development at a molecular level, it is highly desirable to deduce the identities of genes directly targeted by c-Myb. Experiments presented in this thesis to determine if *Bcl2l1* is a direct target of c-Myb utilized the current standard approach, which is one that examines the binding of a transcription factor by ChIP to consensus binding sites within a cis-regulatory region of a predicted target gene. However, transcription factors can bind to a site with low match to its consensus sequence with the help of anchoring protein-protein interactions or tether to a site in the genome through protein-protein interactions entirely independent of its DNA binding domain (Fig. 3.20). Considering recent genome wide transcription factor binding studies, demonstrating that less than 10% of site-specific transcription factors has over 50% of their binding sites within 2.5 kb of transcription start sites (Rozowsky et al., 2009), it is not surprising that the traditional ChIP approach has only been moderately successful in the identification of novel targets of such factors. In fact, transcription factors that bind exclusively to proximal promoter regions are likely to be the exception rather than the rule and c-Myb itself has been shown to participate in long-range transcriptional regulation (Tahirov et al., 2002). Thus our failure to detect c-Myb

localization at the three conserved MREs within the known promoter region of *Bcl2l1* does not preclude the ability of c-Myb to directly regulate *Bcl2l1* transcription.

Limitations of the traditional ChIP approach to identify direct c-Myb target genes could be addressed by a genome wide c-Myb binding study. ChIP-seq combines traditional ChIP with a sequencing technology that allows overlapping immunoprecipitated DNA fragments to be aligned with the mouse genome sequence, which provides unbiased and genome wide mapping of transcription factor binding with very high resolution. Our development of an anti-c-Myb ChIP method has laid the foundation for successful future ChIP-seq experiments in *Tcrα*$^{-/-}$ DP thymocytes. Failure to detect binding in the vicinity of the *Bcl2l1* locus by anti-c-Myb ChIP-seq analysis would preclude the ability of c-Myb to directly regulate *Bcl2l1* transcription. In this case, comparison of ChIP-seq results against our existing mRNA expression microarray has the powerful potential of identifying functionally relevant c-Myb binding sites and direct c-Myb targets that might mediate c-Myb induced transcription of *Bcl2l1*. Promising candidate mediators of c-Myb induced *Bcl2l1* transcription can then be verified by analyzing their ability to promote Bcl-xL expression, survival and bind to *Bcl2l1* using the *in vitro* transduction assay described in this thesis and ChIP. Finally, hierarchical organization of direct and secondary target genes by combining ChIP-seq and mRNA microarray data sets will facilitate the mapping of novel pathways regulated by c-Myb and further our understanding of c-Myb activity in the DP stage of T cell development.

A

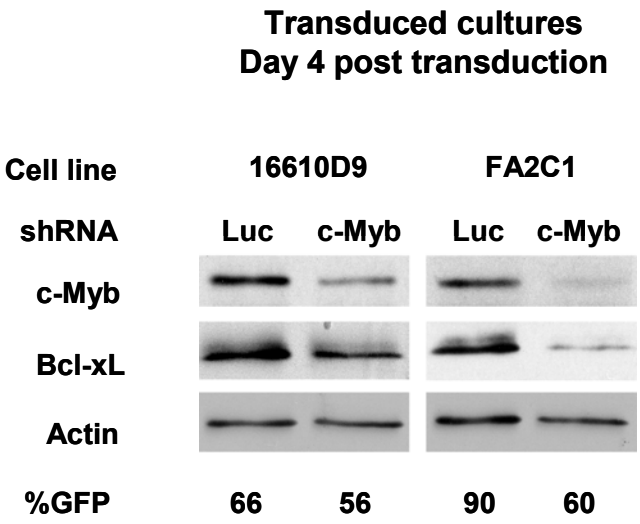
Transduced cultures
Day 4 post transduction
Cell line
16610D9
FA2C1
shRNA
Luc
c-Myb
Luc
c-Myb
c-Myb
Bcl-xL
Actin
%GFP
66
56
90
60

B

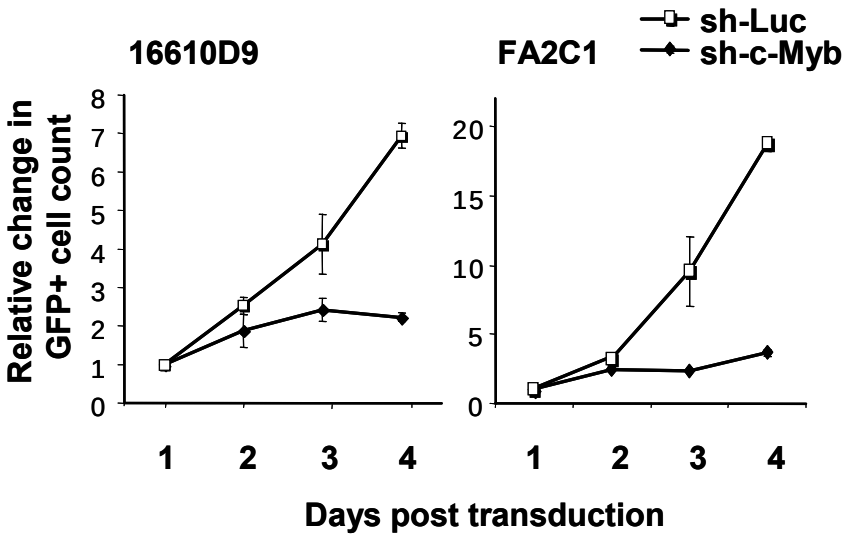
16610D9
FA2C1
sh-Luc
sh-c-Myb
Relative change in GFP+ cell count
0
1
2
3
4
5
6
7
8
0
5
10
15
20
1
2
3
4
Days post transduction

Figure 4.1 c-Myb knock-down results in decreased Bcl-xL expression and growth kinetics of two mouse thymoma lines. (A) 16610D9 and FA2C1 cell lines were transduced with either the negative control sh-Luc shRNA or sh-c-Myb and analyzed four days later for c-Myb and Bcl-xL protein expression by western blot. Percentage GFP^+ transduced cells at the time of harvest is indicated below the gel images. (B) Line graphs show the relative change in the GFP^+ cell count derived from the percentage GFP^+ cells measured by flow cytometry and the total viable cell count. Error bars indicate SEM for two experimental replicates. Preliminary results are representative of one experiment.

Is Bcl-xL a mediator of c-Myb dependent tumorogenesis?

Expression of the *Myb* proto-oncogene is strictly regulated during normal development of the hematopoietic system, colonic crypts and breast epithelium (Ramsay and Gonda, 2008). Aberrant *Myb* expression in the same tissues has been linked to tumorigenesis (Persson et al., 2009; Ramsay and Gonda, 2008). Pertinent to T cell development are recent findings from two groups linking gene duplication events at the *Myb* locus and translocations that juxtapose the *Tcrβ* and *Myb* loci to a significant portion of human T cell acute lymphoblastic leukemias (T-ALL) (Clappier et al., 2007; Lahortiga et al., 2007). Aberrant c-Myb expression in these tumors leads to a block in differentiation and contributes to increased cell survival and proliferation. Our finding that c-Myb regulates the expression of another proto-oncogene, *Bcl2l1*, during T cell development raises the distinct possibility that Bcl-xL might be a mediator of c-Myb dependent oncogenic events.

It is well established that genes involved in the inhibition of apoptosis can confer growth advantage and increased tumorigenicity (Hashimoto et al., 1997; Oka et al., 1999). Expression of Bcl-xL in the NCI-60 cell line panel, containing 60 of the most extensively characterized cancer cells lines derived from various tissue origins, strongly correlated with resistance to most chemotherapeutic agents (Amundson et al., 2000). Like c-Myb, Bcl-xL protein plays a major role in colorectal tumor development and progression (Krajewska et al., 1996) making it an attractive mediator of c-Myb in colorectal cancers. Indeed, one study reported a correlation between c-Myb over-expression and enhanced Bcl-xL protein levels in primary colorectal cancers (Biroccio et

al., 2001). In this study, 90% of patients that demonstrated over-expression c-Myb also over-expressed Bcl-xL and co-expression of the two predicted poor prognosis. In addition, the authors established that forced c-Myb expression in a human colon carcinoma cell line effectively induced Bcl-xL expression. These findings are consistent with Bcl-xL being an oncogenic effector of c-Myb in colorectal cancers.

We have obtained preliminary evidence supporting a role of c-Myb in the regulation of Bcl-xL expression in transformed T cells. shRNA mediated knock-down of c-Myb correlates with both decreased Bcl-xL expression and growth kinetics in two cell lines, 16610D9 and FA2C1 (Bain et al., 1999; Reschly et al., 2006), derived from *p53*$^{-/-}$ thymomas (Fig. 4.1). This experiment provides the first evidence linking c-Myb with Bcl-xL expression in transformed T cells. To verify if the observed c-Myb dependent growth advantage is mediated by Bcl-xL, it will be crucial to measure growth kinetics following simultaneous knockdown of c-Myb and over-expression of Bcl-xL. To establish Bcl-xL as a mediator of c-Myb dependent oncogenesis, it will be important to screen human T cell malignancies with aberrant c-Myb expression for Bcl-xL dependence and c-Myb dependent Bcl-xL expression. This can be achieved by RNAi mediated knockdown of c-Myb or Bcl-xL expression followed by analysis of Bcl-xL expression and tumor cell survival respectively.

How is c-Myb mRNA expression regulated during T cell development?

Upstream signals that mediate the dynamic changes in *Myb* expression observed during T cell development remain a mystery. The known importance of the dosage of c-Myb

expression during normal development and oncogenesis directs attention to this issue. Our results demonstrating normal c-Myb protein expression in *Rorγ*$^{-/-}$ and *Tcf1*$^{-/-}$ thymocytes preclude a regulatory role of RORγt or TCF-1 function in c-Myb expression. Recently, our collaborators demonstrated that the c-Myb specific micro RNA miR150 is abundantly expressed in mature T and B cells but not their progenitors (Xiao et al., 2007). Thus, post-transcriptional regulation is a potential source of signals that modulate *Myb* expression during T cell development. Lessons learned from developing B cells have established a clear relationship between miR150 and c-Myb expression. However, the physiological relevance of miR150 during T cell development remains unclear. Thymocytes develop normally in *miR150*$^{-/-}$ mice and premature miR150 transgene expression has little to no detectable effect on T cell development (Xiao et al., 2007; Zhou et al., 2007). This is in stark contrast to our published observations in c-Myb deficient mice and strongly argues against miR150 as a major regulator of *Myb* expression during T cell development.

As previously discussed, pre-TCR and αβ-TCR signals initiate gene expression programs that drive the later stages of T cell development. Upon a closer look at the dynamic changes in *Myb* mRNA expression during T cell development, an apparent connection can be drawn between the peaks of c-Myb expression and the absence of pre-TCR or αβ-TCR mediated signals (Fig. 1.2). Thus, it is possible that *Myb* mRNA expression is subject of negative regulation by TCR controlled events during thymopoiesis. This possibility is supported by the identification of *Myb* as a gene that is down-reglated upon positive selection, by mRNA expression microarray studies in mice

(Mick et al., 2004) and humans (Hoffmann et al., 2003) as well as our observation that Myb mRNA drastically decreases upon PMA and ionophore stimulation *in vitro* (Fig. 3.2). A similar role for pre-TCR signaling in regulating *Myb* expression has not been tested and can be addressed by monitoring changes in *Myb* mRNA expression following anti-CD3 crosslinking of *Rag* deficient thymocytes. The demonstration of a trend of pre-TCR/αβ-TCR signaling and down-regulation of c-Myb expression in thymocytes would position c-Myb as a mediator of TCR instructed changes in gene expression and significantly advance the current understanding of c-Myb biology in T cell development.

The expression and function of E-protein family members is strictly regulated by pre-TCR and αβ-TCR mediated signaling (Fig. 1.2 and 1.3). The four E proteins [E12 (*Tcfe2a*), E47 (*Tcfe2a*), E2-2 (*Tcf4*), and HEB (*Tcf12*)] are widely expressed basic helix-loop-helix proteins that bind to a canonical site (CANNTG) in the genome as homo- and heterodimers, where they can either activate or repress transcription. Id3 is a negative regulator of E protein activity that is induced by pre-TCR and αβ-TCR signals in thymocytes following β-selection and positive selection (Bain et al., 2001; Xi et al., 2006). The implication is that Id3 might be necessary to decrease E protein activity in response to β-selection and positive-selection signals, resulting in a net change in activity that perfectly matches the dynamic changes of c-Myb mRNA expression during T cell development. Similar to c-Myb deficient thymocytes, those deficient in E protein function display increased spontaneous cell death at the DP stage prohibiting extended usage of 3' located *Jα* segments, a decrease in the percentage of CD4SP thymocytes and an increase in the percentage of CD8SP thymocytes (Jones and Zhuang, 2007). Another

fascinating role of E-proteins is their maintenance of an undifferentiated pre-selection phenotype in thymocytes awaiting either β-selection or positive selection to enforce the TCR controlled developmental checkpoints. Initial evidence described in Appendix 2 suggest that c-Myb might play a similar role during positive selection. In addition, established downstream effectors of E proteins during T cell development include Gfi1, Klf2, CXCR4, CCR7 and FOXO1, all of which are similarly up- or down-regulated in c-Myb deficient pre-selection DP thymocytes (See Appendix 1). These similarities in the function and expression of E-proteins and c-Myb may be reflective of their involvement in a common pathway during T cell development. In support of this hypothesis, a search in an mRNA microarray dataset performed on thymocytes doubly deficient for E2A and HEB (Jones and Zhuang, 2007) identified a ~75% decrease in *Myb* expression while transcripts encoding E-protein family members and Id proteins were not significantly changed in $Myb^{f/f}$ $Tcr\alpha^{-/-}$ DP thymocytes (microarray data not shown). These findings are consistent with E-proteins being an upstream regulator of c-Myb expression (Fig. 4.2). Thus, results demonstrating that during DP to SP thymocyte differentiation i) CCR7 is regulated by Klf2, Gfi1, c-Myb and E-proteins, ii) Klf-2 is regulated by Gfi1, c-Myb, and E-proteins, iii) Gfi1 expression is under the control of both c-Myb and E-proteins, iv) the expression c-Myb is regulated by E-proteins, position c-Myb in a genetic pathway initiated by a pre-TCR signal and ending in effector functions that maintain the survival and immature phenotype of the pre-selection DP thymocyte compartment (Fig. 4.2). This hypothetical scenario is further discussed in Appendix 2.

The establishment of a genetic relationship between E-proteins and c-Myb requires additional analysis of c-Myb mRNA and protein expression in thymocytes deficient in E-protein function. Due to existing functional redundancy, inactivation of both E2A and HEB is required to severely impact DP thymocyte development. Therefore, the potential role of E-proteins to regulate c-Myb expression in DP thymocytes is likely best addressed in Cd4-Cre transgenic mice carrying floxed alleles of *tcfe2a* and *tcf12* (Jones and Zhuang, 2007). In addition, experiments demonstrating the ability of exogenous c-Myb to restore developmental defects and aberrant gene expression caused by E-protein deficiency will be instrumental. This can be achieved by MIGR1-c-Myb transduction of *Tcfe2a* and *Tcf12* deficient thymocytes using the in vitro add-back system established in this thesis (Fig. 3.14)

The role of c-Myb in DP to SP thymocyte differentiation

We have previously demonstrated that deletion at the *Myb* locus in DP thymocytes results in a decreased CD4SP compartment that can not be prevented by the expression of a MHC class II restricted transgenic TCR (Bender et al., 2004). This finding was confirmed by two other groups (Lieu et al., 2004; Maurice et al., 2007), and attributed to a decrease in the expression of GATA-3 (Maurice et al., 2007). However, these studies did not address the αβ-TCR independent survival defect that occurs in c-Myb deficient pre-selection DP thymocytes and causes biased *Tcrα* repertoire that could adversely affect both positive selection and CD4/CD8 lineage decision. Experiments in this thesis demonstrate that the expression of Bcl-2tg expression directed to the T cell lineage could

prevent premature apoptosis provides a tractable genetic system useful for the investigation of the contributions of c-Myb in DP to SP thymocyte differentiation. Initial characterization of *Myb*$^{f/f}$ Bcl-2tg confirms a function for c-Myb in the development of CD4SP thymocytes that is independent of premature apoptosis. In addition, Bcl-2tg expression revealed a previously unrecognized increase in the percentage of CD69^{+} post-selection DP thymocytes and CD8SP thymocytes in c-Myb deficient mice consistent with enhanced positive selection and differentiation towards the CD8SP lineage. Thus interpretations of c-Myb function in DP to SP differentiation must take into consideration the complex roles of c-Myb in promoting survival and CD4SP lineage development, as well as potentially suppressing positive selection and CD8SP lineage development. It is possible that accelerated positive selection is yielding increased development towards the CD8SP lineage in c-Myb deficient mice due to a lack of additional signals required for CD4 lineage differentiation. Three potential sources of such signals are discussed below.

CD4/CD8 cell fate is thought to be the combined outcome of the kinetics of membrane proximal TCR signaling and downstream transcription and chromatin remodelling events (Singer et al., 2008) (Fig. 1.4). One crucial membrane proximal signal that might conceivably be impaired in c-Myb deficient DP thymocytes is that conveyed by the CD4 co-receptor. The *Cd4* gene utilizes both positive and negative *cis*-regulatory elements for its expression in the thymus (Ellmeier et al., 1999) both of which have been reported to be targets of c-Myb regulation (Allen et al., 2001; Siu et al., 1992). However, normal amounts of surface CD4 are detected on DP thymocytes and mature splenic T lacking c-Myb (Bender et al., 2004), challenging the physiological effect of c-

Myb on *Cd4* expression. Nonetheless, given that small changes in *Cd4* expression can perturb CD4SP lineage differentiation (Sarafova et al., 2009) and that cells expressing class II MHC specific TCR can differentiate down the CD8SP lineage in CD4 deficient mice, it is desirable to properly examine the role of c-Myb in tuning the expression of *Cd4* during T cell development. To test whether loss of CD4 expression is causing the defect, a constitutively expressed Cd4 transgene that has been shown to reconstitute the CD4SP compartment in *Cd4* deficient mice (Law et al., 1994) could be introduced to c-Myb deficient mice. Crossing $Myb^{f/f}$ Cd4-tg mice with a MHC class II restricted TCR transgenic strain would facilitate analysis of CD4SP thymocyte development. The prediction would be that c-Myb likely regulates *Cd4* expression if thymic representation of $Myb^{f/f}$ CD4SP cells is readily restored by forced *Cd4* expression in mice that lack c-Myb.

A nuclear signal that might be impaired in c-Myb deficient DP thymocytes is that mediated by GATA3. GATA3 is a transcription factor that plays an established role in CD4SP lineage specification and Th-POK expression. Despite convincing evidence demonstrating direct binding of c-Myb to the GATA3 promoter to promote GATA3 transcription in post-selection DP thymocytes (Maurice et al., 2007), it is difficult to reconcile the discrepancies between Gata3 and c-Myb in terms of expression pattern and function during DP to SP thymocyte differentiation. GATA3 expression is induced after productive αβ-TCR engagement of DP thymocytes, a signal that is likely responsible for the rapid down-regulation of *Myb* expression (Fig. 3.2). Next, unlike DP c-Myb deficient DP thymocytes, GATA3 deficient thymocytes do not display impaired survival or

increased production of CD8SP thymocytes. Most importantly, an exogenous source of GATA3 failed to reconstitute the *Myb*$^{f/f}$ CD4SP compartment (Personal communication with Dr Jose Alberola-Ila, Oklahoma Medical Research Foundation, Oklahoma City, OK), strongly argueing against the possibility of GATA3 being immediately downstream of c-Myb in the transcriptional network regulating CD4SP development. Evidence supporting a direct regulation of *Gata3* by c-Myb was generated in a system where premature apoptosis in c-Myb deficient thymocytes was not controlled (Maurice et al., 2007). We argue that the relationship between c-Myb and GATA3 remains an outstanding issue that should be examined further using *Myb*$^{f/f}$ Bcl-2tg mice.

A second nuclear factor potentially deficient in DP thymocytes that lack c-Myb is Gfi1, a transcriptional repressor that is significantly down-regulated by 2.3 fold in c-Myb deficient pre-selection DP thymocytes (Table A4). Loss of Gfi1 does not impinge on DP thymocyte survival, but negatively regulates the generation of CD4SP thymocytes while accelerating the generation of CD8 SP cells in the same fashion as *Myb*$^{f/f}$ Bcl-2tg thymocytes (Yucel et al., 2003). In addition to this intriguing phenotypic resemblance, we identified several genes repressed by both c-Myb and Gfi1 including Klf2, Traf5 and Maf (Table A2, A4 and A5) (Yucel et al., 2003). Taken together, these correlative observations are in accordance with Gfi1 functioning down-stream of c-Myb in the regulation of DP to SP thymocyte differentiation (Fig. 4.2). Gfi1-GFP reporter mice are available and could provide a useful tool in examining c-Myb dependent Gfi1 expression (Yucel et al., 2004). To identify down-stream mediators of c-Myb function pertinent in

DP to SP differentiation, anti-c-Myb ChIP-seq analysis in control thymocytes will also be of high priority.

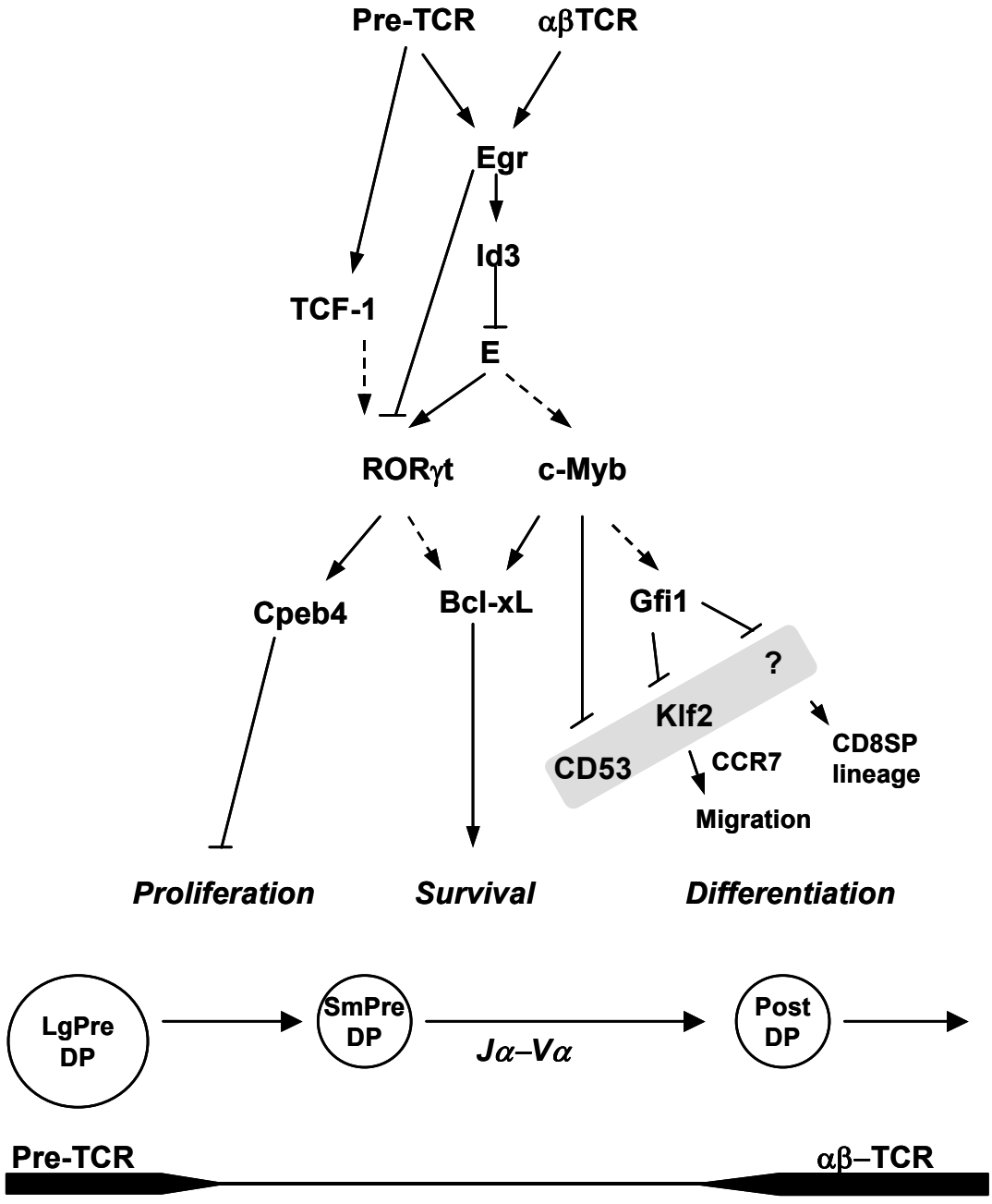

Figure 4.2 Model for how c-Myb might fit into the network of transcription factors that regulates the pre-selection DP thymocyte phenotype. This model builds upon Figures 1.3 and 3.20 as well as phenotypic and gene expression analysis of *Myb*$^{f/f}$ Cd4-Cre DP thymocytes in comparison with RORγt and E-protein deficient mice. It proposes that c-Myb might act down-stream of E-proteins, much like RORγt. In contrast to RORγt, c-Myb is likely to be required for the maintenance rather than the establishment of the small pre-selection DP thymocyte phenotype.

APPENDIX

Myb mRNA expression, as shown in chapter III, is abundant in pre-selection DP thymocytes and low both prior to and following this stage during T cell development. This intriguing pattern of expression suggests that c-Myb may play an important role in enforcing a pre-selection DP thymocyte specific gene expression profile. To better understand the contributions of c-Myb during this stage, we interrogated >34,000 cDNA probes by Affymetrix microarray expression analysis to identify genes that are differentially expressed in $Myb^{f/w}$ $Tcr\alpha^{-/-}$ and $Myb^{f/f}$ $Tcr\alpha^{-/-}$ DP thymocytes. Based on the main goal of this thesis, the microarray experiment was primarily designed to identify candidate c-Myb target genes that mediate protection from apoptosis through the intrinsic pathway in pre-selection DP thymocytes. Appendix 1 will present and discuss results from the microarray that lead to the identification of *Bcl2l1* as a mediator of c-Myb in pre-selection DP thymocytes. Appendix 2 will present and discuss microarray results consistent with a role of c-Myb in maintaining an undifferentiated gene expression profile in unsignaled DP thymocytes.

Appendix 1. Identification of potential c-Myb target genes involved in the regulation of pre-selection DP thymocyte survival by mRNA microarray

To attain high statistical power, the microarray was carried out using four independent biological replicates. cDNA of DP thymocytes from four $Myb^{f/w}$ $Tcr\alpha^{-/-}$ and four $Myb^{f/f}$

Tcrα$^{-/-}$ mice were individually hybridized to Mouse Genome 430 2.0 Gene Chips. The resulting dataset was subjected to the Student's *t*-test and a two-fold change ($p<0.01$) cutoff and identified 254 known genes to be upregulated and 219 known genes to be down-regulated in *Myb*$^{f/f}$ *Tcrα*$^{-/-}$ compared to *Myb*$^{f/w}$ *Tcrα*$^{-/-}$ DP thymocytes (Table A1).

Differential expression was validated by qRT-PCR or flow cytometry for a selection of gene products with known function in T cell development (Table A2 and Fig. A1). As negative control, qRT-PCR was carried out measuring two transcripts (*Rorγ* and *Tcf1*) that did not meet our selection criteria. qRT-PCR as well as flow cytometry analysis confirmed the direction of differential expression as identified by the microarray for all of the transcripts subjected to validation (Fig. A1 and A2), attesting to the overall quality of this dataset. In addition, the amplitude or absence of differential expression detected by qRT-PCR closely adhered to that identified by the microarray for genes that were up-regulated or unchanged in the absence of c-Myb. However, this was less so the case with transcripts that were down-regulated in the absence of c-Myb where the decrease in the expression of *Smarce1* and *Gfi1* detected by qRT-PCR was less and more pronounced respectively than that measured by the microarray. This is not surprising as the presence of infrequent transcripts is less likely to be accurately measured by either method. However, it is an observation that must be taken into consideration when interpreting the microarray results.

Table A1 Summary of microarray identified genes

≥2 fold change in expression p<0.01 (Student's *t*-test)	Upregulated	Down-regulated
Probe Sets	365	296
Known genes	254	215
Rikens	26	30
Unknown ESTs without Riken ID	42	35

Table A2 Validation of Microarray data by qRT-PCR

Gene Name	Microarray	qRT-PCR
Smarce1	-7.55	-1.7
Gfi1	-2.33	-7.047
Camk4	-3.035	-2.78
Bcl2l1	-2.36	-2.12
Sh2d1a	-2.63	-1.75
Ccnd3	-2.2	-2.34
Socs3	3.72	1.84
Foxo1	2.615	2.31
Gmap4	3.445	2.69
Gadd45b	3.45	3.03
Dtx1	8.01	6.93
Maf	50.4	48.34
Fosl2	114.885	100.77
Rorγ	1.21	1.135
Tcf1	-1.12	-1.04

Table A3 Regulation of programmed cell death ontology group analysis

Gene name	Fold Change	Genbank	Probe set	Apoptosis regulation
Lig4	-3.484	AW545311	1439487_at	negative regulation
Bcl6	-2.683	U41465	1450381_a_at	negative regulation
Bcl6	-2.05	U41465	1421818_at	negative regulation
Sh2d1a	-2.566	NM_011364	1449393_at	positive regulation
Bcl2l1	**-2.357**	**U51279**	**1426050_at**	**negative regulation**
Trp53inp1	-2.176	AW495711	1416927_at	positive regulation
Plekhf1	2.653	BC002120	1424671_at	positive regulation
Sgms1	4	BE629162	1426576_at	negative regulation
Sgms1	6.352	AW985925	1436499_at	negative regulation
Sgms1	6.41	BE629162	1426575_at	negative regulation
Il2ra	7.6	AF054581	1420691_at	positive regulation
Il2ra	8.942	AF054581	1420692_at	positive regulation

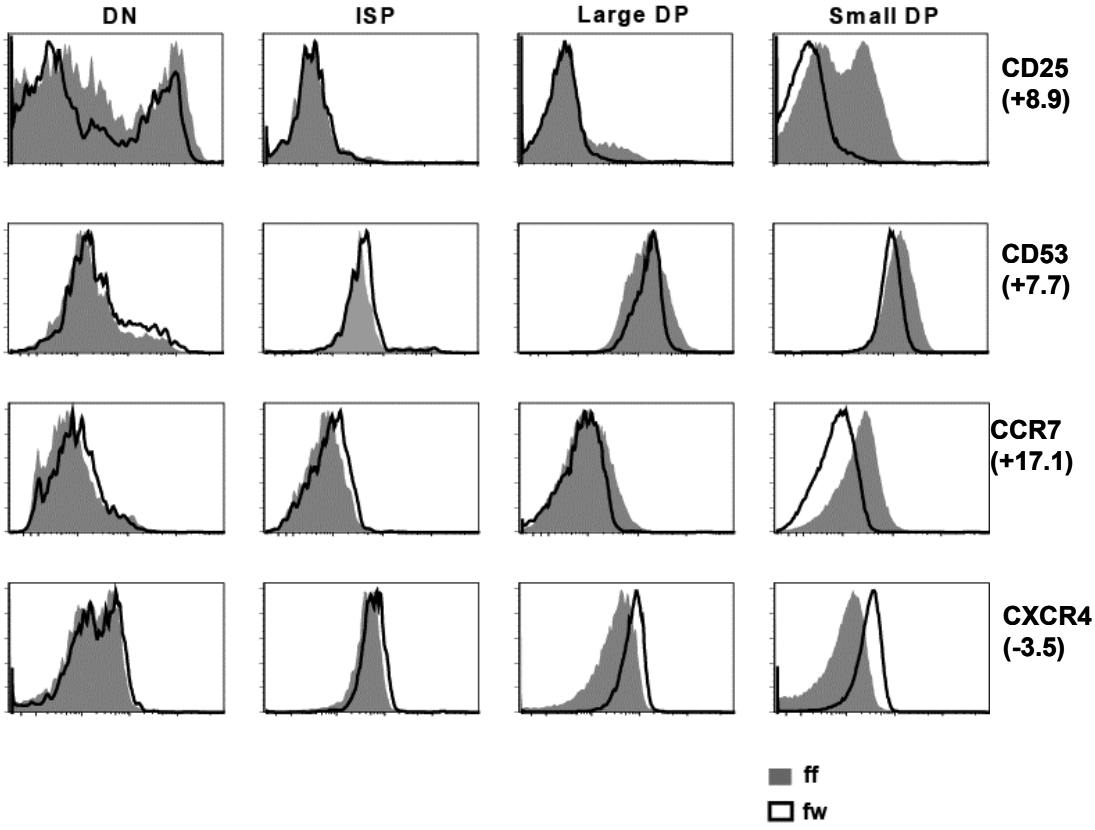

Figure A1 Validation of Microarray results by flow cytometry. *Myb*$^{f/f}$ *Tcrα*$^{-/-}$ and *Myb*$^{f/w}$ *Tcrα*$^{-/-}$ thymocytes were stained for surface expression of CD3, CD4 and CD8 and one of the following gene products, CD25, CD53, CCR7 and CXCR4. These genes were identified by mRNA microarray analysis to be significantly changed in c-Myb deficient pre-selection DP thymocytes as indicated to right of the histograms. Flow cytometry analysis confirms the microarray measured direction of change and demonstrates that the change in protein expression is mainly limited to the small pre-selection DP thymocyte subset.

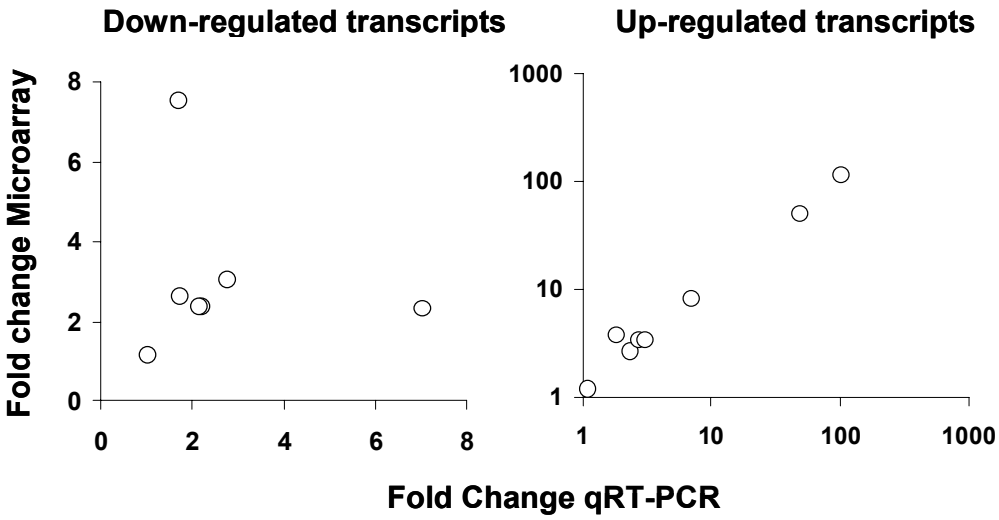

Figure A2 Validation of Microarray results with qRT-PCR. Graphs show fold decrease expression of several genes detected by microarray analysis plotted against those detected (left) and increase (right) in mRNA by qRT-PCR analysis. Genes are listed in Table A2.

As previously described, DP thymocytes derived from co-culturing *Myb*$^{f/f}$ *Tcrα*$^{-/-}$ DN thymocytes with OP9-DL1 stromal cells faithfully recapitulates the survival defect observed in those differentiated *in vivo* (Fig. 3.13). Furthermore, transduction of co-culture with retrovirus encoding the full length *Myb* cDNA efficiently restores this survival defect (Fig. 3.14). To further validate that genes identified by the microarray are indeed regulated by c-Myb we employed this in vitro add-back system and measured the ability of exogenous c-Myb to restore differential expression of several genes in c-Myb deficient DP thymocytes. In vitro differentiated *Myb*$^{f/f}$ *Tcrα*$^{-/-}$ and *Myb*$^{f/w}$ *Tcrα*$^{-/-}$ DP thymocytes transduced with either the negative control MIGR1 virus or MIGR1-c-Myb were electronically sorted, total cellular RNA was extracted and qRT-PCR carried out as previously described (Fig. 3.14). Consistent with the microarray results, the direction of differential expression recapitulated in co-culture derived *Myb*$^{f/f}$ *Tcrα*$^{-/-}$ DP thymocytes (Fig. A3). Altered gene expression due to the loss of c-Myb was at least in part restored by exogenous c-Myb in all cases but one (*Gfi1*), suggesting that the microarray has succeeded in identifying true c-Myb target genes. Several reasons may contribute to the failure of exogenous c-Myb to restore *Gfi1* mRNA expression. First, c-Myb induced up-regulation of *Gfi1* maybe highly dosage dependent and therefore not detectable upon over-expression with MIGR1-c-Myb. Second, c-Myb may regulate *Gfi1* expression in the presence of signals provided by the thymic microenvironment but not by OP9-DL1 stromal cells. Third, Gfi1 may be indirectly regulated by c-Myb and re-upregulation may not be detectable at the time of the assay. Finally, the fold change of down-regulated

messages might be more difficult to accurately measure due to the scarcity of cDNA templates for qRT-PCR.

As described in Chapter III, our work has demonstrated that large and small pre-selection DP thymocytes differ significantly in their behavior and regulation and that while the large cells comprise around 10% of the *Myb*$^{f/w}$ *Tcrα*$^{-/-}$ DP compartment, this percentage is doubled in the *Myb*$^{f/f}$ *Tcrα*$^{-/-}$ DP compartment. Unfortunately, at the time of this microarray assay, these differences were not yet clear to us. Since microarrays measure the average changes in gene expression, a transcript that is at least 20-fold enriched in large compared to small pre-selection DP thymocytes can show up as 2-fold induced in c-Myb deficient thymocytes when averaged over the entire DP population. By not distinguishing between small and large cells in our experimental design, differentially expressed genes may in some cases reflect the differential representation of large versus small pre-selection DP thymocytes rather than differential expression due to the loss of c-Myb within the small DP subset. This is a significant caveat that must be kept in mind when considering the microarray dataset and emphasizes the need for careful result validation in sorted small pre-selection DP thymocytes from control and mutant mice whenever a gene of interest is pursued based on this microarray.

This thesis work demonstrates first-hand that changes in the expression of genes involved in survival regulation can be masked by an ensuing survival defect. While we were able to detect decreased *Bcl2l1* mRNA expression in small c-Myb deficient pre-selection DP thymocytes, changes on the protein level were completely masked by the survival defect and exposed only when survival is artificially maintained by Bcl-2tg

expression or Z-VAD treatment *in vitro*. The impact of pre-mature apoptosis on our ability to detect differences in the mRNA expression profile of c-Myb deficient DP thymocytes has not been tested. It is likely that a microarray comparing c-Myb sufficient and deficient DP thymocytes in the presence of Bcl-2tg expression will enhance differences in c-Myb regulated genes, particularly those involved in survival. Second, since apoptosis is a process that involves *de novo* transcription, the presence of a Bcl-2tg might facilitate the identification of genes responsible for increased apoptosis by purging changes in gene expression that occur as a result of ongoing apoptosis. Thus, in hindsight, the use of Bcl-2tg expressing control and mutant pre-selection DP thymocytes may have been even more effective in identifying the cause of the survival defect as well as provide better insight into the role of c-Myb in DP to SP development.

To detect changes in the expression of genes involved in survival regulation, we performed ontology analysis (Fig. A4). Out of the 365 and 296 probe sets that identified up- and down-regulated genes respectively, only 12 probe sets specific for the transcripts of 8 genes belonged to the gene ontology group Regulation of programmed cell death (GO:0043067) under the domain of Biological processes (Ashburner et al., 2000) (Table A3). We focused our attention on the 3 positive regulators of programmed cell death that were up-regulated in the absence of c-Myb (*Trp53inp1*, *Plekhf* and *Il2ra*) and the 3 negative regulators of programmed cell death that were down-regulated in the absence of c-Myb (*Lig4*, *Bcl6* and *Bcl2l1*). From these 6 genes, we deemed a statistically significant 2.4 fold decrease in *Bcl2l1* mRNA to be most pertinent to an increase in intrinsic apoptosis.

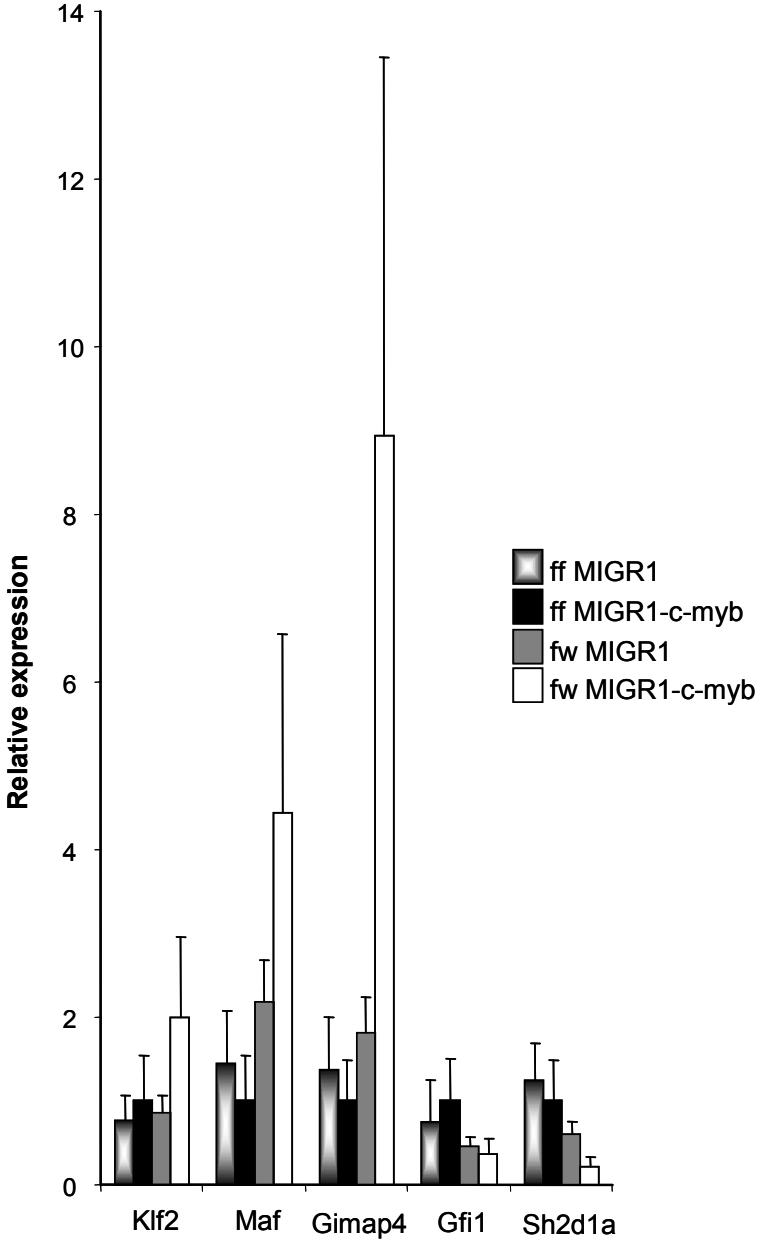

Figure A3 Assaying the ability of exogenous c-Myb to restore the expression of putative target genes identified by the microarray in pre-selection DP thymocytes.

Using the assay developed in Figure 3.14, *Myb*$^{f/f}$ *Tcrα*$^{-/-}$ and *Myb*$^{f/w}$ *Tcrα*$^{-/-}$ thymocytes were co-cultured with OP9-DL1 stromal cells and transduced with MIGR1 alone or MIGR1-c-Myb. Transduced DP thymocytes were electronically sorted 3 days post-transduction and assayed by qRT-PCR for the mRNA expression of several putative c-Myb target genes identified by microarray analysis.

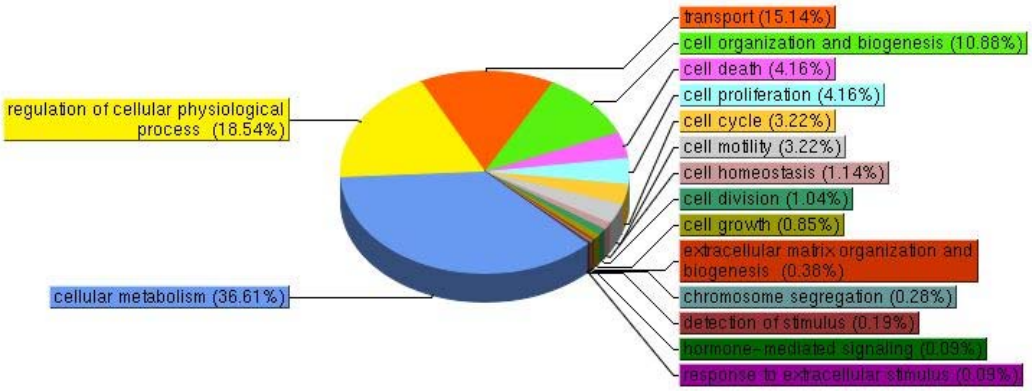

Figure A4 Gene ontology groups. Venn diagram was generated using the GeneSifter software (VizX Labs LLC, Seattle, WA) and shows the ontology distribution of genes that were identified as significantly changed above two fold by microarray analysis.

Appendix 2. c-Myb and the maintenance of a pre-selection DP gene expression signature

Positive selection ensures that peripheral T cells are tolerant but not ignorant to self-MHC and drives major developmental programs including thymocyte survival, migration into a new microenvironment, TCR tuning of antigenic responsiveness, and T lineage commitment. A previous study comparing the mRNA profile in post-selection DP thymocytes from class I MHC restricted OT-I TCR transgenic mice with OT-I *Tap*$^{-/-}$ pre-selection DP thymocytes identified 120 genes that changed significantly in expression during positive selection (Mick et al., 2004). A manual comparison of these 120 genes against our microarray gene list displaying ≥2 fold ($p<0.05$) differential expression in the absence of c-Myb identified an overlap consisting of 24 transcripts (Fig. A5). Out of these 24 genes, 15 genes were induced and 9 genes were down-regulated by normal positive selection. In the first group of 15 genes, 14 genes were elevated in c-Myb deficient pre-selection DP thymocytes including positive selection hallmarks such as *Cd53*, *Ccr7, Klf2* and *Btla* (Han et al., 2004; Tomlinson et al., 1995; Witt and Robey, 2004), and all but 2 of the second group of 9 genes showed decreased expression in c-Myb deficient pre-selection DP thymocytes. This analysis reveals a higher than expected similarity to a post-selection gene expression profile in c-Myb deficient *Tcrα*$^{-/-}$ DP thymocytes, and is consistent with the notion that c-Myb may play a role in the maintenance of an undifferentiated pre-selection DP thymocyte phenotype prior to positive selection during T cell development.

Coordinated changes in chemokine receptor expression including increased CCR7 (Kwan and Killeen, 2004) and decreased CXCR4 expression (Suzuki et al., 1999) are associated with normal positive selection and play an important role in thymocyte migration from the cortex into the medulla and subsequently into secondary lymphoid organs in the periphery. Microarray results demonstrate a 17.1 fold increase in *Ccr7* mRNA expression and a 3.5 fold decrease in *Cxcr4* mRNA expression (Table A4 and 5). These differences in mRNA expression translated to significant changes in the cell surface protein expression in c-Myb deficient small pre-selection DP thymocytes (Fig. A1) and are consistent with aberrant differentiation. Of special interest is the increase in CCR7 as the genetic pathway leading to its expression appears to be positively regulated in c-Myb deficient DP thymocytes. Upon normal positive selection, the expression of the transcription factor Klf2 is induced and facilitates up-regulation of CCR7 (Carlson et al., 2006). c-Myb deficient DP thymocytes, this occurs independently of αβ TCR, possibly through decreased expression of Gfi1, a transcription repressor reported to suppress *Klf2* expression (Yucel et al., 2003). Our observation provides a concrete example of a genetic pathway normally associated with positive selection that has been improperly initiated in unsignaled pre-selection DP thymocytes that lack c-Myb, contributing to a post-selection-like phenotype. However, altered chemokine receptor expression due to the loss c-Myb is unlikely to be sufficient for thymic egress without proper self-peptide/MHC interactions as evidenced by the lack of splenic T lineage cells in $Myb^{f/f}$ $Tcr\alpha^{-/-}$ mice with or without Bcl-2tg expression (data not shown). Thus despite the appearance of aberrant differentiation, the αβ-TCR controlled repertoire selection checkpoint remains intact in $Myb^{f/f}$ $Tcr\alpha^{-/-}$ mice.

If aberrant differentiation of unsignaled DP thymocytes is not sufficient to override the repertoire selection checkpoint in c-Myb deficient mice, is it still physiologically important? Our observation that *Myb*$^{f/f}$ Bcl-2tg mice have an increased percentage of CD69^{+} DP thymocytes and an increased overall SP:DP ratio is consistent with enhanced positive selection. Thus we hypothesize that the improper regulation of signaling molecules and nuclear factors in c-Myb deficient pre-selection DP thymocytes is indeed relevant and could possibly induce a 'poised' state where the threshold of αβ-TCR engagement required for differentiation is lowered. To further interrogate this notion we monitored the up-regulation of surface CD69 in *Myb*$^{f/f}$ and *Myb*$^{f/w}$ thymocytes upon anti-CD3 crosslinking *in vitro*. Thymocytes were analyzed at 3 and 8 hours post culture prior to the event of overwhelming DP cell death due to lack of c-Myb. *Myb*$^{f/f}$ DP thymocytes displayed augmented up-regulation of CD69 compared to *Myb*$^{f/w}$ thymocytes, consistent with increased sensitivity towards αβ-TCR induced activation (Fig. A6). The notion of an increased sensitivity of c-Myb deficient DP thymocytes towards αβ-TCR signaling predicts not only enhanced positive selection but also enhanced negative selection and dysregulated CD4/CD8 lineage decision. Indeed, our observation that c-Myb deficient DP thymocytes exhibit an αβ-TCR independent survival defect does not rule out a role for c-Myb in the survival of DP thymocytes during repertoire selection. Thus, c-Myb function in pre-selection DP thymocytes appears to be twofold, to promote survival and to prevent differentiation.

In conclusion, our finding that DP thymocytes doubly deficient in αβ-TCR and c-Myb undergo phenotypic changes that are hallmarks of αβ-TCR mediated positive

selection is consistent with a scenario where high expression of c-Myb in pre-selection DP thymocytes regulates the positive selection checkpoint by extending the survival window to allow sufficient *Tcrα* recombination while preventing improper differentiation until a qualified αβ-TCR signal down-regulates c-Myb expression of DP thymocytes. Such a role was previously linked to the E-protein family of transcription factors. Similar to c-Myb deficient DP thymocytes, those deficient in E-protein function exhibit enhanced positive selection that results in faster production of mature CD8 T cells (Bain et al., 1999). While the generation of mature CD8 T cells still requires proper self-MHC interactions in thymocytes singly deficient for *Tcfe2a (Bain et al., 1999)*, the repertoire selection checkpoint is entirely overridden in mice doubly deficient in *Tcfe2a* and *Tcf12* where CD8 T cells can develop in a αβ-TCR independent fashion (Jones and Zhuang, 2007). These similarities hint that c-Myb might function in the same genetic pathway as E-protein family members during T cell development (discussed in Chapter IV). Our observations that abundant c-Myb contributes to the maintenance of an immature phenotype lends new support to the old notion that c-Myb function negatively regulates differentiation during hematopoiesis and provides grounds for pertinent studies in the future.

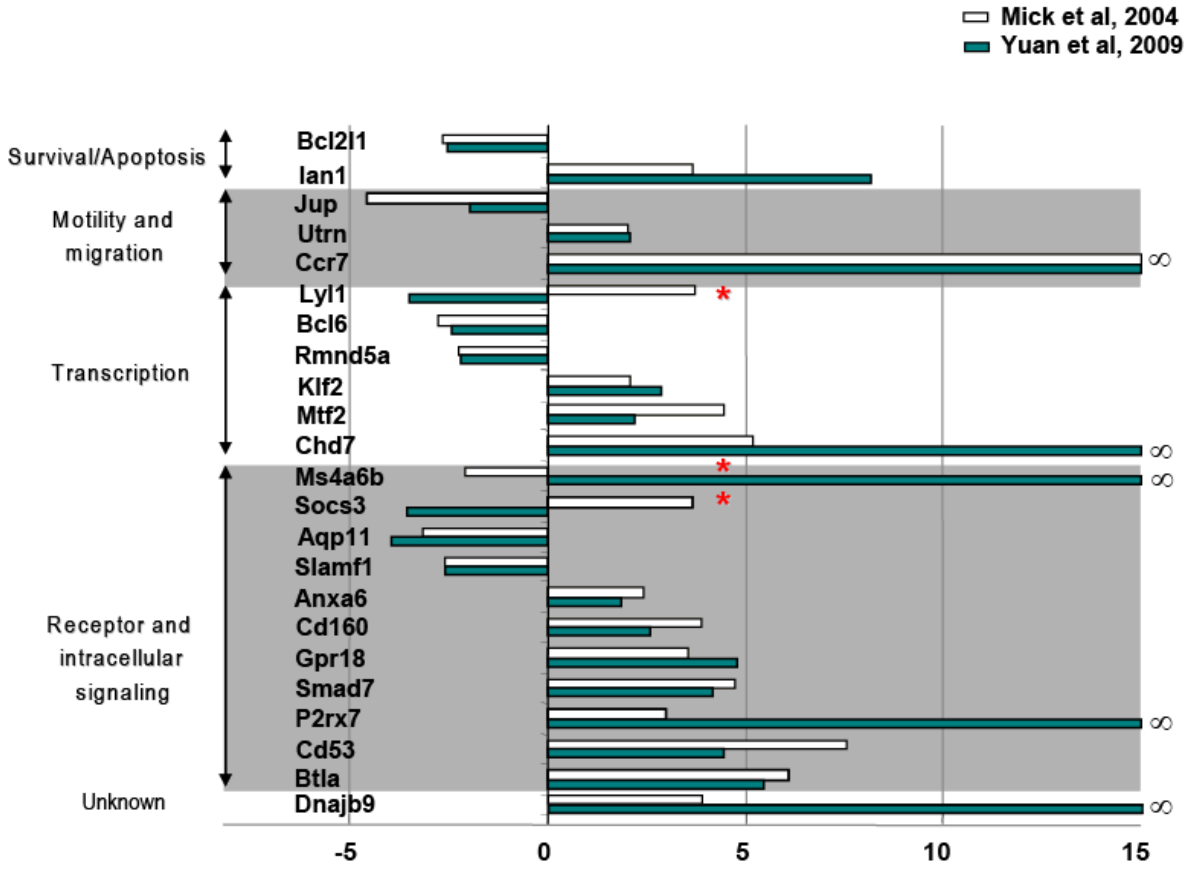

Figure A5 Comparison of *Myb*$^{f/f}$ *Tcrα*$^{-/-}$ and *Myb*$^{f/w}$ *Tcrα*$^{-/-}$ DP microarray results to a positive selection microarray study. Mick et al identified 120 genes that were significantly changed (>3 fold p<0.01) (Mick et al., 2004) upon positive selection. Twenty-three of these genes were significantly altered (>2 fold p<0.05) in our microarray study comparing *Myb*$^{f/f}$ *Tcrα*$^{-/-}$ to *Myb*$^{f/w}$ *Tcrα*$^{-/-}$ DP thymocyte mRNA profiles. Average fold change identified by both studies are plotted next to each other. Asterisks highlight changes identified by both studies that are of opposite directions.

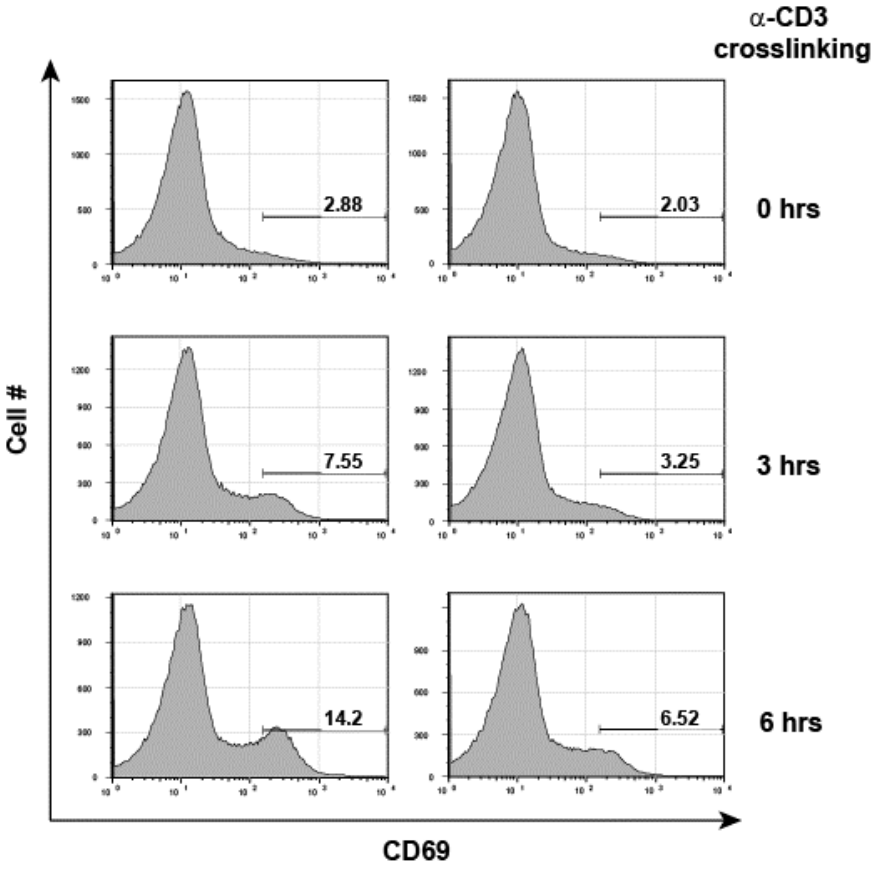

Figure A6 ***Myb*$^{f/f}$ DP thymocytes exhibit accelerated up-regulation of CD69 upon anti-CD3 stimulation.** Total thymocytes were cultured for the indicated times with 3 μg/ml plate-immobilized anti-CD3. Cells were stained for CD4, CD8 and CD69 and analyzed by flow cytometry. Histograms show CD69 distribution through a $CD4^+CD8^+$ gate and represent preliminary results from one experiment.

Table A4 List of up-regulated genes (365 probe sets). Validated differential expression is shown in bold.

Fold Change	Genbank	Probe set	Gene name
226.41	**BM245170**	**1437247_at**	***Fosl2***
205.57	NM_008365	1421628_at	*Il18r1*
59.93	**AV284857**	**1437473_at**	***Maf***
42.51	AV323441	1447849_s_at	-
41.83	BB159247	1438536_at	*5830411N06Rik*
40.87	**AV284857**	**1456060_at**	***Maf***
27.14	**BM240693**	**1435828_at**	***Maf***
25.28	NM_021344	1418743_a_at	*Tesc*
21.33	NM_011407	1418612_at	*Slfn1*
17.77	NM_016851	1418301_at	*Irf6*
17.51	AV247387	1456545_at	*Il18rap*
17.1	**BB204380**	**1423466_at**	***Ccr7***
16.25	AV341509	1440662_at	*Rgl1*
15.35	BB766747	1436395_at	*Card6*
15.33	BB256507	1447016_at	*Tbc1d1*
14.92	AV261931	1423222_at	*Cap2*
14.72	AK002529	1432205_a_at	*C130038G02Rik*
14.6	BB022640	1456967_at	*Trim66*
14.41	AI595932	1421027_a_at	*Mef2c*
14.09	AV238183	1460405_at	*Arhgef10l*
13.61	NM_030698	1421600_a_at	*Trim26*
13.2	BB770967	1437445_at	*Trpm1*
13.17	BB525541	1457691_at	*Phgdhl1*
13.02	NM_134159	1419671_a_at	*Il17rc*
12.32	AK016639	1454545_at	*4933403L11Rik*
12.11	AV352375	1444073_at	*Maf*
12.09	C76146	1442900_at	-
11.68	**AF054581**	**1420692_at**	***Il2ra***
11.59	BB007136	1457044_at	*4732474O15Rik*
11.56	AV321994	1443078_at	-
11.19	AF230395	1424929_a_at	*Trim26*
11.18	BB314321	1456376_at	-
11.12	BC005679	1448793_a_at	*Sdc4*
11.12	AF329969	1422231_a_at	*Tnfrsf25*
10.83	NM_007969	1417160_s_at	*Expi*
10.64	NM_010553	1421291_at	*Il18rap*
10.17	BB533095	1437279_x_at	*Sdc1*

10.14	BB200905	1458265_at	-
9.94	AK009336	1453552_at	*1600029D21Rik*
9.66	AK018108	1428837_at	*Klhl14*
9.59	NM_021344	1418744_s_at	*Tesc*
9.53	BI788645	1415943_at	*Sdc1*
9.34	AV222628	1456210_at	*5430407P10Rik*
9.22	AW492978	1446994_at	*Exosc2*
9.2	AI550758	1444605_at	*1700061F12Rik*
9.01	BM242490	1437356_at	*Phgdhl1*
9	AI595932	1421028_a_at	*Mef2c*
8.72	**AF054581**	**1420691_at**	***Il2ra***
8.54	BB349272	1440802_at	-
8.53	BG075874	1456453_at	*Evl*
8.44	BB387637	1436491_at	*6330500D04Rik*
8.43	NM_011426	1422161_at	*Siglec1*
8.3	NM_013693	1419607_at	*Tnf*
8.28	AK004874	1425518_at	*Rapgef4*
8.15	BE629162	1426575_at	*Tmem23*
8.14	NM_022431	1449539_at	*Ms4a11*
8.01	BG068695	1459180_at	-
8.01	**AB015422**	**1425822_a_at**	***Dtx1***
7.99	BB536254	1445349_at	-
7.74	AV047342	1421138_a_at	*Pkib*
7.71	AA415783	1447963_at	*EG624824*
7.69	**NM_007651**	**1448617_at**	***Cd53***
7.66	NM_010735	1420353_at	*Lta*
7.38	AK003707	1428472_at	*Spsb1*
7.37	BB480970	1440037_at	*Pbx1*
7.34	BI526033	1455085_at	*1700086L19Rik*
7.11	NM_031880	1422721_at	*Tnk1*
7.07	NM_009513	1418588_at	*Nrsn1*
7.03	W13191	1426464_at	*Nr1d1*
7.02	BB163080	1445711_at	*St6gal1*
6.95	AW552781	1460083_at	*Adam10*
6.94	BB553926	1441569_at	*E330009P21Rik*
6.85	AB067534	1425374_at	*Oas3*
6.79	AK018204	1433014_at	*Kcnd2*
6.7	BB558800	1437056_x_at	*Crispld2*
6.68	NM_026134	1421591_at	*Cylc1*
6.67	AV231424	1436932_at	*Grhl3*
6.66	AK018308	1432310_at	*6530401F13Rik*
6.57	BB280300	1451507_at	*Mef2c*
6.55	BB327547	1444426_at	*F730031O20Rik*
6.49	BQ031259	1435455_at	*C79267*

6.46	NM_013566	1418741_at	*Itgb7*
6.38	BQ173895	1435078_at	*Tanc2*
6.38	NM_008489	1448550_at	*Lbp*
6.34	AW985925	1436499_at	*Tmem23*
6.34	AK005699	1453056_at	*Slc16a13*
6.27	BB357585	1426340_at	*Slc1a3*
6.19	BB426676	1439661_at	*Slc16a14*
6.18	BG069616	1452202_at	*Pde2a*
6.18	**BM240873**	**1455656_at**	***Btla***
6.18	NM_019688	1421622_a_at	*Rapgef4*
6.13	AK017142	1433137_at	*Dlgap1*
6.11	BI788645	1448158_at	*Sdc1*
6.09	NM_133707	1417798_at	*1810019J16Rik*
6.06	NM_017379	1419518_at	*Tuba8*
6.05	NM_009973	1418221_at	*Csn1s2b*
6.05	BB667844	1434442_at	*D5Ertd593e*
5.98	BB739558	1453177_at	*4631426E05Rik*
5.95	AK020505	1460537_at	*Ebf2*
5.94	AK016058	1432191_at	-
5.84	BG261907	1417436_at	*Large*
5.68	BM221121	1439946_at	*Mef2c*
5.65	BB446316	1457410_at	-
5.62	BG967663	1455106_a_at	-
5.58	X57960	1427452_at	*Rpl7*
5.56	AV021455	1428156_at	*Gng2*
5.48	AV333298	1456180_at	*Rbm24*
5.44	AF193796	1425874_at	*Hoxc13*
5.36	AW764291	1430622_at	*St6gal1*
5.32	BI988638	1443885_at	-
5.3	BC018470	1424775_at	*Oas1g*
5.25	NM_015766	1449222_at	*Ebi3*
5.21	NM_024458	1449179_at	*Pdc*
5.17	BG070552	1455279_at	-
5.17	BB291414	1439357_at	*Il17re*
5.17	NM_013694	1422419_s_at	*Tnp2*
5.16	AI606844	1459733_at	*Pea15*
5.15	AV245300	1446139_at	*AI661453*
5.15	**BB804123**	**1459744_at**	***Cd53***
5.15	BB541393	1460093_at	-
5.1	AV221299	1439015_at	*Gfra1*
5.09	NM_009801	1448752_at	*Car2*
5.08	AI195854	1447948_at	*A430107O13Rik*
5.07	NM_007746	1419208_at	*Map3k8*
5.06	AI447329	1444776_at	*2700005E23Rik*

5.05	BB277054	1435918_at	*BC055107*
5.02	BC013442	1416316_at	*Slc27a2*
5	AK004775	1460470_at	*Acoxl*
4.92	BG075800	1420928_at	*St6gal1*
4.89	BB745401	1434758_at	*Crispld2*
4.88	AK013138	1417823_at	*Gcat*
4.85	NM_007965	1450106_a_at	*Evl*
4.8	BE534815	1450440_at	*Gfra1*
4.77	AK015567	1433097_at	*4930473M17Rik*
4.76	BB362600	1442997_at	*Odz3*
4.76	BC003755	1424127_at	*Eya2*
4.76	BG061923	1445518_at	*Zeb2*
4.74	BG973910	1426566_s_at	*Il17re*
4.65	BB528273	1446471_at	-
4.63	NM_009977	1419202_at	*Cst7*
4.62	BM730637	1436204_at	*1110059G02Rik*
4.62	NM_011517	1449534_at	*Sycp3*
4.54	AF300870	1449129_a_at	*Kcnip3*
4.53	AW546029	1440885_at	*Evl*
4.53	BB345595	1443267_at	*Tanc2*
4.52	BB094679	1459811_at	*Mtf2*
4.49	NM_011909	1418191_at	*Usp18*
4.48	BB426320	1440711_at	*C630001G18Rik*
4.45	AV028075	1446769_at	*2810439F02Rik*
4.44	NM_011579	1449009_at	*Tgtp*
4.42	BC023470	1426893_at	*C230093N12Rik*
4.36	AW550625	1427883_a_at	*Col3a1*
4.36	BB215882	1457556_at	-
4.33	BI156044	1455582_at	-
4.31	BB038663	1446563_at	-
4.29	BM939365	1444020_at	*Ncan*
4.29	BG064103	1423602_at	*Traf1*
4.28	AK019034	1460458_at	*Crispld2*
4.26	BB054454	1445404_at	*Kif27*
4.25	NM_008454	1420490_at	*Klk1b26*
4.23	NM_007628	1449177_at	*Ccna1*
4.23	AK017352	1453439_at	*Amtn*
4.2	BI329779	1457263_at	-
4.19	BB424718	1456632_at	*Bcl11a*
4.18	BB218245	1445452_at	*Traf1*
4.15	BE629162	1426576_at	*Tmem23*
4.15	BG070037	1421037_at	*Npas2*
4.11	AK009888	1429602_at	*Cd164l2*
4.1	AI846432	1447536_at	*Lysmd2*

4.07	AW125876	1458624_at	*Rbm24*
4.07	AW553781	1434920_a_at	*Evl*
4.05	NM_016846	1449124_at	*Rgl1*
4.05	AV270913	1435444_at	*Atf6*
4.04	AV259665	1438967_x_at	*Amhr2*
4.02	AV307961	1454752_at	*Rbm24*
4	BC016208	1451229_at	*Hdac11*
3.97	AI661342	1444203_at	-
3.92	AV365582	1437967_at	-
3.91	NM_021360	1422251_at	*Neurl*
3.9	NM_017473	1448723_at	*Rdh7*
3.89	D43690	1449108_at	*Fdx1*
3.87	NM_023224	1422666_at	*Cblc*
3.84	BC024872	1418580_at	*Rtp4*
3.81	BB175186	1443457_at	-
3.78	BB195596	1446739_at	*St6gal1*
3.76	NM_008040	1422350_at	*Fpr-rs3*
3.76	AK012114	1432103_a_at	*Sh3gl3*
3.76	BB776961	1423551_at	*Cdh13*
3.73	**BC005577**	**1424375_s_at**	***Gimap4***
3.72	BB241535	1455899_x_at	*Socs3*
3.7	BE947744	1440288_at	*Ptchd2*
3.69	BB135602	1437636_at	-
3.63	NM_025891	1418467_at	*Smarcd3*
3.63	BG145550	1439141_at	*Gpr18*
3.61	BB282778	1439324_at	*D230004J03Rik*
3.61	AK005500	1452783_at	*Fndc3b*
3.6	AI596360	1420150_at	*Spsb1*
3.6	AW106963	1423439_at	*Pck1*
3.59	AV278455	1430883_at	*4933402C05Rik*
3.51	AV300716	1447621_s_at	*2610307O08Rik*
3.5	BB136012	1447803_x_at	*Capg*
3.5	NM_009350	1418682_at	*Tenr*
3.49	BB208816	1443120_at	*Pdzd4*
3.48	AY090098	1426278_at	*Ifi27*
3.47	NM_009910	1449925_at	*Cxcr3*
3.47	BB768495	1425467_a_at	*Plp1*
3.46	BE990881	1447479_at	-
3.45	BG070844	1426273_at	*Lmbr1*
3.41	NM_010591	1417409_at	*Jun*
3.4	AK004593	1448863_a_at	*Tnfaip1*
3.4	AI790191	1458409_at	*Slc7a8*
3.38	AK004593	1417865_at	*Tnfaip1*
3.37	BC022130	1451239_a_at	*Slc26a1*

3.36	**NM_008037**	**1422931_at**	***Fosl2***
3.34	D14636	1424704_at	*Runx2*
3.33	AK010908	1460437_at	*Pscd4*
3.3	AV277444	1437176_at	*AI451557*
3.29	BE947686	1444653_at	-
3.27	AK007540	1452948_at	*Tnfaip8l2*
3.26	BC006026	1424305_at	*Igj*
3.24	AK006127	1429845_at	*Ptrh1*
3.24	NM_011716	1448411_at	*Wfs1*
3.24	**BG071113**	**1459170_at**	***Foxo1***
3.22	BB662566	1448023_at	*Kalrn*
3.2	AK015846	1454560_at	*4930519N06Rik*
3.18	AV231340	1435541_at	*Btc*
3.16	BC005577	1424374_at	*Gimap4*
3.14	BC015076	1448265_x_at	*Eva1*
3.13	NM_011361	1416041_at	*Sgk*
3.12	NM_008353	1418166_at	*Il12rb1*
3.1	BG069300	1438103_at	*Pcdhgc3*
3.08	NM_019417	1417928_at	*Pdlim4*
3.06	BC012262	1424250_a_at	*Arhgef3*
3.05	BG973910	1452109_at	*Il17re*
3.01	AK018666	1426951_at	*Crim1*
2.99	AF153199	1421977_at	*Mmp19*
2.98	BG064539	1433833_at	*Fndc3b*
2.96	BC002008	1416022_at	*Fabp5*
2.94	NM_133662	1419647_a_at	*Ier3*
2.92	NM_007599	1450355_a_at	*Capg*
2.91	BB235437	1440157_at	*Scml4*
2.89	BB831725	1456212_x_at	-
2.89	AV209206	1457021_x_at	*Amhr2*
2.89	AV259880	1428736_at	*Gramd3*
2.88	NM_133942	1417965_at	*Plekha1*
2.88	BB034038	1435710_at	*AI661384*
2.88	BC011108	1425440_x_at	*Slc41a3*
2.87	BG074777	1442288_at	*Anxa6*
2.86	AK014544	1428595_at	*Slc6a19*
2.84	AK014058	1452751_at	*Ebf3*
2.83	BC023470	1426894_s_at	*C230093N12Rik*
2.75	NM_009097	1416896_at	*Rps6ka1*
2.75	BC002092	1448916_at	*Mafg*
2.74	NM_007423	1416645_a_at	*Afp*
2.73	NM_133809	1418998_at	*Kmo*
2.73	BB824091	1441793_at	*Rnf39*
2.71	AV259880	1428737_s_at	*Gramd3*

2.7	NM_007744	1449183_at	*Comt*
2.7	BC002120	1424671_at	*Plekhf1*
2.7	BC012692	1417826_at	*Akr1e1*
2.7	AK012853	1430029_a_at	*Tspan31*
2.7	AV309418	1456174_x_at	*Ndrg1*
2.68	BB446952	1452982_at	*Igf1r*
2.66	NM_011558	1450521_a_at	-
2.65	BC021548	1424032_at	*Hvcn1*
2.6	BB006809	1417780_at	*Lass4*
2.6	NM_009025	1415850_at	*Rasa3*
2.59	BI660199	1424034_at	-
2.58	AK019325	1431591_s_at	*Gm9706*
2.58	BB280444	1441508_at	*ENSMUSG00000062298*
2.58	BC013525	1449374_at	*Pipox*
2.57	BM208226	1436513_at	*Tanc2*
2.57	BB160562	1437800_at	-
2.56	BG069348	1422086_at	*Tbx19*
2.56	AK020831	1429214_at	*Adamtsl2*
2.55	BI453402	1431352_s_at	*Pvt1*
2.54	BE983573	1447654_at	-
2.54	BC026209	1452016_at	*Alox5ap*
2.52	BC002008	1416021_a_at	*Fabp5*
2.5	**AI462296**	**1416982_at**	***Foxo1***
2.48	AI527359	1438840_x_at	*Apoa1*
2.48	NM_013472	1415818_at	*Anxa6*
2.46	C85657	1428909_at	*FNt05*
2.46	AV254560	1437090_at	*Ccdc63*
2.46	NM_023320	1417128_at	*Plekho1*
2.44	BB436898	1447610_at	-
2.42	NM_019871	1418958_at	*Amac1*
2.41	BB353000	1457469_at	-
2.4	BB446560	1440162_x_at	-
2.4	AI462296	1416981_at	*Foxo1*
2.38	AV303043	1439373_x_at	*Wnt5b*
2.36	NM_010591	1448694_at	*Jun*
2.35	BB009122	1438169_a_at	*Frmd4b*
2.35	NM_025982	1416556_at	*Tspan31*
2.34	AK005036	1428780_at	*Tha1*
2.33	NM_134068	1448985_at	*Dusp22*
2.33	NM_007568	1421161_at	*Btc*
2.33	BC021916	1460351_at	*S100a11*
2.32	BC028561	1428038_at	*Gm568*
2.32	**AI462296**	**1416983_s_at**	***Foxo1***
2.31	AI845421	1445524_at	*Ddc*

2.31	BE986579	1444095_a_at	-
2.29	BC027152	1451340_at	*Arid5a*
2.28	AK014746	1431580_at	*Luzp2*
2.27	BB538661	1434755_at	*Coro2b*
2.26	BC024597	1451998_at	*Tasp1*
2.26	BC006692	1423883_at	*Acsl1*
2.26	AI987929	1450977_s_at	*Ndrg1*
2.25	AI414399	1421243_at	*Rnf144*
2.25	BC017647	1424663_at	*BC017647*
2.24	BB550183	1438211_s_at	-
2.23	BB119177	1435137_s_at	-
2.22	BB530448	1442640_at	*Slfn5*
2.21	BC005776	1424810_at	*Tasp1*
2.21	BQ175246	1451200_at	*Kif1b*
2.21	AK004593	1417866_at	*Tnfaip1*
2.21	BI076834	1427932_s_at	-
2.21	BE311335	1426944_at	*Fbxw8*
2.2	BG067753	1452123_s_at	*Frmd4b*
2.2	BI413218	1450643_s_at	*Acsl1*
2.2	NM_008681	1420760_s_at	*Ndrg1*
2.18	BB528391	1423596_at	*Nek6*
2.18	BI413218	1422526_at	*Acsl1*
2.18	NM_011150	1448380_at	*Lgals3bp*
2.18	BB375402	1438316_a_at	*Ccdc102a*
2.17	AI551328	1458911_at	*C230086A09Rik*
2.17	BC004651	1448241_at	*Gm2a*
2.16	AU018569	1449698_at	-
2.16	BE980124	1426565_at	*Igf1r*
2.14	NM_011633	1448861_at	*Traf5*
2.14	NM_013711	1449097_at	*Txnrd2*
2.14	BQ176116	1454693_at	*Hdac4*
2.13	AV329070	1434359_at	*6330500D04Rik*
2.12	BF714880	1426604_at	-
2.12	BG966339	1434112_at	-
2.12	BB320171	1446108_at	*Ank2*
2.12	NM_033602	1419006_s_at	*Peli2*
2.12	NM_019494	1419698_at	*Cxcl11*
2.11	BM119683	1455442_at	*Slc6a19*
2.11	AI987929	1450976_at	*Ndrg1*
2.11	NM_011604	1421352_at	*Tlr6*
2.1	NM_018781	1421486_at	*Egr3*
2.09	**NM_008452**	**1448890_at**	***Klf2***
2.09	BB175494	1429427_s_at	*Tcf7l2*
2.08	BB707122	1452160_at	*Tiparp*

2.08	BC022734	1424265_at	*Npl*
2.06	BB334959	1456747_x_at	*Cd99l2*
2.06	AV326297	1456334_s_at	-
2.05	NM_021888	1450630_at	*Qtrt1*
2.05	BG868450	1428381_a_at	*2700038C09Rik*
2.02	AF175771	1418398_a_at	*Tspan32*
2.02	BB707122	1452161_at	*Tiparp*
2.02	BB705379	1453212_at	*Zfp383*
2.01	BM242294	1460555_at	*6330500D04Rik*
2	BQ031101	1452603_at	*5330431N19Rik*
2	AK013026	1429246_a_at	*Anxa6*

Table A5 List of down-regulated genes (296 probe sets). Validated differential expression is shown in bold.

Fold Change	Genbank	Probe set	Gene name
-18.14	AW493093	1444596_at	*Pax7*
-17.15	NM_009640	1421441_at	*Angpt1*
-15.31	BC014728	1424178_at	*Tmem38a*
-14.68	BF124648	1433683_at	*Rbm35b*
-12.33	NM_013707	1419707_at	*Krtap14*
-12.14	BB486127	1427149_at	*Plekha6*
-11.77	BC011440	1425398_at	*Hist1h2bc*
-11.36	NM_007820	1421741_at	*Cyp3a16*
-11.07	BG866612	1421439_at	*Wnt8b*
-11.07	BE957024	1457414_at	*Frmd4a*
-10.64	BE993937	1434008_at	*Scn4b*
-10.09	BB278723	1440233_at	*A930013B10Rik*
-9.65	BG070333	1446263_at	-
-9.47	BB767129	1428795_at	*1110021L09Rik*
-9.21	AK005537	1431647_a_at	*Ceacam13*
-9.19	AV379247	1449807_x_at	-
-9.19	NM_021374	1421493_a_at	*Rgs20*
-8.89	NM_017396	1419704_at	*Cyp3a41*
-8.81	AF093620	1419098_at	*Stom*
-8.72	AK015485	1454135_at	*4930458K08Rik*
-8.71	BM250725	1437515_at	*Mrpplf4*
-8.61	BB522820	1455203_at	*A930003A15Rik*
-8.3	AK009168	1453945_at	*2310005E17Rik*
-8.27	AV122850	1431642_at	*Eif2s3y*
-8.18	NM_007400	1421171_at	*Adam12*
-7.95	BE635120	1444313_at	-
-7.83	AK018444	1453659_at	*Cenpo*
-7.82	AK010738	1432018_at	*Ascl2*
-7.7	BQ287036	1443765_at	*1810058N05Rik*
-7.59	AK015525	1431639_at	*4930468A15Rik*
-7.55	AK017922	1430822_at	*Smarce1*
-7.26	NM_021567	1449054_a_at	*Pcbp4*
-7.25	AK006819	1431871_at	*Txndc3*
-7.25	NM_007400	1421172_at	*Adam12*
-7.15	BQ180352	1419389_at	*Pde10a*
-7.06	BB750000	1456919_at	*A930013B10Rik*
-7.02	AW553423	1458243_at	-

-6.99	NM_011303	1448390_a_at	*Dhrs3*
-6.95	NM_022316	1448321_at	*Smoc1*
-6.91	AI854627	1440229_at	*2310034G01Rik*
-6.66	BB313996	1456826_at	*Taok2*
-6.57	BG069218	1434584_a_at	*LOC384077*
-6.52	AI315015	1435371_x_at	*Ces3*
-6.5	BC012658	1417925_at	*Ccl22*
-6.5	AK004908	1427321_s_at	*Cxadr*
-6.38	AV209602	1443661_at	-
-6.34	BG066773	1460329_at	*B4galt6*
-6.24	BG065957	1449654_s_at	-
-6.16	AV301853	1438926_at	*Rpl36a*
-6.06	BB255018	1445275_at	*C130092O11Rik*
-6.05	NM_054098	1460197_a_at	*Steap4*
-6.04	BG068967	1446016_at	-
-6	BB376573	1428569_at	-
-5.98	BB463553	1439400_x_at	*5430433E21Rik*
-5.96	AV336506	1440891_at	*Gria4*
-5.95	BB239244	1445238_at	*Ccl21b*
-5.93	AJ307017	1452509_at	*Usp9y*
-5.84	NM_011979	1420723_at	*Vnn3*
-5.83	BB762344	1458711_at	-
-5.62	BB270688	1441302_at	-
-5.56	BG079457	1459925_at	*Lman2l*
-5.54	BB279458	1456675_at	*AA536749*
-5.53	BI076734	1447170_at	-
-5.48	BG968304	1421290_at	*Hspb7*
-5.4	AK008498	1429378_x_at	*AY761184*
-5.35	BF471959	1434913_at	*Hmgcll1*
-5.32	BB200698	1439657_at	*Kcnk2*
-5.32	BF714674	1457602_at	-
-5.31	BB453858	1443536_at	*Slc7a11*
-5.31	AK014058	1428349_s_at	*Ebf3*
-5.21	BB245038	1457156_at	*Trhde*
-5.15	NM_028146	1449307_at	*Dbndd1*
-5.08	NM_133205	1450329_a_at	*Arr3*
-5.05	BG072064	1458731_at	-
-5.04	U08020	1423669_at	*Col1a1*
-5.03	BB211614	1458104_a_at	*BC038167*
-4.98	AK015582	1433317_at	*Tmem116*
-4.96	AK013485	1432413_at	*Trappc9*
-4.95	AW990746	1460051_at	*BC038613*
-4.88	AK016947	1430155_at	*4933427E11Rik*
-4.83	NM_013906	1418270_at	*Adamts8*

-4.83	BC024774	1425408_a_at	*2610034M16Rik*
-4.77	AW537404	1459959_at	*Gldc*
-4.76	BB516668	1444232_at	*Prkg1*
-4.75	BB333100	1440531_at	*Rbm11*
-4.74	BE457796	1439897_at	*Nebl*
-4.68	BB546375	1443304_at	*Mtl5*
-4.61	BM245880	1433825_at	*Ntrk3*
-4.59	AW537651	1439190_at	*Fhad1*
-4.55	BG073852	1459555_at	-
-4.52	AV282552	1445868_at	*Cpeb3*
-4.51	AU067824	1433969_at	*Cdkl4*
-4.48	BB561487	1437293_x_at	-
-4.46	NM_008553	1450164_at	*Ascl1*
-4.41	BG069012	1459207_at	-
-4.4	BB454472	1459348_at	*Ebf1*
-4.39	BB811311	1437268_at	*Lancl3*
-4.34	AK015417	1432457_at	*4930448F12Rik*
-4.31	AV380908	1456804_at	*EG627821*
-4.3	C76110	1447078_at	-
-4.26	NM_030265	1450370_a_at	*Kcnip4*
-4.23	AK021065	1454517_at	*C030011I16Rik*
-4.18	NM_007762	1418810_at	*Crhr1*
-4.15	BF730550	1438078_at	-
-4.15	BB185152	1441652_at	*Bmpr2*
-4.07	AF302127	1418487_at	*Ripk4*
-4.04	AK015076	1433089_at	-
-4	BM114398	1429401_at	*Stox2*
-3.99	AV274554	1436547_at	*Dgke*
-3.96	BC025502	1424842_a_at	*Arhgap24*
-3.96	BG068973	1446112_at	-
-3.94	AW124671	1443680_at	*Otx2os1*
-3.93	AA266367	1436419_a_at	*1700097N02Rik*
-3.92	BB795572	1455377_at	*Ttll7*
-3.91	AV354142	1449796_at	*Prph1*
-3.87	BB132695	1425571_at	*Slamf1*
-3.87	BB355074	1446638_at	*Ptpru*
-3.86	NM_011990	1420413_at	*Slc7a11*
-3.85	BM211306	1436749_at	*Mesdc2*
-3.79	BB453314	1439066_at	*Angpt1*
-3.78	BB174864	1435126_at	*Dusp15*
-3.78	AK016250	1432167_at	-
-3.78	BG068519	1440476_at	*D6Ertd474e*
-3.73	BB128517	1424987_at	*5430435G22Rik*
-3.73	BF020653	1441805_at	-

-3.72	AF356522	1424936_a_at	*Dnahc8*
-3.7	AV274889	1455846_at	-
-3.7	AW550459	1445268_at	-
-3.68	BC025863	1451846_at	*Nebl*
-3.64	BE947974	1435809_at	*Ankrd34*
-3.63	L04678	1427387_a_at	*Itgb4*
-3.62	BI143915	1454974_at	*Ntn1*
-3.59	BB451946	1442587_at	*Nrcam*
-3.57	AK014969	1429472_at	*4921525O09Rik*
-3.56	AW123182	1440127_a_at	-
-3.55	AW545311	1439487_at	*Lig4*
-3.5	**D87747**	**1448710_at**	***Cxcr4***
-3.47	BG068554	1447158_at	-
-3.47	NM_008038	1450583_s_at	-
-3.45	BB347455	1457251_x_at	-
-3.45	**AI323528**	**1420197_at**	***Gadd45b***
-3.45	BC021368	1426302_at	*Tmprss4*
-3.4	BB549567	1437725_x_at	*Tm2d2*
-3.4	NM_008440	1450108_at	*Kif1a*
-3.38	BE691430	1453503_at	*Spink12*
-3.36	NM_009397	1450829_at	*Tnfaip3*
-3.34	AK005854	1451009_at	*Rnf151*
-3.32	AK013891	1428855_at	*H13*
-3.28	BB482300	1459825_x_at	*Igf2bp1*
-3.24	BB246182	1454953_at	*Rnf157*
-3.21	NM_008905	1417801_a_at	*Ppfibp2*
-3.19	BE954273	1436146_at	*4930481A15Rik*
-3.18	NM_133657	1418821_at	*Cyp2a12*
-3.18	BF235516	1420841_at	*Ptprf*
-3.16	AF109769	1425679_a_at	*Mapk8ip1*
-3.14	NM_029509	1418776_at	*5830443L24Rik*
-3.12	BB163668	1434902_at	*Rnf157*
-3.1	AV047063	1447606_x_at	*Aqp11*
-3.1	AI550443	1436630_at	*Aqp11*
-3.1	BB246182	1434427_a_at	*Rnf157*
-3.1	BB209139	1441974_at	*Camk4*
-3.09	AI648923	1455411_at	*Aqp11*
-3.08	BM214359	1420993_at	*B3gnt5*
-3.07	BE686667	1440874_at	*Slco5a1*
-3.06	BB741330	1438509_at	-
-3.04	BB205754	1440072_at	*Glcci1*
-3.02	AK016530	1430784_a_at	*4932417H02Rik*
-3.01	NM_008348	1448731_at	*Il10ra*
-2.99	BB464727	1438565_at	*A830010M20Rik*

-2.95	AV293368	1434140_at	*Mcf2l*
-2.94	NM_008846	1421833_at	*2900009I07Rik*
-2.92	BF660296	1421941_at	*Camk4*
-2.89	BI465649	1458906_at	-
-2.87	BC014714	1423858_a_at	*Hmgcs2*
-2.85	BI076809	1434929_at	*BC035044*
-2.82	BB280100	1438590_at	*Rapgef3*
-2.82	BC016493	1425112_at	*Ankrd27*
-2.81	BM241351	1433699_at	*Tnfaip3*
-2.81	BB229969	1457141_at	-
-2.8	BB554351	1435211_at	*Ttc12*
-2.8	AA266367	1455692_x_at	*1700097N02Rik*
-2.78	BF472491	1429254_at	*Aqp11*
-2.78	BB230205	1440945_at	-
-2.77	AV312506	1447836_x_at	-
-2.76	BF235516	1420842_at	*Ptprf*
-2.75	NM_134112	1422293_a_at	*Kctd1*
-2.75	BB604994	1419892_at	*1110021J02Rik*
-2.75	BB283644	1457261_at	*A930025H08Rik*
-2.74	AK017076	1431297_a_at	*4933436C20Rik*
-2.72	BM247146	1438295_at	*Glcci1*
-2.72	NM_007956	1421244_at	*Esr1*
-2.71	U41465	1450381_a_at	*Bcl6*
-2.7	BB132695	1425569_a_at	*Slamf1*
-2.67	M31649	1427766_at	*EG667790*
-2.67	AV327791	1436117_at	*A830010M20Rik*
-2.67	BE948928	1428260_at	*Spg3a*
-2.66	AW060821	1447929_at	*Ssh3*
-2.63	BB150687	1457700_at	*4732474A20Rik*
-2.63	**NM_011364**	**1449393_at**	***Sh2d1a***
-2.62	AI428101	1419157_at	*Sox4*
-2.6	BF235516	1420843_at	*Ptprf*
-2.59	BB151674	1444431_at	*Rcsd1*
-2.59	AK011417	1453255_at	*Slc43a1*
-2.57	BG069663	1434277_a_at	*Ypel2*
-2.56	AW558771	1428504_at	*Xrcc6*
-2.55	NM_011156	1422796_at	*Prep*
-2.55	NM_023478	1449104_at	*Upk3a*
-2.54	BB132695	1425570_at	*Slamf1*
-2.51	NM_008846	1450389_s_at	*2900009I07Rik*
-2.5	BB709109	1430230_at	*Rcsd1*
-2.48	NM_008075	1450300_at	*Gabrr1*
-2.48	**BE691816**	**1438805_at**	*Ccnd3*
-2.47	BB552737	1456221_at	*Cdh8*

-2.45	BB031322	1442866_at	*Rcsd1*
-2.45	BG073499	1419049_at	*Pcnx*
-2.4	BE457918	1436154_at	-
-2.39	BB012489	1422642_at	*Cdc42ep3*
-2.39	BM121794	1438452_at	*Nebl*
-2.38	AK006478	1431734_a_at	*Dnajb4*
-2.37	AK008844	1429796_at	*Kalrn*
-2.36	BB159263	1424248_at	*Arpp21*
-2.36	BM935811	1422444_at	*Itga6*
-2.36	**U51279**	**1426050_at**	***Bcl2l1***
-2.35	AK005731	1428705_at	*1700007K13Rik*
-2.34	AK004902	1431833_a_at	*Hmgcs2*
-2.34	BB234335	1441316_at	-
-2.34	BC025206	1425128_at	*B3gnt8*
-2.33	**NM_010278**	**1417679_at**	***Gfi1***
-2.33	BB107412	1429005_at	*Mfhas1*
-2.33	BM118423	1439942_at	*Prep*
-2.32	AK020414	1433241_at	*Rmnd1*
-2.32	BB012489	1450700_at	*Cdc42ep3*
-2.32	BF466091	1448616_at	*Dvl2*
-2.32	BG069663	1454901_at	*Ypel2*
-2.32	M93428	1424825_a_at	*Glycam1*
-2.31	AK016023	1424077_at	*Gdpd1*
-2.3	AK003894	1429402_at	*Glt8d2*
-2.3	AK013449	1429068_at	*A430035B10Rik*
-2.29	BB726971	1439256_x_at	*Gpr137b*
-2.28	AI326328	1438298_a_at	*12-Sep*
-2.27	AF248636	1425086_a_at	*Slamf6*
-2.27	AW495711	1416927_at	*Trp53inp1*
-2.26	BB205273	1441115_at	*Rnf125*
-2.26	BB760479	1450402_at	*Pparbp*
-2.25	BF018155	1453069_at	*Pik3cb*
-2.24	BB323256	1438433_at	*Whdc1*
-2.24	AK018009	1431527_at	*Cd164*
-2.24	NM_009624	1418586_at	*Adcy9*
-2.24	BM935811	1422445_at	*Itga6*
-2.24	BB159263	1451280_at	*Arpp21*
-2.23	**BG143624**	**1444323_at**	*Ccnd3*
-2.2	BI659732	1431068_at	*Rmnd5a*
-2.2	AK009736	1429775_a_at	*Gpr137b*
-2.2	BQ174669	1434962_x_at	*Ccl27*
-2.2	AV334527	1435871_at	*Elavl3*
-2.19	BB023955	1440558_at	*Atp9b*
-2.19	AK016023	1424076_at	*Gdpd1*

-2.19	BE690800	1457828_at	*Stam*
-2.19	AI528824	1449937_at	*Pp11r*
-2.18	BB199960	1442061_at	*Btbd7*
-2.18	BC020532	1424471_at	*Rapgef3*
-2.17	NM_007619	1450457_at	*Cbl*
-2.17	AK003894	1429403_x_at	*Glt8d2*
-2.17	BC021410	1425914_a_at	*Armcx4*
-2.16	BB378464	1440007_at	*Slc43a1*
-2.15	NM_027884	1449405_at	*Tns1*
-2.14	BB667823	1429399_at	*Rnf125*
-2.12	AK012007	1430083_at	*2610307P16Rik*
-2.12	**NM_007632**	**1415907_at**	***Ccnd3***
-2.11	AB015595	1418489_a_at	*Calcrl*
-2.1	NM_027884	1419283_s_at	*Tns1*
-2.1	AV313371	1437561_at	*Trat1*
-2.09	AV306734	1420852_a_at	*B3gnt2*
-2.08	AI788952	1419821_s_at	*Idh1*
-2.07	BC022643	1452249_at	*Prickle1*
-2.07	AV205521	1438437_a_at	-
-2.06	U41465	1421818_at	*Bcl6*
-2.06	BF020504	1435405_at	*Setd4*
-2.06	NM_010585	1460203_at	*Itpr1*
-2.06	BE983452	1457037_at	*Zbtb2*
-2.05	BB807812	1439666_at	*2010001J22Rik*
-2.05	AK012553	1431751_a_at	*Mpped2*
-2.04	BB200607	1435084_at	*C730049O14Rik*
-2.04	BB239651	1457773_at	*Slamf6*
-2.04	BF578163	1421337_at	*Elf4*
-2.03	BE692425	1439956_at	*Ms4a6c*
-2.03	BC017147	1425558_at	*Klc3*
-2.03	BG073499	1419047_at	*Pcnx*
-2.03	AV023018	1455602_x_at	*Rpe*
-2.02	U12434	1451910_a_at	*Cd6*
-2.02	NM_010585	1417279_at	*Itpr1*
-2.02	AV025559	1436991_x_at	*Gsn*
-2.01	NM_031257	1417289_at	*Plekha2*
-2.01	BB549997	1426620_at	*Chst10*
-2.01	AW911766	1459896_at	*Pogk*
-2	BE863648	1429653_at	*Gse1*
-2	AI528824	1449938_at	*Pp11r*

References

Akashi, K., Kondo, M., von Freeden-Jeffry, U., Murray, R., and Weissman, I. L. (1997). Bcl-2 rescues T lymphopoiesis in interleukin-7 receptor-deficient mice. Cell *89*, 1033-1041.

Allen, R. D., 3rd, Bender, T. P., and Siu, G. (1999). c-Myb is essential for early T cell development. Genes Dev *13*, 1073-1078.

Allen, R. D., 3rd, Kim, H. K., Sarafova, S. D., and Siu, G. (2001). Negative regulation of CD4 gene expression by a HES-1-c-Myb complex. Mol Cell Biol *21*, 3071-3082.

Alm-Kristiansen, A. H., Saether, T., Matre, V., Gilfillan, S., Dahle, O., and Gabrielsen, O. S. (2008). FLASH acts as a co-activator of the transcription factor c-Myb and localizes to active RNA polymerase II foci. Oncogene *27*, 4644-4656.

Amundson, S. A., Myers, T. G., Scudiero, D., Kitada, S., Reed, J. C., and Fornace, A. J., Jr. (2000). An informatics approach identifying markers of chemosensitivity in human cancer cell lines. Cancer Res *60*, 6101-6110.

Anderson, M. S., Venanzi, E. S., Klein, L., Chen, Z., Berzins, S. P., Turley, S. J., von Boehmer, H., Bronson, R., Dierich, A., Benoist, C., and Mathis, D. (2002). Projection of an immunological self shadow within the thymus by the aire protein. Science *298*, 1395-1401.

Ashburner, M., Ball, C. A., Blake, J. A., Botstein, D., Butler, H., Cherry, J. M., Davis, A. P., Dolinski, K., Dwight, S. S., Eppig, J. T.*, et al.* (2000). Gene ontology: tool for the unification of biology. The Gene Ontology Consortium. Nat. Genet. *25*, 25-29.

Aziz, N., Miglarese, M. R., Hendrickson, R. C., Shabanowitz, J., Sturgill, T. W., Hunt, D. F., and Bender, T. P. (1995). Modulation of c-Myb-induced transcription activation by a phosphorylation site near the negative regulatory domain. Proc Natl Acad Sci U S A *92*, 6429-6433.

Badiani, P., Corbella, P., Kioussis, D., Marvel, J., and Weston, K. (1994). Dominant interfering alleles define a role for c-Myb in T-cell development. Genes Dev *8*, 770-782.

Bain, G., Cravatt, C. B., Loomans, C., Alberola-Ila, J., Hedrick, S. M., and Murre, C. (2001). Regulation of the helix-loop-helix proteins, E2A and Id3, by the Ras-ERK MAPK cascade. Nat Immunol *2*, 165-171.

Bain, G., Quong, M. W., Soloff, R. S., Hedrick, S. M., and Murre, C. (1999). Thymocyte maturation is regulated by the activity of the helix-loop-helix protein, E47. J Exp Med *190*, 1605-1616.

Balciunaite, G., Ceredig, R., and Rolink, A. G. (2005). The earliest subpopulation of mouse thymocytes contains potent T, significant macrophage, and natural killer cell but no B-lymphocyte potential. Blood *105*, 1930-1936.

Bao, Q., and Shi, Y. (2007). Apoptosome: a platform for the activation of initiator caspases. Cell Death Differ *14*, 56-65.

Bender, T. P., Kremer, C. S., Kraus, M., Buch, T., and Rajewsky, K. (2004). Critical functions for c-Myb at three checkpoints during thymocyte development. Nat. Immunol. *5*, 721-729.

Bender, T. P., and Kuehl, W. M. (1987a). Differential expression of the c-myb proto-oncogene marks the pre-B cell/B cell junction in murine B lymphoid tumors. J Immunol *139*, 3822-3827.

Bender, T. P., and Kuehl, W. M. (1987b). Differential expression of the c-myb proto-oncogene marks the pre-B cell/B cell junction in murine B lymphoid tumors. J. Immunol. *139*, 3822-3827.

Berge, T., Matre, V., Brendeford, E. M., Saether, T., Luscher, B., and Gabrielsen, O. S. (2007). Revisiting a selection of target genes for the hematopoietic transcription factor c-Myb using chromatin immunoprecipitation and c-Myb knockdown. Blood Cells Mol Dis *39*, 278-286.

Biedenkapp, H., Borgmeyer, U., Sippel, A. E., and Klempnauer, K. H. (1988). Viral myb oncogene encodes a sequence-specific DNA-binding activity. Nature *335*, 835-837.

Bies, J., Markus, J., and Wolff, L. (2002). Covalent attachment of the SUMO-1 protein to the negative regulatory domain of the c-Myb transcription factor modifies its stability and transactivation capacity. J Biol Chem *277*, 8999-9009.

Bies, J., and Wolff, L. (1997). Oncogenic activation of c-Myb by carboxyl-terminal truncation leads to decreased proteolysis by the ubiquitin-26S proteasome pathway. Oncogene *14*, 203-212.

Biroccio, A., Benassi, B., D'Agnano, I., D'Angelo, C., Buglioni, S., Mottolese, M., Ricciotti, A., Citro, G., Cosimelli, M., Ramsay, R. G.*, et al.* (2001). c-Myb and Bcl-x overexpression predicts poor prognosis in colorectal cancer: clinical and experimental findings. Am J Pathol *158*, 1289-1299.

Boehm, T., and Bleul, C. C. (2007). The evolutionary history of lymphoid organs. Nat Immunol *8*, 131-135.

Borgulya, P., Kishi, H., Uematsu, Y., and von Boehmer, H. (1992). Exclusion and inclusion of alpha and beta T cell receptor alleles. Cell *69*, 529-537.

Bortner, D. M., and Ostrowski, M. C. (1991). Analysis of the v-myb structural components important for transactivation of gene expression. Nucleic Acids Res *19*, 1533-1539.

Bosselut, R., Guinter, T. I., Sharrow, S. O., and Singer, A. (2003). Unraveling a revealing paradox: Why major histocompatibility complex I-signaled thymocytes "paradoxically"

appear as CD4+8lo transitional cells during positive selection of CD8+ T cells. J Exp Med *197*, 1709-1719.

Bouillet, P., Metcalf, D., Huang, D. C., Tarlinton, D. M., Kay, T. W., Kontgen, F., Adams, J. M., and Strasser, A. (1999). Proapoptotic Bcl-2 relative Bim required for certain apoptotic responses, leukocyte homeostasis, and to preclude autoimmunity. Science *286*, 1735-1738.

Brandle, D., Muller, C., Rulicke, T., Hengartner, H., and Pircher, H. (1992). Engagement of the T-cell receptor during positive selection in the thymus down-regulates RAG-1 expression. Proc. Natl. Acad. Sci. USA *89*, 9529-9533.

Carlson, C. M., Endrizzi, B. T., Wu, J., Ding, X., Weinreich, M. A., Walsh, E. R., Wani, M. A., Lingrel, J. B., Hogquist, K. A., and Jameson, S. C. (2006). Kruppel-like factor 2 regulates thymocyte and T-cell migration. Nature *442*, 299-302.

Carpinelli, M. R., Hilton, D. J., Metcalf, D., Antonchuk, J. L., Hyland, C. D., Mifsud, S. L., Di Rago, L., Hilton, A. A., Willson, T. A., Roberts, A. W.*, et al.* (2004). Suppressor screen in Mpl-/- mice: c-Myb mutation causes supraphysiological production of platelets in the absence of thrombopoietin signaling. Proc Natl Acad Sci U S A *101*, 6553-6558.

Chai, J., Shiozaki, E., Srinivasula, S. M., Wu, Q., Datta, P., Alnemri, E. S., and Shi, Y. (2001). Structural basis of caspase-7 inhibition by XIAP. Cell *104*, 769-780.

Chen, J., Kremer, C. S., and Bender, T. P. (2006). The carbonic anhydrase I locus contains a c-Myb target promoter and modulates differentiation of murine erythroleukemia cells. Oncogene *25*, 2758-2772.

Chen, L., Willis, S. N., Wei, A., Smith, B. J., Fletcher, J. I., Hinds, M. G., Colman, P. M., Day, C. L., Adams, J. M., and Huang, D. C. (2005). Differential targeting of prosurvival Bcl-2 proteins by their BH3-only ligands allows complementary apoptotic function. Mol Cell *17*, 393-403.

Cheng, E. H., Wei, M. C., Weiler, S., Flavell, R. A., Mak, T. W., Lindsten, T., and Korsmeyer, S. J. (2001). BCL-2, BCL-X(L) sequester BH3 domain-only molecules preventing BAX- and BAK-mediated mitochondrial apoptosis. Mol Cell *8*, 705-711.

Cheng, L. E., Chan, F. K., Cado, D., and Winoto, A. (1997). Functional redundancy of the Nur77 and Nor-1 orphan steroid receptors in T-cell apoptosis. Embo J *16*, 1865-1875.

Chinnaiyan, A. M., O'Rourke, K., Tewari, M., and Dixit, V. M. (1995). FADD, a novel death domain-containing protein, interacts with the death domain of Fas and initiates apoptosis. Cell *81*, 505-512.

Clappier, E., Cuccuini, W., Kalota, A., Crinquette, A., Cayuela, J. M., Dik, W. A., Langerak, A. W., Montpellier, B., Nadel, B., Walrafen, P.*, et al.* (2007). The C-MYB locus is involved in chromosomal translocation and genomic duplications in human T-

cell acute leukemia (T-ALL), the translocation defining a new T-ALL subtype in very young children. Blood *110*, 1251-1261.

Cobb, R. M., Oestreich, K. J., Osipovich, O. A., and Oltz, E. M. (2006). Accessibility control of V(D)J recombination. Adv Immunol *91*, 45-109.

Dai, P., Akimaru, H., Tanaka, Y., Hou, D. X., Yasukawa, T., Kanei-Ishii, C., Takahashi, T., and Ishii, S. (1996a). CBP as a transcriptional coactivator of c-Myb. Genes Dev *10*, 528-540.

Dai, P., Akimaru, H., Tanaka, Y., Hou, D. X., Yasukawa, T., Kanei-Ishii, C., Takahashi, T., and Ishii, S. (1996b). CBP as a transcriptional coactivator of c-Myb. Genes. Dev. *10*, 528-540.

Davodeau, F., Difilippantonio, M., Roldan, E., Malissen, M., Casanova, J. L., Couedel, C., Morcet, J. F., Merkenschlager, M., Nussenzweig, A., Bonneville, M., and Malissen, B. (2001). The tight interallelic positional coincidence that distinguishes T-cell receptor Jalpha usage does not result from homologous chromosomal pairing during ValphaJalpha rearrangement. Embo J *20*, 4717-4729.

Deveraux, Q. L., Takahashi, R., Salvesen, G. S., and Reed, J. C. (1997). X-linked IAP is a direct inhibitor of cell-death proteases. Nature *388*, 300-304.

Drabsch, Y., Hugo, H., Zhang, R., Dowhan, D. H., Miao, Y. R., Gewirtz, A. M., Barry, S. C., Ramsay, R. G., and Gonda, T. J. (2007). Mechanism of and requirement for estrogen-

regulated MYB expression in estrogen-receptor-positive breast cancer cells. Proc Natl Acad Sci U S A *104*, 13762-13767.

Du, C., Fang, M., Li, Y., Li, L., and Wang, X. (2000). Smac, a mitochondrial protein that promotes cytochrome c-dependent caspase activation by eliminating IAP inhibition. Cell *102*, 33-42.

Duprey, S. P., and Boettiger, D. (1985). Developmental regulation of c-myb in normal myeloid progenitor cells. Proc. Natl. Acad. Sci. USA *82*, 6937-6941.

Dzhagalov, I., Dunkle, A., and He, Y. W. (2008). The anti-apoptotic Bcl-2 family member Mcl-1 promotes T lymphocyte survival at multiple stages. J. Immunol. *181*, 521-528.

Egawa, T. (2009). Runx and ThPOK: A balancing act to regulate thymocyte lineage commitment. J Cell Biochem.

Egerton, M., Shortman, K., and Scollay, R. (1990). The kinetics of immature murine thymocyte development in vivo. Int. Immunol. *2*, 501-507.

Ellmeier, W., Sawada, S., and Littman, D. R. (1999). The regulation of CD4 and CD8 coreceptor gene expression during T cell development. Annu Rev Immunol *17*, 523-554.

Emambokus, N., Vegiopoulos, A., Harman, B., Jenkinson, E., Anderson, G., and Frampton, J. (2003). Progression through key stages of haemopoiesis is dependent on distinct threshold levels of c-Myb. Embo. J. *22*, 4478-4488.

Enari, M., Sakahira, H., Yokoyama, H., Okawa, K., Iwamatsu, A., and Nagata, S. (1998). A caspase-activated DNase that degrades DNA during apoptosis, and its inhibitor ICAD. Nature *391*, 43-50.

Ess, K. C., Witte, D. P., Bascomb, C. P., and Aronow, B. J. (1999). Diverse developing mouse lineages exhibit high-level c-Myb expression in immature cells and loss of expression upon differentiation. Oncogene *18*, 1103-1111.

Ezzat, S., Zhu, X., Loeper, S., Fischer, S., and Asa, S. L. (2006). Tumor-derived Ikaros 6 acetylates the Bcl-XL promoter to up-regulate a survival signal in pituitary cells. Mol Endocrinol *20*, 2976-2986.

Farnham, P. J. (2009). Insights from genomic profiling of transcription factors. Nat Rev Genet *10*, 605-616.

Feik, N., Bilic, I., Tinhofer, J., Unger, B., Littman, D. R., and Ellmeier, W. (2005). Functional and molecular analysis of the double-positive stage-specific CD8 enhancer E8III during thymocyte development. J Immunol *174*, 1513-1524.

Gallagher, P., Bao, Y., Serrano, S. M., Laing, G. D., Theakston, R. D., Gutierrez, J. M., Escalante, T., Zigrino, P., Moura-da-Silva, A. M., Nischt, R.*, et al.* (2005). Role of the

snake venom toxin jararhagin in proinflammatory pathogenesis: in vitro and in vivo gene expression analysis of the effects of the toxin. Arch. Biochem. Biophys. *441*, 1-15.

Garbe, A. I., and von Boehmer, H. (2007). TCR and Notch synergize in alphabeta versus gammadelta lineage choice. Trends Immunol *28*, 124-131.

Garcia, P., Clarke, M., Vegiopoulos, A., Berlanga, O., Camelo, A., Lorvellec, M., and Frampton, J. (2009). Reduced c-Myb activity compromises HSCs and leads to a myeloproliferation with a novel stem cell basis. Embo J *28*, 1492-1504.

Godfrey, D. I., Kennedy, J., Suda, T., and Zlotnik, A. (1993). A developmental pathway involving four phenotypically and functionally distinct subsets of CD3-CD4-CD8- triple-negative adult mouse thymocytes defined by CD44 and CD25 expression. J. Immunol. *150*, 4244-4252.

Gonda, T. J., Buckmaster, C., and Ramsay, R. G. (1989). Activation of c-myb by carboxy-terminal truncation: relationship to transformation of murine haemopoietic cells in vitro. Embo J *8*, 1777-1783.

Gonda, T. J., Sheiness, D. K., and Bishop, J. M. (1982). Transcripts from the cellular homologs of retroviral oncogenes: distribution among chicken tissues. Mol Cell Biol *2*, 617-624.

Gonzalez, J., Orlofsky, A., and Prystowsky, M. B. (2003). A1 is a growth-permissive antiapoptotic factor mediating postactivation survival in T cells. Blood *101*, 2679-2685.

Gonzalez-Garcia, M., Perez-Ballestero, R., Ding, L., Duan, L., Boise, L. H., Thompson, C. B., and Nunez, G. (1994). bcl-XL is the major bcl-x mRNA form expressed during murine development and its product localizes to mitochondria. Development *120*, 3033-3042.

Goux, D., Coudert, J. D., Maurice, D., Scarpellino, L., Jeannet, G., Piccolo, S., Weston, K., Huelsken, J., and Held, W. (2005). Cooperating pre-T-cell receptor and TCF-1-dependent signals ensure thymocyte survival. Blood *106*, 1726-1733.

Gratiot-Deans, J., Merino, R., Nunez, G., and Turka, L. A. (1994). Bcl-2 expression during T-cell development: early loss and late return occur at specific stages of commitment to differentiation and survival. Proc. Natl. Acad. Sci. USA *91*, 10685-10689.

Grillot, D. A., Gonzalez-Garcia, M., Ekhterae, D., Duan, L., Inohara, N., Ohta, S., Seldin, M. F., and Nunez, G. (1997). Genomic organization, promoter region analysis, and chromosome localization of the mouse bcl-x gene. J. Immunol. *158*, 4750-4757.

Grillot, D. A., Merino, R., and Nunez, G. (1995). Bcl-XL displays restricted distribution during T cell development and inhibits multiple forms of apoptosis but not clonal deletion in transgenic mice. J. Exp. Med. *182*, 1973-1983.

Groettrup, M., Ungewiss, K., Azogui, O., Palacios, R., Owen, M. J., Hayday, A. C., and von Boehmer, H. (1993). A novel disulfide-linked heterodimer on pre-T cells consists of the T cell receptor beta chain and a 33 kd glycoprotein. Cell *75*, 283-294.

Guo, J., Hawwari, A., Li, H., Sun, Z., Mahanta, S. K., Littman, D. R., Krangel, M. S., and He, Y. W. (2002). Regulation of the TCRalpha repertoire by the survival window of CD4(+)CD8(+) thymocytes. Nat. Immunol. *3*, 469-476.

Han, P., Goularte, O. D., Rufner, K., Wilkinson, B., and Kaye, J. (2004). An inhibitory Ig superfamily protein expressed by lymphocytes and APCs is also an early marker of thymocyte positive selection. J Immunol *172*, 5931-5939.

Hashimoto, S., Koji, T., Kohara, N., Kanematsu, T., and Nakane, P. K. (1997). Frequency of apoptosis relates inversely to invasiveness and metastatic activity in human colorectal cancer. Virchows Arch *431*, 241-248.

He, Y. W. (2000). The role of orphan nuclear receptor in thymocyte differentiation and lymphoid organ development. Immunol Res *22*, 71-82.

Hengartner, M. O. (2000). The biochemistry of apoptosis. Nature *407*, 770-776.

Hoffmann, R., Bruno, L., Seidl, T., Rolink, A., and Melchers, F. (2003). Rules for gene usage inferred from a comparison of large-scale gene expression profiles of T and B lymphocyte development. J. Immunol. *170*, 1339-1353.

Huang, C., and Kanagawa, O. (2001a). Ordered and coordinated rearrangement of the TCR alpha locus: role of secondary rearrangement in thymic selection. J. Immunol. *166*, 2597-2601.

Huang, C., and Kanagawa, O. (2001b). Ordered and coordinated rearrangement of the TCR alpha locus: role of secondary rearrangement in thymic selection. J Immunol *166*, 2597-2601.

Huang, C. Y., Sleckman, B. P., and Kanagawa, O. (2005). Revision of T cell receptor {alpha} chain genes is required for normal T lymphocyte development. Proc. Natl. Acad. Sci. USA *102*, 14356-14361.

Hugo, H., Cures, A., Suraweera, N., Drabsch, Y., Purcell, D., Mantamadiotis, T., Phillips, W., Dobrovic, A., Zupi, G., Gonda, T. J.*, et al.* (2006). Mutations in the MYB intron I regulatory sequence increase transcription in colon cancers. Genes Chromosomes Cancer *45*, 1143-1154.

Ioannidis, V., Beermann, F., Clevers, H., and Held, W. (2001). The beta-catenin--TCF-1 pathway ensures CD4(+)CD8(+) thymocyte survival. Nat. Immunol. *2*, 691-697.

Ivanov, II, McKenzie, B. S., Zhou, L., Tadokoro, C. E., Lepelley, A., Lafaille, J. J., Cua, D. J., and Littman, D. R. (2006). The orphan nuclear receptor RORgammat directs the differentiation program of proinflammatory IL-17+ T helper cells. Cell *126*, 1121-1133.

Jones, M. E., and Zhuang, Y. (2007). Acquisition of a functional T cell receptor during T lymphocyte development is enforced by HEB and E2A transcription factors. Immunity *27*, 860-870.

Jost, P. J., Grabow, S., Gray, D., McKenzie, M. D., Nachbur, U., Huang, D. C., Bouillet, P., Thomas, H. E., Borner, C., Silke, J.*, et al.* (2009). XIAP discriminates between type I and type II FAS-induced apoptosis. Nature *460*, 1035-1039.

Jung, D., and Alt, F. W. (2004). Unraveling V(D)J recombination; insights into gene regulation. Cell *116*, 299-311.

Kanei-Ishii, C., Ninomiya-Tsuji, J., Tanikawa, J., Nomura, T., Ishitani, T., Kishida, S., Kokura, K., Kurahashi, T., Ichikawa-Iwata, E., Kim, Y.*, et al.* (2004). Wnt-1 signal induces phosphorylation and degradation of c-Myb protein via TAK1, HIPK2, and NLK. Genes Dev *18*, 816-829.

Klempnauer, K. H., Bonifer, C., and Sippel, A. E. (1986). Identification and characterization of the protein encoded by the human c-myb proto-oncogene. Embo. J. *5*, 1903-1911.

Klempnauer, K. H., Gonda, T. J., and Bishop, J. M. (1982). Nucleotide sequence of the retroviral leukemia gene v-myb and its cellular progenitor c-myb: the architecture of a transduced oncogene. Cell *31*, 453-463.

Krajewska, M., Moss, S. F., Krajewski, S., Song, K., Holt, P. R., and Reed, J. C. (1996). Elevated expression of Bcl-X and reduced Bak in primary colorectal adenocarcinomas. Cancer Res *56*, 2422-2427.

Kwan, J., and Killeen, N. (2004). CCR7 directs the migration of thymocytes into the thymic medulla. J Immunol *172*, 3999-4007.

Lahortiga, I., De Keersmaecker, K., Van Vlierberghe, P., Graux, C., Cauwelier, B., Lambert, F., Mentens, N., Beverloo, H. B., Pieters, R., Speleman, F.*, et al.* (2007). Duplication of the MYB oncogene in T cell acute lymphoblastic leukemia. Nat. Genet. *39*, 593-595.

Lang, G., White, J. R., Argent-Katwala, M. J., Allinson, C. G., and Weston, K. (2005). Myb proteins regulate the expression of diverse target genes. Oncogene *24*, 1375-1384.

Law, Y. M., Yeung, R. S., Mamalaki, C., Kioussis, D., Mak, T. W., and Flavell, R. A. (1994). Human CD4 restores normal T cell development and function in mice deficient in murine CD4. J Exp Med *179*, 1233-1242.

Lee, P. P., Fitzpatrick, D. R., Beard, C., Jessup, H. K., Lehar, S., Makar, K. W., Perez-Melgosa, M., Sweetser, M. T., Schlissel, M. S., Nguyen, S.*, et al.* (2001). A critical role for Dnmt1 and DNA methylation in T cell development, function, and survival. Immunity *15*, 763-774.

Levin, S. D., Anderson, S. J., Forbush, K. A., and Perlmutter, R. M. (1993). A dominant-negative transgene defines a role for p56lck in thymopoiesis. Embo J *12*, 1671-1680.

Lieu, Y. K., Kumar, A., Pajerowski, A. G., Rogers, T. J., and Reddy, E. P. (2004). Requirement of c-myb in T cell development and in mature T cell function. Proc. Natl. Acad. Sci. USA *101*, 14853-14858.

Lin, B., Kolluri, S. K., Lin, F., Liu, W., Han, Y. H., Cao, X., Dawson, M. I., Reed, J. C., and Zhang, X. K. (2004). Conversion of Bcl-2 from protector to killer by interaction with nuclear orphan receptor Nur77/TR3. Cell *116*, 527-540.

Linette, G. P., Li, Y., Roth, K., and Korsmeyer, S. J. (1996). Cross talk between cell death and cell cycle progression: BCL-2 regulates NFAT-mediated activation. Proc Natl Acad Sci U S A *93*, 9545-9552.

Lipsick, J. S. (1996). One billion years of Myb. Oncogene *13*, 223-235.

Liston, A., Lesage, S., Wilson, J., Peltonen, L., and Goodnow, C. C. (2003). Aire regulates negative selection of organ-specific T cells. Nat Immunol *4*, 350-354.

Liu, F., Lei, W., O'Rourke, J. P., and Ness, S. A. (2006). Oncogenic mutations cause dramatic, qualitative changes in the transcriptional activity of c-Myb. Oncogene *25*, 795-805.

Locksley, R. M., Reiner, S. L., Hatam, F., Littman, D. R., and Killeen, N. (1993). Helper T cells without CD4: control of leishmaniasis in CD4-deficient mice. Science *261*, 1448-1451.

Lu, J., Guo, S., Ebert, B. L., Zhang, H., Peng, X., Bosco, J., Pretz, J., Schlanger, R., Wang, J. Y., Mak, R. H.*, et al.* (2008). MicroRNA-mediated control of cell fate in megakaryocyte-erythrocyte progenitors. Dev Cell *14*, 843-853.

Luscher, B., and Eisenman, R. N. (1988). c-myc and c-myb protein degradation: effect of metabolic inhibitors and heat shock. Mol Cell Biol *8*, 2504-2512.

Ma, A., Pena, J. C., Chang, B., Margosian, E., Davidson, L., Alt, F. W., and Thompson, C. B. (1995). Bclx regulates the survival of double-positive thymocytes. Proc Natl Acad Sci U S A *92*, 4763-4767.

Malissen, M., Trucy, J., Jouvin-Marche, E., Cazenave, P. A., Scollay, R., and Malissen, B. (1992). Regulation of TCR alpha and beta gene allelic exclusion during T-cell development. Immunol Today *13*, 315-322.

Mandal, M., Borowski, C., Palomero, T., Ferrando, A. A., Oberdoerffer, P., Meng, F., Ruiz-Vela, A., Ciofani, M., Zuniga-Pflucker, J. C., Screpanti, I.*, et al.* (2005). The BCL2A1 gene as a pre-T cell receptor-induced regulator of thymocyte survival. J Exp Med *201*, 603-614.

Mandal, M., Crusio, K. M., Meng, F., Liu, S., Kinsella, M., Clark, M. R., Takeuchi, O., and Aifantis, I. (2008). Regulation of lymphocyte progenitor survival by the proapoptotic activities of Bim and Bid. Proc Natl Acad Sci U S A *105*, 20840-20845.

Maraskovsky, E., O'Reilly, L. A., Teepe, M., Corcoran, L. M., Peschon, J. J., and Strasser, A. (1997). Bcl-2 can rescue T lymphocyte development in interleukin-7 receptor-deficient mice but not in mutant rag-1-/- mice. Cell *89*, 1011-1019.

Marsden, V. S., O'Connor, L., O'Reilly, L. A., Silke, J., Metcalf, D., Ekert, P. G., Huang, D. C., Cecconi, F., Kuida, K., Tomaselli, K. J.*, et al.* (2002). Apoptosis initiated by Bcl-2-regulated caspase activation independently of the cytochrome c/Apaf-1/caspase-9 apoptosome. Nature *419*, 634-637.

Mason, K. D., Carpinelli, M. R., Fletcher, J. I., Collinge, J. E., Hilton, A. A., Ellis, S., Kelly, P. N., Ekert, P. G., Metcalf, D., Roberts, A. W.*, et al.* (2007). Programmed anuclear cell death delimits platelet life span. Cell *128*, 1173-1186.

Masuda, K., Kakugawa, K., Nakayama, T., Minato, N., Katsura, Y., and Kawamoto, H. (2007). T cell lineage determination precedes the initiation of TCR beta gene rearrangement. J Immunol *179*, 3699-3706.

Maurice, D., Hooper, J., Lang, G., and Weston, K. (2007). c-Myb regulates lineage choice in developing thymocytes via its target gene Gata3. Embo. J. *26*, 3629-3640.

McCann, S., Sullivan, J., Guerra, J., Arcinas, M., and Boxer, L. M. (1995). Repression of the c-myb gene by WT1 protein in T and B cell lines. J Biol Chem *270*, 23785-23789.

McMurry, M. T., and Krangel, M. S. (2000). A role for histone acetylation in the developmental regulation of VDJ recombination. Science *287*, 495-498.

Mick, V. E., Starr, T. K., McCaughtry, T. M., McNeil, L. K., and Hogquist, K. A. (2004). The regulated expression of a diverse set of genes during thymocyte positive selection in vivo. J. Immunol. *173*, 5434-5444.

Misslitz, A., Bernhardt, G., and Forster, R. (2006). Trafficking on serpentines: molecular insight on how maturating T cells find their winding paths in the thymus. Immunol Rev *209*, 115-128.

Mo, X., Kowenz-Leutz, E., Laumonnier, Y., Xu, H., and Leutz, A. (2005). Histone H3 tail positioning and acetylation by the c-Myb but not the v-Myb DNA-binding SANT domain. Genes Dev *19*, 2447-2457.

Mucenski, M. L., McLain, K., Kier, A. B., Swerdlow, S. H., Schreiner, C. M., Miller, T. A., Pietryga, D. W., Scott, W. J., Jr., and Potter, S. S. (1991). A functional c-myb gene is required for normal murine fetal hepatic hematopoiesis. Cell *65*, 677-689.

Mukai, H. Y., Motohashi, H., Ohneda, O., Suzuki, N., Nagano, M., and Yamamoto, M. (2006). Transgene insertion in proximity to the c-myb gene disrupts erythroid-megakaryocytic lineage bifurcation. Mol Cell Biol *26*, 7953-7965.

Ness, S. A. (2003). Myb protein specificity: evidence of a context-specific transcription factor code. Blood Cells Mol Dis *31*, 192-200.

Newton, K., Harris, A. W., and Strasser, A. (2000). FADD/MORT1 regulates the pre-TCR checkpoint and can function as a tumour suppressor. Embo J *19*, 931-941.

Nomura, T., Sakai, N., Sarai, A., Sudo, T., Kanei-Ishii, C., Ramsay, R. G., Favier, D., Gonda, T. J., and Ishii, S. (1993). Negative autoregulation of c-Myb activity by homodimer formation through the leucine zipper. J Biol Chem *268*, 21914-21923.

Nomura, T., Tanikawa, J., Akimaru, H., Kanei-Ishii, C., Ichikawa-Iwata, E., Khan, M. M., Ito, H., and Ishii, S. (2004). Oncogenic activation of c-Myb correlates with a loss of negative regulation by TIF1beta and Ski. J. Biol. Chem. *279*, 16715-16726.

Oberdoerffer, P., Kanellopoulou, C., Heissmeyer, V., Paeper, C., Borowski, C., Aifantis, I., Rao, A., and Rajewsky, K. (2005). Efficiency of RNA interference in the mouse hematopoietic system varies between cell types and developmental stages. Mol Cell Biol *25*, 3896-3905.

Oelgeschlager, M., Janknecht, R., Krieg, J., Schreek, S., and Luscher, B. (1996). Interaction of the co-activator CBP with Myb proteins: effects on Myb-specific transactivation and on the cooperativity with NF-M. Embo J *15*, 2771-2780.

Ohoka, Y., Kuwata, T., Tozawa, Y., Zhao, Y., Mukai, M., Motegi, Y., Suzuki, R., Yokoyama, M., and Iwata, M. (1996). In vitro differentiation and commitment of CD4+ CD8+ thymocytes to the CD4 lineage, without TCR engagement. Int. Immunol. *8*, 297-306.

Oka, K., Qi, B., and Yutsudo, M. (1999). Tumorigenic conversion resulting from inhibition of apoptosis in a nontumorigenic HeLa-derived hybrid cell line. Cancer Res *59*, 1816-1819.

Opferman, J. T. (2008). Apoptosis in the development of the immune system. Cell. Death. Differ. *15*, 234-242.

Opferman, J. T., Letai, A., Beard, C., Sorcinelli, M. D., Ong, C. C., and Korsmeyer, S. J. (2003). Development and maintenance of B and T lymphocytes requires antiapoptotic MCL-1. Nature *426*, 671-676.

Pear, W. S., Miller, J. P., Xu, L., Pui, J. C., Soffer, B., Quackenbush, R. C., Pendergast, A. M., Bronson, R., Aster, J. C., Scott, M. L., and Baltimore, D. (1998). Efficient and rapid induction of a chronic myelogenous leukemia-like myeloproliferative disease in mice receiving P210 bcr/abl-transduced bone marrow. Blood *92*, 3780-3792.

Pearson, R., and Weston, K. (2000). c-Myb regulates the proliferation of immature thymocytes following beta-selection. Embo J *19*, 6112-6120.

Penit, C., Lucas, B., and Vasseur, F. (1995). Cell expansion and growth arrest phases during the transition from precursor (CD4-8-) to immature (CD4+8+) thymocytes in normal and genetically modified mice. J. Immunol. *154*, 5103-5113.

Persson, M., Andren, Y., Mark, J., Horlings, H. M., Persson, F., and Stenman, G. (2009). Recurrent fusion of MYB and NFIB transcription factor genes in carcinomas of the breast and head and neck. Proc Natl Acad Sci U S A.

Peschon, J. J., Morrissey, P. J., Grabstein, K. H., Ramsdell, F. J., Maraskovsky, E., Gliniak, B. C., Park, L. S., Ziegler, S. F., Williams, D. E., Ware, C. B.*, et al.* (1994). Early lymphocyte expansion is severely impaired in interleukin 7 receptor-deficient mice. J Exp Med *180*, 1955-1960.

Petrie, H. T., Livak, F., Burtrum, D., and Mazel, S. (1995). T cell receptor gene recombination patterns and mechanisms: cell death, rescue, and T cell production. J. Exp. Med. *182*, 121-127.

Petrie, H. T., Livak, F., Schatz, D. G., Strasser, A., Crispe, I. N., and Shortman, K. (1993). Multiple rearrangements in T cell receptor alpha chain genes maximize the production of useful thymocytes. J. Exp. Med. *178*, 615-622.

Pfaffl, M. W. (2001). A new mathematical model for relative quantification in real-time RT-PCR. Nucleic. Acids. Res. *29*, e45.

Plachetka, A., Chayka, O., Wilczek, C., Melnik, S., Bonifer, C., and Klempnauer, K. H. (2008). C/EBPbeta induces chromatin opening at a cell-type-specific enhancer. Mol Cell Biol *28*, 2102-2112.

Radtke, F., Wilson, A., Stark, G., Bauer, M., van Meerwijk, J., MacDonald, H. R., and Aguet, M. (1999). Deficient T cell fate specification in mice with an induced inactivation of Notch1. Immunity *10*, 547-558.

Ramsay, R. G., and Gonda, T. J. (2008). MYB function in normal and cancer cells. Nat Rev Cancer *8*, 523-534.

Rathmell, J. C., Farkash, E. A., Gao, W., and Thompson, C. B. (2001). IL-7 enhances the survival and maintains the size of naive T cells. J. Immunol. *167*, 6869-6876.

Rathmell, J. C., Lindsten, T., Zong, W. X., Cinalli, R. M., and Thompson, C. B. (2002). Deficiency in Bak and Bax perturbs thymic selection and lymphoid homeostasis. Nat. Immunol. *3*, 932-939.

Rathmell, J. C., Vander Heiden, M. G., Harris, M. H., Frauwirth, K. A., and Thompson, C. B. (2000). In the absence of extrinsic signals, nutrient utilization by lymphocytes is insufficient to maintain either cell size or viability. Mol. Cell. *6*, 683-692.

Ravichandran, K. S. (2003). "Recruitment signals" from apoptotic cells: invitation to a quiet meal. Cell *113*, 817-820.

Reschly, E. J., Spaulding, C., Vilimas, T., Graham, W. V., Brumbaugh, R. L., Aifantis, I., Pear, W. S., and Kee, B. L. (2006). Notch1 promotes survival of E2A-deficient T cell lymphomas through pre-T cell receptor-dependent and -independent mechanisms. Blood *107*, 4115-4121.

Riedl, S. J., Renatus, M., Schwarzenbacher, R., Zhou, Q., Sun, C., Fesik, S. W., Liddington, R. C., and Salvesen, G. S. (2001). Structural basis for the inhibition of caspase-3 by XIAP. Cell *104*, 791-800.

Riegert, P., and Gilfillan, S. (1999). A conserved sequence block in the murine and human TCR J alpha region: assessment of regulatory function in vivo. J. Immunol. *162*, 3471-3480.

Rothenberg, E. V. (2009). Decision by committee: new light on the CD4/CD8-lineage choice. Immunol Cell Biol *87*, 109-112.

Rozowsky, J., Euskirchen, G., Auerbach, R. K., Zhang, Z. D., Gibson, T., Bjornson, R., Carriero, N., Snyder, M., and Gerstein, M. B. (2009). PeakSeq enables systematic scoring of ChIP-seq experiments relative to controls. Nat Biotechnol *27*, 66-75.

Sakamoto, H., Dai, G., Tsujino, K., Hashimoto, K., Huang, X., Fujimoto, T., Mucenski, M., Frampton, J., and Ogawa, M. (2006). Proper levels of c-Myb are discretely defined at distinct steps of hematopoietic cell development. Blood *108*, 896-903.

Sakura, H., Kanei-Ishii, C., Nagase, T., Nakagoshi, H., Gonda, T. J., and Ishii, S. (1989). Delineation of three functional domains of the transcriptional activator encoded by the c-myb protooncogene. Proc Natl Acad Sci U S A *86*, 5758-5762.

Sala, A., Nicolaides, N. C., Engelhard, A., Bellon, T., Lawe, D. C., Arnold, A., Grana, X., Giordano, A., and Calabretta, B. (1994). Correlation between E2F-1 requirement in

the S phase and E2F-1 transactivation of cell cycle-related genes in human cells. Cancer Res *54*, 1402-1406.

Salmena, L., Lemmers, B., Hakem, A., Matysiak-Zablocki, E., Murakami, K., Au, P. Y., Berry, D. M., Tamblyn, L., Shehabeldin, A., Migon, E.*, et al.* (2003). Essential role for caspase 8 in T-cell homeostasis and T-cell-mediated immunity. Genes Dev *17*, 883-895.

Sambandam, A., Maillard, I., Zediak, V. P., Xu, L., Gerstein, R. M., Aster, J. C., Pear, W. S., and Bhandoola, A. (2005). Notch signaling controls the generation and differentiation of early T lineage progenitors. Nat Immunol *6*, 663-670.

Sandberg, M. L., Sutton, S. E., Pletcher, M. T., Wiltshire, T., Tarantino, L. M., Hogenesch, J. B., and Cooke, M. P. (2005). c-Myb and p300 regulate hematopoietic stem cell proliferation and differentiation. Dev Cell *8*, 153-166.

Sano, Y., and Ishii, S. (2001). Increased affinity of c-Myb for CREB-binding protein (CBP) after CBP-induced acetylation. J Biol Chem *276*, 3674-3682.

Sarafova, S. D., Van Laethem, F., Adoro, S., Guinter, T., Sharrow, S. O., Feigenbaum, L., and Singer, A. (2009). Upregulation of CD4 Expression during MHC Class II-Specific Positive Selection Is Essential for Error-free Lineage Choice. Immunity.

Scaffidi, C., Fulda, S., Srinivasan, A., Friesen, C., Li, F., Tomaselli, K. J., Debatin, K. M., Krammer, P. H., and Peter, M. E. (1998). Two CD95 (APO-1/Fas) signaling pathways. Embo J *17*, 1675-1687.

Schmitt, T. M., Ciofani, M., Petrie, H. T., and Zuniga-Pflucker, J. C. (2004). Maintenance of T cell specification and differentiation requires recurrent notch receptor-ligand interactions. J Exp Med *200*, 469-479.

Schmitt, T. M., and Zuniga-Pflucker, J. C. (2002). Induction of T cell development from hematopoietic progenitor cells by delta-like-1 in vitro. Immunity *17*, 749-756.

Shen, H. Q., Lu, M., Ikawa, T., Masuda, K., Ohmura, K., Minato, N., Katsura, Y., and Kawamoto, H. (2003). T/NK bipotent progenitors in the thymus retain the potential to generate dendritic cells. J Immunol *171*, 3401-3406.

Shortman, K., Egerton, M., Spangrude, G. J., and Scollay, R. (1990). The generation and fate of thymocytes. Semin Immunol *2*, 3-12.

Sidman, C. L., Marshall, J. D., and Von Boehmer, H. (1992). Transgenic T cell receptor interactions in the lymphoproliferative and autoimmune syndromes of lpr and gld mutant mice. Eur J Immunol *22*, 499-504.

Singer, A. (2002). New perspectives on a developmental dilemma: the kinetic signaling model and the importance of signal duration for the CD4/CD8 lineage decision. Curr Opin Immunol *14*, 207-215.

Singer, A., Adoro, S., and Park, J. H. (2008). Lineage fate and intense debate: myths, models and mechanisms of CD4- versus CD8-lineage choice. Nat. Rev. Immunol. *8*, 788-801.

Siu, G., Wurster, A. L., Lipsick, J. S., and Hedrick, S. M. (1992). Expression of the CD4 gene requires a Myb transcription factor. Mol Cell Biol *12*, 1592-1604.

Smith, K. G., Strasser, A., and Vaux, D. L. (1996). CrmA expression in T lymphocytes of transgenic mice inhibits CD95 (Fas/APO-1)-transduced apoptosis, but does not cause lymphadenopathy or autoimmune disease. Embo J *15*, 5167-5176.

Starr, T. K., Jameson, S. C., and Hogquist, K. A. (2003). Positive and negative selection of T cells. Annu. Rev. Immunol. *21*, 139-176.

Strasser, A., Harris, A. W., and Cory, S. (1991). bcl-2 transgene inhibits T cell death and perturbs thymic self-censorship. Cell *67*, 889-899.

Sudo, T., Nishikawa, S., Ohno, N., Akiyama, N., Tamakoshi, M., and Yoshida, H. (1993). Expression and function of the interleukin 7 receptor in murine lymphocytes. Proc Natl Acad Sci U S A *90*, 9125-9129.

Sullivan, J., Feeley, B., Guerra, J., and Boxer, L. M. (1997). Identification of the major positive regulators of c-myb expression in hematopoietic cells of different lineages. J Biol Chem *272*, 1943-1949.

Sun, Z., Unutmaz, D., Zou, Y. R., Sunshine, M. J., Pierani, A., Brenner-Morton, S., Mebius, R. E., and Littman, D. R. (2000). Requirement for RORgamma in thymocyte survival and lymphoid organ development. Science *288*, 2369-2373.

Suzuki, G., Sawa, H., Kobayashi, Y., Nakata, Y., Nakagawa, K., Uzawa, A., Sakiyama, H., Kakinuma, S., Iwabuchi, K., and Nagashima, K. (1999). Pertussis toxin-sensitive signal controls the trafficking of thymocytes across the corticomedullary junction in the thymus. J Immunol *162*, 5981-5985.

Tahirov, T. H., Sato, K., Ichikawa-Iwata, E., Sasaki, M., Inoue-Bungo, T., Shiina, M., Kimura, K., Takata, S., Fujikawa, A., Morii, H.*, et al.* (2002). Mechanism of c-Myb-C/EBP beta cooperation from separated sites on a promoter. Cell *108*, 57-70.

Takahama, Y., and Nakauchi, H. (1996). Phorbol ester and calcium ionophore can replace TCR signals that induce positive selection of CD4 T cells. J. Immunol. *157*, 1508-1513.

Tanaka, Y., Patestos, N. P., Maekawa, T., and Ishii, S. (1999). B-myb is required for inner cell mass formation at an early stage of development. J Biol Chem *274*, 28067-28070.

Taylor, D., Badiani, P., and Weston, K. (1996). A dominant interfering Myb mutant causes apoptosis in T cells. Genes Dev *10*, 2732-2744.

Teh, H. S., Kisielow, P., Scott, B., Kishi, H., Uematsu, Y., Bluthmann, H., and von Boehmer, H. (1988). Thymic major histocompatibility complex antigens and the alpha beta T-cell receptor determine the CD4/CD8 phenotype of T cells. Nature *335*, 229-233.

Testi, R., D'Ambrosio, D., De Maria, R., and Santoni, A. (1994). The CD69 receptor: a multipurpose cell-surface trigger for hematopoietic cells. Immunol. Today. *15*, 479-483.

Thomas, M. D., Kremer, C. S., Ravichandran, K. S., Rajewsky, K., and Bender, T. P. (2005). c-Myb is critical for B cell development and maintenance of follicular B cells. Immunity *23*, 275-286.

Thompson, S. D., Pelkonen, J., and Hurwitz, J. L. (1990). First T cell receptor alpha gene rearrangements during T cell ontogeny skew to the 5' region of the J alpha locus. J Immunol *145*, 2347-2352.

Tomlinson, M. G., Hanke, T., Hughes, D. A., Barclay, A. N., Scholl, E., Hunig, T., and Wright, M. D. (1995). Characterization of mouse CD53: epitope mapping, cellular distribution and induction by T cell receptor engagement during repertoire selection. Eur J Immunol *25*, 2201-2205.

Toscani, A., Mettus, R. V., Coupland, R., Simpkins, H., Litvin, J., Orth, J., Hatton, K. S., and Reddy, E. P. (1997). Arrest of spermatogenesis and defective breast development in mice lacking A-myb. Nature *386*, 713-717.

Toth, C. R., Hostutler, R. F., Baldwin, A. S., Jr., and Bender, T. P. (1995). Members of the nuclear factor kappa B family transactivate the murine c-myb gene. J Biol Chem *270*, 7661-7671.

Turka, L. A., Schatz, D. G., Oettinger, M. A., Chun, J. J., Gorka, C., Lee, K., McCormack, W. T., and Thompson, C. B. (1991). Thymocyte expression of RAG-1 and RAG-2: termination by T cell receptor cross-linking. Science *253*, 778-781.

Tyznik, A. J., Sun, J. C., and Bevan, M. J. (2004). The CD8 population in CD4-deficient mice is heavily contaminated with MHC class II-restricted T cells. J Exp Med *199*, 559-565.

Ueno, T., Saito, F., Gray, D. H., Kuse, S., Hieshima, K., Nakano, H., Kakiuchi, T., Lipp, M., Boyd, R. L., and Takahama, Y. (2004). CCR7 signals are essential for cortex-medulla migration of developing thymocytes. J Exp Med *200*, 493-505.

Veis, D. J., Sorenson, C. M., Shutter, J. R., and Korsmeyer, S. J. (1993). Bcl-2-deficient mice demonstrate fulminant lymphoid apoptosis, polycystic kidneys, and hypopigmented hair. Cell *75*, 229-240.

Verbeek, S., Izon, D., Hofhuis, F., Robanus-Maandag, E., te Riele, H., van de Wetering, M., Oosterwegel, M., Wilson, A., MacDonald, H. R., and Clevers, H. (1995). An HMG-box-containing T-cell factor required for thymocyte differentiation. Nature *374*, 70-74.

Verhagen, A. M., Ekert, P. G., Pakusch, M., Silke, J., Connolly, L. M., Reid, G. E., Moritz, R. L., Simpson, R. J., and Vaux, D. L. (2000). Identification of DIABLO, a mammalian protein that promotes apoptosis by binding to and antagonizing IAP proteins. Cell *102*, 43-53.

Verschelde, C., Michonneau, D., Trescol-Biemont, M. C., Berberich, I., Schimpl, A., and Bonnefoy-Berard, N. (2006). Overexpression of the antiapoptotic protein A1 promotes the survival of double positive thymocytes awaiting positive selection. Cell. Death. Differ. *13*, 1213-1221.

Villey, I., Caillol, D., Selz, F., Ferrier, P., and de Villartay, J. P. (1996). Defect in rearrangement of the most 5' TCR-J alpha following targeted deletion of T early alpha (TEA): implications for TCR alpha locus accessibility. Immunity *5*, 331-342.

Villunger, A., Marsden, V. S., Zhan, Y., Erlacher, M., Lew, A. M., Bouillet, P., Berzins, S., Godfrey, D. I., Heath, W. R., and Strasser, A. (2004). Negative selection of semimature CD4(+)8(-)HSA+ thymocytes requires the BH3-only protein Bim but is independent of death receptor signaling. Proc Natl Acad Sci U S A *101*, 7052-7057.

von Boehmer, H. (2004). Selection of the T-cell repertoire: receptor-controlled checkpoints in T-cell development. Adv Immunol *84*, 201-238.

von Boehmer, H., Aifantis, I., Feinberg, J., Lechner, O., Saint-Ruf, C., Walter, U., Buer, J., and Azogui, O. (1999). Pleiotropic changes controlled by the pre-T-cell receptor. Curr Opin Immunol *11*, 135-142.

von Freeden-Jeffry, U., Solvason, N., Howard, M., and Murray, R. (1997). The earliest T lineage-committed cells depend on IL-7 for Bcl-2 expression and normal cell cycle progression. Immunity *7*, 147-154.

Wang, F., Huang, C. Y., and Kanagawa, O. (1998). Rapid deletion of rearranged T cell antigen receptor (TCR) Valpha-Jalpha segment by secondary rearrangement in the thymus: role of continuous rearrangement of TCR alpha chain gene and positive selection in the T cell repertoire formation. Proc. Natl. Acad. Sci. USA *95*, 11834-11839.

Wang, Q. F., Lauring, J., and Schlissel, M. S. (2000). c-Myb binds to a sequence in the proximal region of the RAG-2 promoter and is essential for promoter activity in T-lineage cells. Mol Cell Biol *20*, 9203-9211.

Wang, Z., Zang, C., Rosenfeld, J. A., Schones, D. E., Barski, A., Cuddapah, S., Cui, K., Roh, T. Y., Peng, W., Zhang, M. Q., and Zhao, K. (2008). Combinatorial patterns of histone acetylations and methylations in the human genome. Nat Genet *40*, 897-903.

Weinreich, M. A., and Hogquist, K. A. (2008). Thymic emigration: when and how T cells leave home. J Immunol *181*, 2265-2270.

Westin, E. H., Gallo, R. C., Arya, S. K., Eva, A., Souza, L. M., Baluda, M. A., Aaronson, S. A., and Wong-Staal, F. (1982). Differential expression of the amv gene in human hematopoietic cells. Proc. Natl. Acad. Sci. USA *79*, 2194-2198.

Weston, K., and Bishop, J. M. (1989). Transcriptional activation by the v-myb oncogene and its cellular progenitor, c-myb. Cell *58*, 85-93.

Wilkinson, R. W., Anderson, G., Owen, J. J., and Jenkinson, E. J. (1995). Positive selection of thymocytes involves sustained interactions with the thymic microenvironment. J Immunol *155*, 5234-5240.

Willis, S. N., Fletcher, J. I., Kaufmann, T., van Delft, M. F., Chen, L., Czabotar, P. E., Ierino, H., Lee, E. F., Fairlie, W. D., Bouillet, P*., et al.* (2007). Apoptosis initiated when BH3 ligands engage multiple Bcl-2 homologs, not Bax or Bak. Science *315*, 856-859.

Wilson, A., Held, W., and MacDonald, H. R. (1994). Two waves of recombinase gene expression in developing thymocytes. J Exp Med *179*, 1355-1360.

Wilson, A., MacDonald, H. R., and Radtke, F. (2001). Notch 1-deficient common lymphoid precursors adopt a B cell fate in the thymus. J Exp Med *194*, 1003-1012.

Witt, C. M., and Robey, E. A. (2004). The ins and outs of CCR7 in the thymus. J Exp Med *200*, 405-409.

Woo, C. H., Sopchak, L., and Lipsick, J. S. (1998). Overexpression of an alternatively spliced form of c-Myb results in increases in transactivation and transforms avian myelomonoblasts. J Virol *72*, 6813-6821.

Woronicz, J. D., Calnan, B., Ngo, V., and Winoto, A. (1994). Requirement for the orphan steroid receptor Nur77 in apoptosis of T-cell hybridomas. Nature *367*, 277-281.

Xi, H., and Kersh, G. J. (2004a). Early growth response gene 3 regulates thymocyte proliferation during the transition from CD4-CD8- to CD4+CD8+. J Immunol *172*, 964-971.

Xi, H., and Kersh, G. J. (2004b). Sustained early growth response gene 3 expression inhibits the survival of CD4/CD8 double-positive thymocytes. J. Immunol. *173*, 340-348.

Xi, H., Schwartz, R., Engel, I., Murre, C., and Kersh, G. J. (2006). Interplay between RORgammat, Egr3, and E proteins controls proliferation in response to pre-TCR signals. Immunity *24*, 813-826.

Xiao, C., Calado, D. P., Galler, G., Thai, T. H., Patterson, H. C., Wang, J., Rajewsky, N., Bender, T. P., and Rajewsky, K. (2007). MiR-150 controls B cell differentiation by targeting the transcription factor c-Myb. Cell *131*, 146-159.

Yannoutsos, N., Wilson, P., Yu, W., Chen, H. T., Nussenzweig, A., Petrie, H., and Nussenzweig, M. C. (2001). The role of recombination activating gene (RAG) reinduction in thymocyte development in vivo. J Exp Med *194*, 471-480.

Yin, X. M., Wang, K., Gross, A., Zhao, Y., Zinkel, S., Klocke, B., Roth, K. A., and Korsmeyer, S. J. (1999). Bid-deficient mice are resistant to Fas-induced hepatocellular apoptosis. Nature *400*, 886-891.

Yu, Q., Erman, B., Bhandoola, A., Sharrow, S. O., and Singer, A. (2003). In vitro evidence that cytokine receptor signals are required for differentiation of double positive thymocytes into functionally mature CD8+ T cells. J Exp Med *197*, 475-487.

Yu, Q., Erman, B., Park, J. H., Feigenbaum, L., and Singer, A. (2004). IL-7 receptor signals inhibit expression of transcription factors TCF-1, LEF-1, and RORgammat: impact on thymocyte development. J. Exp. Med. *200*, 797-803.

Yu, Q., Park, J. H., Doan, L. L., Erman, B., Feigenbaum, L., and Singer, A. (2006). Cytokine signal transduction is suppressed in preselection double-positive thymocytes and restored by positive selection. J. Exp. Med. *203*, 165-175.

Yuan, W. (2000). Intron 1 rather than 5' flanking sequence mediates cell type-specific expression of c-myb at level of transcription elongation. Biochim Biophys Acta *1490*, 74-86.

Yucel, R., Karsunky, H., Klein-Hitpass, L., and Moroy, T. (2003). The transcriptional repressor Gfi1 affects development of early, uncommitted c-Kit+ T cell progenitors and CD4/CD8 lineage decision in the thymus. J Exp Med *197*, 831-844.

Yucel, R., Kosan, C., Heyd, F., and Moroy, T. (2004). Gfi1:green fluorescent protein knock-in mutant reveals differential expression and autoregulation of the growth factor independence 1 (Gfi1) gene during lymphocyte development. J Biol Chem *279*, 40906-40917.

Yue, H. H., Diehl, G. E., and Winoto, A. (2005). Loss of TRAIL-R does not affect thymic or intestinal tumor development in p53 and adenomatous polyposis coli mutant mice. Cell Death Differ *12*, 94-97.

Zhao, H., Kalota, A., Jin, S., and Gewirtz, A. M. (2009). The c-myb proto-oncogene and microRNA-15a comprise an active autoregulatory feedback loop in human hematopoietic cells. Blood *113*, 505-516.

Zhou, B., Wang, S., Mayr, C., Bartel, D. P., and Lodish, H. F. (2007). miR-150, a microRNA expressed in mature B and T cells, blocks early B cell development when expressed prematurely. Proc Natl Acad Sci U S A *104*, 7080-7085.

Zong, W. X., Lindsten, T., Ross, A. J., MacGregor, G. R., and Thompson, C. B. (2001). BH3-only proteins that bind pro-survival Bcl-2 family members fail to induce apoptosis in the absence of Bax and Bak. Genes Dev *15*, 1481-1486.

Zor, T., De Guzman, R. N., Dyson, H. J., and Wright, P. E. (2004). Solution structure of the KIX domain of CBP bound to the transactivation domain of c-Myb. J Mol Biol *337*, 521-534.